

INVESTIGATION OF THE PATHOGENESIS
OF SAIMIRIINE HERPESVIRUS 1
IN BALB/C MICE

By

MELANIE ANN BRESHEARS

Bachelor of Science
Oklahoma State University
Stillwater, Oklahoma
1995

Doctor of Veterinary Medicine
Oklahoma State University
Stillwater, Oklahoma
1998

Submitted to the Faculty of the
Graduate College of the
Oklahoma State University
in partial fulfillment of
the requirements for
the Degree of
DOCTOR OF PHILOSOPHY
July, 2004

INVESTIGATION OF THE PATHOGENESIS
OF SAIMIRIINE HERPESVIRUS 1
IN BALB/C MICE

Thesis Approved:

Jerry W. Ritchey

Thesis Adviser

Richard Eberle

Roger J. Panciera

Jerry T. Saliki

Al Carlozzi

Dean of the Graduate College

ACKNOWLEDGEMENTS

I wish to express my sincere appreciation to my major advisor, Dr. Jerry Ritchey, and my co-advisor, Dr. Richard Eberle, for intelligent and constructive guidance, abundant helpfulness and invaluable support throughout my graduate program. I am indebted to Dr. Ritchey for his untiring mentorship, wise counsel and constant encouragement. To Dr. Eberle, I am grateful for his invaluable direction and supervision, quiet reassurance and tolerance of my preoccupation with pathology. My sincere appreciation extends to other committee members: To Dr. Roger Panciera for his patient and persistent encouragement and unwearied confidence in me and to Dr. Jerry Saliki for his insightful and intelligent input and willingness to serve.

I would like to express my deep gratitude to Ms. Darla Black for her excellent instruction and unfaltering helpfulness in the laboratory and her kind encouragement. I am grateful to Dr. Charlotte Ownby and Dr. Nicholas Cross for the opportunity to serve several enjoyable semesters as a histology teaching assistant. Also, I would like to thank Dr. Ownby and the Electron Microscopy Lab for valuable assistance with confocal microscopy and the OADDL Histopathology Laboratory for technical expertise in processing countless specimens. I am thankful to Ms. Sandra Horton and Ms. Monica Mattmuller at North Carolina State University for technical assistance with immunohistochemical staining. I am also grateful to Dr. Mark Payton for his assistance with the statistical analysis of data. I wish to express my sincere appreciation to Howard Hughes Medical Institute for supporting me as a Predoctoral Fellow.

Finally, I wish to express special appreciation to my parents, to whom this thesis work is dedicated, for their boundless love, understanding and support.

TABLE OF CONTENTS

Chapter	Page
I. INTRODUCTION.....	2
II. REVIEW OF THE LITERATURE.....	4
The Family <i>Herpesviridae</i>	4
Alphaherpesviruses.....	7
Simian Alphaherpesviruses.....	14
References.....	34
III. CHARACTERIZATION OF GROSS AND HISTOLOGICAL LESIONS IN BALB/C MICE EXPERIMENTALLY INFECTED WITH <i>Saimiriine herpesvirus 1</i> (SaHV-1).....	46
Summary.....	46
Introduction.....	47
Materials and Methods.....	49
Results.....	52
Discussion.....	56
Acknowledgements.....	61
References.....	62
IV. CONSTRUCTION AND <i>IN VIVO</i> DETECTION OF AN ENHANCED GREEN FLUORESCENT PROTEIN-EXPRESSING STRAIN OF <i>Saimiriine herpesvirus 1</i> (SaHV- 1).....	72
Summary.....	72
Introduction.....	73
Materials and Methods.....	74
Results.....	81
Discussion.....	87
Acknowledgements.....	91
References.....	92
V. TEMPORAL PROGRESSION OF VIRAL REPLICATION AND GROSS AND HISTOLOGICAL LESIONS IN BALB/C MICE EPIDERMALLY INOCULATED WITH <i>Saimiriine herpesvirus 1</i> (SaHV-1).....	102
Summary.....	102
Introduction.....	103

Materials and Methods.....	106
Results.....	109
Discussion.....	116
References.....	122
VI. SUMMARY AND CONCLUSIONS.....	135
Appendix I.....	142
Appendix II.....	143

LIST OF TABLES

CHAPTER III

Table		Page
1.	Clinical Signs and Gross Lesions	65
2.	Microscopical Lesions	66

CHAPTER IV

1.	Clinical Signs and Seropositivity	101
----	-----------------------------------	-----

CHAPTER V

1.	Clinical Signs and Gross Lesions	128
2.	Comparison of ID50, CNSD50 and LD50	129
3.	Temporal Development of Histological Lesions	130
4.	Temporal Development of GFP Expression	131

LIST OF FIGURES

CHAPTER III

Figure		Page
1.	Typical skin lesion, characterized by foci of necrosis in the epidermis (arrows) and hair follicles (arrowheads) accompanied by an inflammatory infiltrate. H&E. Bar, 200 μm .	67
2.	Lumbar spinal cord segment from a mouse given 10^3 PFU. This animal appeared neurologically normal but had a skin lesion on the left hindlimb and was killed at day 21 p.i. In the left dorsal funiculus and horn there is a focus of intense mononuclear infiltrate and microglial proliferation surrounded by rarefaction. H&E. Bar, 300 μm .	67
3.	Higher magnification of mononuclear infiltrate and microglial proliferation in the dorsal funiculus shown in Fig. 2. H&E. Bar, 200 μm .	68
4.	More distal lumbar spinal cord segment from the animal shown in as Figs. 2 and 3. A mononuclear infiltrate between neuronal cell bodies is present bilaterally in the dorsal root ganglia (arrows). H&E. Bar, 300 μm .	68
5.	Thoracic spinal cord segment from a mouse in the 10^6 PFU group, with unilateral hindlimb paralysis. This animal was killed at day 6 p.i. Note the severe, diffuse vacuolation in the grey matter. On higher magnification, necrosis of neurons and glial cells was evident, as well as a mild mononuclear infiltrate. H&E. Bar, 300 μm .	69
6.	Lumbar spinal cord from mouse that received 10^5 PFU. The animal developed unilateral hindlimb paralysis and was killed at day 60 p.i. There is marked asymmetry of the cord secondary to loss of the unilateral dorsal horn and funiculus. Meninges indicated by arrows. H&E. Bar, 300 μm .	69

7. Immunohistochemical labeling of skin lesion from mouse shown in Fig. 1. Intense labelling of viral antigen is present in the follicular epithelium (arrows). Mayer's hematoxylin counterstain. Bar, 200 μ m. 70
8. Immunohistochemical labeling of lumbar spinal cord from a mouse that received 10^6 PFU. Note the intense viral signal in the left dorsal horn and funiculus. Viral signal is present in both neurons and surrounding glial cells. Mayer's hematoxylin counterstain. Bar, 200 μ m. 70
9. ELISA results for HVS1-specific IgG at 16 (■) and 21 (□) days p.i. The various mouse groups are indicated by the dose (PFU) of virus administered ("0 PFU" indicates controls). OD, optical density. 71

CHAPTER IV

1. Insertion of GFP expression cassette into the SaHV-1 genome. The GFP expression cassette was constructed by flanking the GFP ORF (□) with BV UL19 promoter (≡) and UL18/19/20 transcriptional termination sequences (▣) (A). The GFP expression cassette was inserted into an *Eco*RI restriction site inserted by mutagenic PCR between juxtaposed polyadenylation/ mRNA termination sequences within the SaHV-1 UL26-UL27 intergenic space (B). The viral ORFs (■) and mRNA transcripts shown below by arrows are based on that of HSV1 (McGeoch *et al.*, 1988; Dolan *et al.*, 1998) and BV (Ohsawa *et al.*, 2003; Perelygina *et al.*, 2003), and are consistent with available SaHV-1 sequence data. The reassembled 6 Kbp *Kpn*I fragment was excised from the vector, gel-purified, and co-transfected with genomic SaHV-1 DNA in Vero cells to generate recombinant virus. 96
2. Characterization of wtHVS1, HVS1rG1 and HVS1rG3. Restriction maps for the region of the genome in wtHVS1 based on sequence data (A) and predicted for the recombinant viruses (B) are shown. The location of PCR primers and their products as described in the text are shown beneath the maps. Actual PCR products amplified are shown in (C). A Southern blot using the 6 Kbp fragment (pUQK3) from wtHVS1 as probe is shown in (D) and is described in the text. 97

3. Time course of replication of wild-type and recombinant HVS1. Cell associated virus (top) and extracellular virus (bottom) is indicated as follows: wtHVS1, (■); HVS1rG1, (△); and HVS1rG3, (○). 98
4. Skin and spinal cord lesions in mice given 10^6 PFU HVS1rG, 6 days p.i. Sections of skin (A,E,G) were cut from the same tissue block; skin section C is from a similar lesion in a different animal. In the H&E stained section of skin (A), necrotic keratinocytes (arrow) are surrounded by keratinocytes with intranuclear inclusions (arrowheads). Immunostaining with anti-HVS1 antibody (C) and with anti-GFP antibody (E) demonstrates the presence of viral antigen (C) and GFP (E) within skin lesions. In (C), mast cells (arrow) stain non-specifically with the anti-HVS1 polyclonal antibody. Confocal microscopy (G) reveals a focus of green fluorescence (arrow) that corresponds with the same lesion in (A) and (E); hairshafts exhibit autofluorescence (arrowhead). Sections of thoracic spinal cord (B,D,F,H) were cut from the same tissue block. In the H&E stained section (B), inflammatory cells consisting primarily of neutrophils infiltrate the ipsilateral dorsal grey horn. The anti HVS-1 immunostain (D) and the anti-GFP immunostain (F) demonstrate the presence of HVS1 antigen and GFP, respectively. Viral antigen and GFP are localized primarily within neurons of this region. Confocal microscopy reveals corresponding green fluorescence (H). Bar markers in skin photos (A,C,E,G) equal 50 μm . Bars markers in spinal cord photos (B,D,F,H) equal 125 μm . 99

CHAPTER V

1. **Figure 1.** All tissues are from Balb/c mice epidermally inoculated with 10^6 PFU of SaHV-1rG. 132
- A.** Haired skin. Characteristic skin lesion at the inoculation site 24 hours p.i. There is moderate swelling of epidermal keratinocytes, many of which have distinct intranuclear inclusion bodies. The underlying dermis contains a mild neutrophilic infiltrate and a fibrinosuppurative mat overlies the focus of infected epidermis. H&E.
- B.** Left dorsal root ganglion, lumbar region. Neuronal necrosis and loss is accompanied by a mild mononuclear inflammatory infiltrate at 6 days p.i. H&E.

C. Lumbar spinal cord. Typical lesion present in the lumbar spinal cord at 6 days p.i. The left dorsal grey horn exhibits regionally extensive neuronal necrosis accompanied by mild neutrophilic and lymphocytic inflammation and rarefaction of the left dorsal funiculus. At higher magnification, intranuclear inclusion bodies can be seen in scattered neurons of the left dorsal grey horn. H&E.

D. Ureter, 6 days p.i. There is marked ureteral ectasia with intense transmural and periureteral neutrophilic and lymphoplasmacytic inflammation. The lumen contains neutrophils admixed with fewer mononuclear cells in a fibrinous background. Ureteral epithelium is dysplastic and contains a small number of transmigrating inflammatory cells but no discrete foci of viral infected cells. This mouse had grossly discernible unilateral hydronephrosis. H&E.

E. Colon. Characteristic colon lesion present at 8 days p.i. Neurons within the myenteric plexus are necrotic and myocytes of the adjacent smooth muscle tunics are moderately vacuolated. H&E.

F. Skin. Confocal image demonstrating GFP expression in SaHV-1 infected epidermal and follicular keratinocytes at 24 hours p.i. This tissue section is from the same lesion illustrated in A.

G. Urinary bladder. Confocal image of SaHV-1 infected focus of urinary bladder epithelium at 6 days p.i.

H. Colon. Confocal image of a colonic myenteric plexus, demonstrating viral replication within numerous neurons between the muscular tunics. This tissue section is from the same specimen as E.

NOMENCLATURE

AtHV-1	spider monkey herpesvirus (<i>Ateline herpesvirus 1</i>)
bp	base pair(s)
BSL3	biosafety level three
BV	monkey B virus (<i>Cercopithecine herpesvirus 1</i>)
CNS	central nervous system
CNSD ₅₀	50% central nervous system disease dose
CPE	cytopathogenic effect
DMEM	Dulbecco's modified Eagle medium
DNA	deoxyribonucleic acid
d.p.i.	days post-inoculation
DRG	dorsal root ganglia
eGFP	enhanced green fluorescent protein
ELISA	enzyme-linked immunosorbent assay
FBS	fetal bovine serum
GFP	green fluorescent protein
H&E	haematoxylin and eosin
HSV	herpes simplex virus
HSV-1	herpes simplex virus type 1 (<i>Human herpesvirus 1</i>)
HSV-2	herpes simplex virus type 2 (<i>Human herpesvirus 2</i>)
HVP-2	Baboon herpesvirus (<i>Cercopithecine herpesvirus 16</i>)
IC	intracerebral
ID ₅₀	50% infectious dose
IHC	immunohistochemistry
IM	intramuscular
IP	intraperitoneal
Kbp	kilobase pairs
LD ₅₀	50% lethal dose
LPV	large plaque variant
MOI	multiplicity of infection
mRNA	messenger ribonucleic acid
ORF	open reading frame
PBS	phosphate-buffered saline
PCR	polymerase chain reaction
PFU	plaque forming unit
p.i.	post-inoculation
SA8	simian agent 8 (<i>Cercopithecine herpesvirus 2</i>)
SaHV-1	squirrel monkey herpesvirus (<i>Saimiriine herpesvirus 1</i>)
SaHV-1rG1	isolate 1 of GFP-expressing recombinant SaHV-1
SaHV-1rG3	isolate 3 of GFP-expressing recombinant SaHV-1
SC	subcutaneous
SDS-PAGE	sodium dodecyl sulfate-polyacrylamide gel electrophoresis
SPV	small plaque variant
VZV	varicella-zoster virus (<i>Human herpesvirus 3</i>)

FOREWARD

This dissertation includes the following two peer-reviewed scientific publications (Chapters III & IV), which are presented in the published journal format.

1. Breshears MA, Eberle R, and Ritchey JW. Characterization of gross and histological lesions in Balb/c mice experimentally infected with *Herpesvirus saimiri 1* (HVS1). *J Comp Pathol* 2001; **125**: 25-33.
2. Breshears MA, Black DH, Ritchey JW, Eberle R. Construction and in vivo detection of an enhanced green fluorescent protein-expressing strain of *Saimiriine herpesvirus 1* (SaHV-1). *Arch Virol* 2003; **148**: 311-327.

Chapter V will be submitted for publication soon and has been written in the format prescribed for *Journal of Comparative Pathology*.

CHAPTER I

INTRODUCTION

Animal models of human disease provide the means for detailed study of pathological processes in a complex biological system and are an important tool in advancing the knowledge of many disease processes. Some of the subjects best suited for biomedical research are non-human primates, owing primarily to their close genetic relationship with humans, which is manifested through similarities in biochemical, physiological, and anatomical features. While these similarities are advantageous for comparison of disease processes between species, they are potentially dangerous since they increase the likelihood of trans-species transmission of infectious agents. As an example, a well-known infectious agent that can result in severe or fatal disease for humans following trans-species spread from the non-human primate host is *Cercopithecine herpesvirus 1* or monkey B virus (BV) of macaques, a member of the subfamily *Alphaherpesvirinae*. Given the significant risk imposed by this virus on workers routinely exposed to macaques as well as the potential for trans-species spread associated with alphaherpesviruses in general, other alphaherpesviruses present in additional primate species are worthy of investigation.

Saimiirine herpesvirus 1 (SaHV-1) is an alphaherpesvirus that is indigenous to squirrel monkeys. It is genetically and antigenically related to BV as well as other primate alphaherpesviruses, including the human herpes simplex viruses (HSV). As a

simian alphaherpesvirus that has been the subject of modest research but not the focus of intense investigation, it provides ample background information upon which to construct a comparative small animal model system while allowing potential for new discovery. A small animal model of SaHV-1 infection would be beneficial in gaining a better understanding of alphaherpesvirus neuropathogenesis, including viruses native to simian hosts in addition to viruses indigenous to humans. An added benefit for the development of a rodent model using SaHV-1 rather than a virus native to humans would be the possibility of later expanding studies to involve squirrel monkeys, the natural host species. The focus of this dissertation is the characterization of a mouse model for investigation of the neuropathogenesis of SaHV-1, using both wild-type virus and a recombinant virus that expresses green fluorescent protein (GFP).

CHAPTER II

REVIEW OF THE LITERATURE

The Family *Herpesviridae*

The *Herpesviridae* are composed of large double-stranded DNA viruses that have a characteristic virion architecture and share four significant biological properties.

Structural features include a core containing linear, double-stranded DNA within a 100-110 nm diameter icosadeltahedral capsid composed of 162 capsomeres. The capsid is surrounded by an amorphous, frequently asymmetric tegument and an outer envelope containing viral glycoprotein spikes on its surface. Viral DNA contained in the core of the mature virion may be packaged in the form of a torus. The molecular weight of the DNA genome varies from 80 to 150 million kD (120 to 230 Kbp) between different herpesviruses, with minimal variation in genome size occurring for any one herpesvirus. The base composition of herpesvirus DNAs varies from 31 to 75 G + C mole percent.

The DNA core is surrounded by a capsid with the previously mentioned structural features characteristic of all herpesviruses. The tegument, which lies between the capsid and the envelope, may vary in thickness depending on the location of the virion within the infected cell. The envelope appears to be derived from patches of altered cellular membranes and contains numerous protrusions of glycoprotein spikes which vary in number and relative amounts. The entire herpes virion varies from 120 to 300 nm in

diameter due to variability in the thickness of the tegument as well as artifactual differences resulting from the state of the envelope. For example, virions with a damaged envelope are permeable to negative stains and during preparation for electron microscopy, attain a diameter much greater than that of virions with intact envelopes [96, 98].

The four significant biological properties shared by all herpesviruses are: i) All herpesviruses specify a large array of enzymes involved in nucleic acid metabolism, DNA synthesis, and protein processing. ii) Viral DNA synthesis and capsid assembly occurs in the nucleus and envelopment of the capsid occurs as it transits through the nuclear membrane. There is argument, however, about transit of the virion through the cytoplasm and single envelopment versus successive de-envelopment and re-envelopment (reviewed in [34]). iii) Production of infectious virus progeny always involves irreversible destruction of the infected cell. iv) Herpesviruses are able to remain latent in their natural hosts, with viral genomes taking the form of closed circular molecules. Other biological properties vary greatly among herpesviruses, such as wide or narrow host cell range, efficiency or rate of viral multiplication, the actual cell type within which latency occurs, and clinical manifestation of disease [96, 98].

Biological properties such as host cell range, length of replicative cycle, and cell type in which latency is established were initially used to divide the family *Herpesviridae* into three subfamilies, the *Alphaherpesvirinae*, *Betaherpesvirinae* and *Gammaherpesvirinae* [1, 95]. These classifications are also supported by the more recently developed criteria of gene sequence and other genetic attributes [55, 99]. *Alphaherpesvirinae* have a variable host cell range, short replicative cycle, spread rapidly

in culture, efficiently destroy infected cells, and are capable of establishing latency, primarily in sensory ganglia [98]. They characteristically initiate infection in mucosal epithelial cells where they replicate and then invade the sensory neurons to establish latent infection in the ganglia [120]. *Betaherpesvirinae* have a restricted host range, long reproductive cycle with slow spread in culture, often with enlargement of infected cells and latency in secretory glands, lymphoreticular cells, kidneys and other tissues [98]. *Gammaherpesvirinae* have a limited host range, may remain latent in lymphoid tissue, and replicate in lymphoblastoid cells with some viruses causing lytic infections in epithelioid or fibroblastic cells [98].

Herpesviruses are widespread in nature with almost all vertebrate species being naturally infected by at least one herpesvirus [98]. Genomic data demonstrate a common evolutionary origin among all herpesviruses [73, 76] as well as divergent patterns that reveal co-speciation or co-evolution of virus and host [74, 75]. As a result, herpesviruses are generally well-adapted to their hosts, rarely causing severe or fatal disease in immunocompetent natural hosts [98]. On the contrary, when aberrant or heterologous hosts are infected with a herpesvirus, especially those belonging to the subfamily *Alphaherpesvirinae*, fatal disease is frequent [98]. For example, pseudorabies virus infection usually produces only mild disease in adult swine, while infection in cattle, goats or dogs is often fatal. Similarly, BV infection produces mild disease in macaques but causes severe encephalomyelitis in humans [96].

Alphaherpesviruses

The subfamily *Alphaherpesvirinae* contains four genera, including *Simplexvirus*, *Varicellovirus*, “Marek’s disease-like viruses” and “Infectious laryngotracheitis-like viruses” [55]. The prototypical member of the *Simplexvirus* genus is *Human herpesvirus 1*, more commonly known as herpes simplex virus type 1 (HSV-1) [97]. Other members of the genus *Simplexvirus* include *Human herpesvirus 2* or human simplex virus type 2 (HSV-2) and several viruses of simian hosts, including *Cercopithecine herpesvirus 1* or monkey B virus, *Cercopithecine herpesvirus 2* or simian agent 8 (SA8), *Cercopithecine herpesvirus 16* also called *Herpesvirus papio 2* (HVP-2), *Ateline herpesvirus 1* (AtHV-1) of spider monkeys, and *Saimiriine herpesvirus 1* (SaHV-1) of squirrel monkeys (see Appendix I for virus names, abbreviations and synonyms). The *Varicellovirus* genus includes the type-member *Human herpesvirus 3* or varicella zoster virus (VZV) and the animal herpesviruses *Suid herpesvirus 1* (commonly known as pseudorabies virus), equine herpesviruses 1 and 4, and *Cercopithecine herpesvirus 9* or simian varicella virus (see Appendix I). Simplexviruses and varicelloviruses vary slightly in genome size, genome sequence arrangement and viral protein expression, but viruses in both genera are often compared to their more completely characterized relative, HSV-1 [57]. Marek’s disease virus is a cell-associated herpesvirus and while it has lymphotropic properties similar to gammaherpesviruses, its genomic organization and molecular structure are similar to those of alphaherpesviruses. The genus of “Marek’s disease-like viruses” also includes nononcogenic herpesviruses of turkeys and chickens that are ubiquitous and not recognized as pathogens in their avian hosts. “Infectious laryngotracheitis-like viruses,” represented by the prototypical laryngotracheitis virus of chickens (*Gallid herpesvirus 1*),

exhibits replication similar to other alphaherpesviruses and causes respiratory disease by infection of upper respiratory tract epithelium.

Pathogenesis of Alphaherpesvirus Infections

In general, the pathogenesis of an HSV-1 infection, the intensively studied prototype of genus *Simplexvirus* of the subfamily *Alphaherpesvirinae*, involves contact of an infectious virus particle with a mucosal surface or abraded skin. Infection occurs when virus replicates within epithelial cells at the site of exposure. From the site of initial infection, virions are centripetally transported within afferent axons to the dorsal root ganglia. It is here that viral latency, an interesting property of alphaherpesviruses, is established. Latent virus can be reactivated and travel centrifugally through the axon to reach the innervated epithelium and replicate, producing vesicles and typical herpetic lesions [120]. The steps in the typical progression of disease from epithelium to the central nervous system will be described in more detail below. The fine points of viral latency and reactivation are beyond the scope of this work, and will not be discussed.

Epithelial Lesions of HSV-1

Moriyama *et al.* [83] reported that mice inoculated with HSV-1 via epidermal scarification of flank skin first have detectable viral antigen in keratinocytes of the epidermal basement layer at 48 hours post-inoculation (p.i.). Morphological changes were not yet apparent, but keratinocytes adjacent to infected cells had detectable viral antigen on the cell membrane although not within the cell. By 72 hours p.i., cells containing antigen were present throughout the epidermis (below the stratum corneum)

including epithelium of hair follicles and sebaceous glands. Ballooning degeneration of keratinocytes within the focus of infection resulted in intraepidermal vesicles. By five days p.i., lesions were covered by adherent crusts and the upper dermis was characterized by coagulation necrosis. Inflammatory cell populations consisting of both mononuclear cells and neutrophils were present in foci beginning early in the disease process [83]. In a microscopic study of HSV and VZV skin lesions of humans, vesicles and pustules were seen either within or beneath the epidermis [79]. Neutrophils were the predominant inflammatory cell type and were present within the epidermis as well as the dermis, where they surrounded small necrotic blood vessels and pilosebaceous units. The severity of the inflammation increased with the duration of both diseases.

In the epidermis, viral spread to neighboring keratinocytes seems to be via extracellular fluid extension or possibly cell-to-cell spread [83]. Restriction of the virus to a small zone surrounding the initial inoculation site is thought to be due to locally extensive cell death and coagulative necrosis in the infected focus. Spread of virus in the dermis may be slowed by the small number of nerve endings present within this layer as well as restriction of HSV-1 spread by the epidermal basement membrane [83]. In fact, Weeks *et al.* [116] reported that the epidermal basement membrane restricts the pathogenesis of HSV-1 and HSV-2 by preventing virus inoculated intradermally (beneath the basement membrane) from gaining access to free nerve endings present within the epidermis. Conversely, virus replicating within the epidermis has ready access to peripheral nerves via free nerve endings that project into the epidermis through the basement membrane [116]. In a different mouse inoculation study, it was demonstrated that infection of shallow abrasions rather than deeper inoculation methods progressed to

disease more rapidly [40]. Similarly, other membranes such as the mature basal lamina of muscle fibers act as a physical barrier to HSV-1 infection [50]. Thus, the route of exposure to the virus has a significant impact on the severity of disease caused by HSV infection.

Neural Invasion and Spread of HSV-1

As first demonstrated by Goodpasture and Teague, HSV-1 has the ability to spread centripetally to the CNS following replication in a peripheral location [41]. Entry of virus into peripheral nerves for intraaxonal transport to the CNS is the next step in the progression of a neuroinvasive alphaherpesvirus infection. In order to be neuroinvasive, a virus must be able to replicate at the initial site of inoculation, enter and be transported in the neurons innervating the site, and also be neurovirulent (have the ability to replicate in nervous tissue). It has been shown that the ability of a virus to cause neuroinvasive disease correlates with the ability of the virus to cause zosteriform disease by replicating in neurons and spreading beyond the initial site of infection via neural circuits [40]. In zosteriform disease, secondary epithelial lesions develop separate from but within the same dermatome as the primary lesion at the inoculation site. For the development of these secondary lesions, virus must be intra-axonally transported retrograde from the initial site to the dorsal root ganglion (DRG), replicate in the DRG, and subsequently undergo anterograde axonal transport to infect epithelium supplied by the same nerve [106, 108].

HSV-1 Transport in Different Classes of Peripheral Nerves

In epidermal inoculation or the zosteriform model, sensory nerves in the epidermis compose the predominant portion of the nervous system exposed to and infected by virus [60, 119]. In the same way, when the virus is inoculated intramuscularly, viral infection is focused on motor neurons within the corresponding spinal cord segments [60, 119]. Furthermore, oral inoculation of mice with HSV has been shown to result in viral infection of the autonomic nervous system, specifically myenteric ganglia within the esophagus and stomach [39]. This study also demonstrated HSV antigen within nerve fibers penetrating into the lamina propria of the gut mucosa [39], while concluding that gastrointestinal (GI) epithelium is not likely to be acutely infected with HSV1 [37, 38]. Thus, it is known that HSV is able to infect sensory, motor, and autonomic divisions of the nervous system, and that the route of exposure may be important in determining which types of neurons are infected.

It has been reported that while HSV-1 transfer occurs through all of the main classes of peripheral neurons, the rate of viral transfer varies between nerve types. Using viral injection into mixed limb nerves, Ugolini determined that retrograde and anterograde HSV-1 transneuronal transfer within sympathetic pathways and small sensory afferents, respectively, is early, robust and synchronized [113]. Transneuronal transfer of virus in these small axons (primarily unmyelinated small cutaneous afferents and sympathetic post-ganglionic axons) preceded transfer in large axons (myelinated cutaneous and muscle afferents and motor axons) [113]. The more rapid transfer of virus within smaller neurons may be due to more efficient viral uptake by these fibers secondary to differences in the type of receptors on the neural surface [8] or because of a

delay in viral penetration secondary to interference by the presence of a myelin sheath [19].

Transsynaptic Transfer of HSV-1.

Once HSV gains access to a neuron, it can be transferred to other neurons in a transsynaptic manner [33, 61, 62, 69, 78, 88, 100, 111, 112]. Virus may travel in the retrograde direction from afferent (sensory) fibers to post-synaptic neurons [61, 62] or may be transported retrograde from efferent (motor) fibers to presynaptic terminals [111, 119]. In either case, the distribution of neurons labeled through transneuronal transfer of virus suggests that virus is preferentially transferred transsynaptically [2, 114]. This feature of alphaherpesviruses has been used extensively to map the neuronal circuitry of the CNS *in vivo* [2, 33, 59, 63, 88, 89, 111-113]. There is some skepticism regarding the specificity of transneuronal transfer of virus, specifically concerning the lytic nature of some viral strains and the presence of viral antigen in glial cells surrounding infected neurons [11]. It is known that the application of a viral envelope containing glycoproteins is essential for the production of infectious progeny virus, and while astrocytes may be able to initiate viral replication, they are not able to provide progeny virus with the necessary envelope [9].

Since astrocytes are the first cell to respond to viral infection in the CNS [10] and because of the very strong affinity of the virus for the astrocyte membrane [114, 115], astrocytes absorb significant amounts of virus that has been released parasynaptically [9]. Thus, the response of astrocytes may play an important role in restricting the spread of infectious virus particles through lytic infections, and thereby contribute to the specificity

of transsynaptic infection [11]. Evidence also exists for nonsynaptic or lateral spread of alphaherpesviruses within peripheral ganglia [12, 64, 68], and the potential for viral passage into unrelated neuronal circuits remains unclear. Nonspecific lateral spread of virus may vary within different types of ganglia (sensory versus autonomic) and the specificity of transsynaptic spread within peripheral ganglia may be influenced by the virulence of the virus strain, with greater non-specific transfer occurring in infections with more virulent strains [103]. In addition, there is evidence that even though axon terminals are the preferred site of virus entry into neurons, virions can enter a neuron at its soma if virus concentration is adequate[11].

Alphaherpesvirus Infections of the Central Nervous System

Alphaherpesviruses typically infect the peripheral nervous system of their natural hosts and although spread to the CNS is possible, it is not common. When alphaherpesviruses do infect the CNS, they maintain the organized pattern of spread indicative of intraaxonal transport and transsynaptic viral transfer [2, 7, 60, 62]. Although relatively rare, CNS infections with the human alpha-herpesviruses result in devastating disease. Of these, HSV is considered to be the most common etiology of sporadic, fatal encephalitis [91]. HSV is also associated with meningitis, myelitis and radiculitis [21]. VZV is another human alphaherpesvirus associated with CNS infections resulting in ganglioneuritis, meningitis and myelitis [31].

Rarely, either VZV or HSV infection can result in urinary retention secondary to motor and sensory neuropathy of the urinary bladder [18, 36, 43, 86, 107, 122] or micturition centers in the brainstem [102]. VZV involvement of the CNS leading to

urinary retention was at the sacral level in 78% of cases, involved the thoracolumbar region in 11% of cases and the higher thoracic cord in 11% of patients [94]. Urinary retention associated with HSV infection of the anogenital region is rare in comparison with VZV and is a result of localized lumbosacral meningomyelitis involving sacral nerves [90] or neuritis of pelvic nerves [42].

Alphaherpesviruses and Cystitis

In a few cases of urine voiding dysfunction associated with either VZV or HSV infections, a herpetic cystitis is present [17, 72, 87]. The most common type of cystitis associated with VZV is an ipsilateral herpetic hemicystitis that is thought to result from the spread of VZV along visceral nerves [18]. In addition, dilation of the renal pelvis and entire ureter ipsilateral to the cutaneous zoster lesion suggests direct neurogenic involvement [18]. In VZV cases, herpetic mucosal lesions may be present in the urethra and urinary bladder [6]. Hemorrhagic cystitis has been associated with HSV-2 infections and results in dysuria with [25] or without extra-urinary herpetic lesions [72, 87]. Cystitis could result from an ascending infection from the external genitalia [20] or via hematogenous spread [25]. Given the evidence for neural spread of VZV to the bladder mucosa, it is expected that neural spread is involved in HSV cystitis as well.

Simian Alphaherpesviruses

Non-human primates are valuable biomedical research resources because of their physiological, anatomical and biochemical similarities to humans. Alphaherpesviruses indigenous to non-human primate species are of special importance for at least two

reasons. First, alphaherpesviruses are well known for spontaneous interspecies transmissibility, which often results in severe or fatal disease for accidentally infected aberrant hosts. Second, some simian alphaherpesviruses lend themselves to use as animal models of human disease because infection of either natural or experimental hosts produces a disease that closely resembles disease associated with alphaherpesvirus infection in humans. The number of herpesviruses that have been isolated from non-human primates is large, and phylogenetic data provide evidence that individual herpesviruses have co-evolved with their host species[74, 75]. This is exemplified by alpha-herpesviruses of Old and New World primates[77].

Old World primates (Catarrhini), (i.e.- macaques, baboons) originate in Africa and Asia, lack prehensile tails and are larger than New World primates. Platyrrhini or New World monkeys originate in South America, have prehensile tails, are relatively small and include squirrel monkeys, spider monkeys, tamarins, marmosets and owl monkeys. (See Appendix II for the taxonomy of selected primates)

Given the potential severity of interspecies infections, the use of monkeys and apes as animal models of human disease lends special importance to the study of simian herpesvirus infections [5]. Certain members of the subfamily *Alphaherpesvirinae* have a highly pathogenic nature in cross-species infections, frequently producing disease with neurologic involvement in species that are not natural hosts. Infection of humans by herpesviruses from the β and γ subfamilies has not been reported although the potential for human zoonotic infections may exist. Therefore the simian alphaherpesviruses are currently considered to be of the greatest importance as potential zoonotic infectious agents [29].

Cercopithecine herpesvirus 1

Cercopithecine herpesvirus 1 or monkey B virus (BV) was the first simian herpesvirus to be identified and characterized. Initial reports were published independently by Gay and Holden in 1933 [35] and Sabin and Wright in 1934 [101]. Each research team isolated virus from the brain and spinal cord of a research physician (identified as Dr. W.B.) who died following the development of acute ascending encephalomyelitis after being bitten on the hand by an apparently normal rhesus monkey (*Macaca mulatta*) [35, 101]. Gay and Holden called the infectious agent W virus and considered it to be a variant of HSV with increased neurotropism [35]. Sabin and Wright provided a comprehensive review of the case in 1934, and based on observed biological properties, the authors considered the isolated virus, which they designated B virus, to be distinct from HSV [101].

B Virus Infection in Macaques

Rhesus, cynomolgus and other Asiatic species of the genus *Macaca* are enzootically infected with BV [118, 121]. BV does not generally cause severe disease in macaques; in fact asymptomatic infection may actually be more common. Like the pathogenesis of HSV in humans [20], BV infection in macaques begins with primary replication in epithelium followed by viral uptake in sensory and autonomic nerve endings and axonal transport to nerve cell bodies in local ganglia where latency is established [118]. Unlike HSV in humans, no vertical transmission of BV between infected females and their offspring has been documented [118]. Animals may become infected at a young age through contact with a virus-shedding animal but most commonly they become infected

at the onset of sexual activity [123, 124]. This is supported by observing that the proportion of macaques with antibody titers to BV increases after dense group caging and in both caged and wild-caught animals, the probability of a positive BV titer is significantly larger for post-pubertal animals [93, 117, 118]. Venereal transmission is thought to be a major route of infection[124], but its actual significance comes to question as it has been established that BV infections occur readily in prepubertal monkeys unless they are caged separately[118]. Obviously, much is unknown regarding the epidemiology of this virus in macaques [118].

Like other alphaherpesviruses, BV can establish latent infections in the natural host that persist throughout life, and may be reactivated and result in virus shedding in saliva or genital secretions, either with or without clinical signs [118, 123, 124]. Latent virus has been detected in trigeminal and lumbosacral sensory ganglia of seropositive macaques [123]. Similar to HSV, it seems that the reactivation of the latent BV is often linked with stress such as capture and shipment, breeding season, or illness [118, 124]. With the seroprevalence of neutralizing antibodies to BV in captive adult macaques ranging from 73% to 100% [92, 93], macaque species are considered to be inherently dangerous to humans because of the risk for BV transmission [13-15, 49].

B Virus Infection in Humans

Since the initial report of human BV infection by Gay and Holden [35] and Sabin and Wright [101] in 1933 and 1934, respectively, fewer than 40 symptomatic human infections with BV have been reported [13, 15, 48, 92, 93, 118]. The most recent case occurred following mucocutaneous exposure to biologic material from a rhesus macaque

through ocular splash without concurrent injury [16]. While these statistics indicate that human BV infection and disease is rare, the consequences of symptomatic BV infection are often severe. Of the 26 well-documented cases of human infection [3, 13, 15, 16, 48, 93, 118], 23 cases (88%) progressed to various degrees of encephalomyelitis which ultimately led to 17 deaths. Monkey-inflicted bites or scratches, saliva contamination of existing wounds, or cuts from monkey tissue culture bottles or needle-stick injuries preceded the onset of disease in 20 of the 26 documented cases [13, 15, 48, 93, 118]. The remaining documented cases include one case of person-to-person transmission [13, 48], mucocutaneous exposure via ocular splash of macaque biologic material [16], cleaning a rhesus skull without protective gloves, two cases of possible respiratory exposure, and one case with an unknown mode of exposure but a history of frequent contact with macaques [93, 118]. The literature contains several other case reports lacking complete documentation [93] and it seems likely that the actual number of human cases is significantly underestimated, especially if one considers presumptive asymptomatic cases [3, 48, 67, 92, 118].

Signs reported in early generalized disease in humans always included fever and often included aches and pains. Variable symptoms included sore throat, vesicular skin lesions, lymphadenitis, and vomiting. These symptoms rapidly progressed to neurological signs such as hyperesthesia, ataxia, and ascending flaccid paralysis. Some cases involved urinary retention, convulsions or mental confusion. In the cases in which spinal taps were reported, cerebrospinal fluid contained increased numbers of leukocytes (predominantly lymphocytes), and elevated protein and glucose [93].

In human cases of BV infection, the tissues and organs that become infected vary with the route of inoculation. In bite wounds or other instances where the skin is the primary source of involvement, virus replicates locally and may result in reddening and swelling of the affected site which progresses to regional lymphangitis and lymphadenitis [118]. After this initial phase of replication, subsequent propagation within the peripheral nervous system progresses to involvement of the spinal cord and eventually, the brain [118]. Unlike the neurologic disease caused by HSV which tends to localize in the temporal lobe of the brain, BV infections can involve all regions of the brain [121] but appear to be more common and severe in the medulla and pons [51, 93, 118]. Microscopic brain lesions include hemorrhagic and necrotic foci, perivascular cuffs of mononuclear cells, edema and degeneration of motor neurons, and in later stages astrocytosis and gliosis [93]. Eosinophilic intranuclear inclusions are not found uniformly, but may be seen in a few cases [51, 93]. Involvement of visceral organs is presumed to be a consequence of a transient viremia and is manifested as multifocal hemorrhagic necrosis, especially of the liver and lung [51, 121], and resembles that reported in HSV-associated visceral infections [20].

Given that thousands of laboratory workers have handled *Macaca* species animals or processed monkey kidney cells without becoming infected, transmission of BV to humans appears to be limited. Even so, the possibility of BV infection needs to be considered for any individual having contact with macaques. Possible infection should be suspected in cases evidenced by contact with a rhesus monkey via bite, scratch, mucocutaneous splash or laboratory accident [14]. Clinical manifestations of disease including the presence of vesicular lesions at the bite site, regional lymphadenopathy,

altered sensation in the extremities, weakness, hyporeflexia, and possibly altered mentation should suggest possible BV infection. Virus isolation in suspected cases should be attempted from vesicular material, pharyngeal swabs, conjunctivae, tissue biopsy, and cerebrospinal fluid. Diagnosis via serological evidence is difficult due to the extensive antigenic cross reactivity between BV and HSV [121].

Currently, the approach to the treatment and prevention of BV disease in humans involves the immediate cleansing of macaque bites, scratches or mucosal surfaces contaminated with macaque biologic materials (Holmes, 1995). Postexposure prophylaxis and treatment involves the utilization of nucleoside analogs such as vidarabine, acyclovir and gangciclovir [118, 121]. In cell culture and in experimentally infected rabbits, acyclovir has been demonstrated to be beneficial in cases of BV infection [118, 121]. It is recommended that oral acyclovir therapy be instituted immediately post-exposure and continued until the cultures of the exposed person are confirmed negative. If culture is positive, therapy should be continued for at least 14 days and if disease develops, intravenous therapy is indicated. Since the use of acyclovir as treatment of BV infections in humans has been limited to a few cases, the efficacy of the drug cannot be unequivocally determined [121].

B Virus Infection in Other Animal Species

BV has been shown to be fatal in other species of monkeys including cebus (capuchin) monkeys [35] and common marmosets (*Callithrix jacchus*) [125], with lesions similar to those observed in BV-infected people. In addition, BV infections with some fatalities but also with evidence for the establishment of latent infection in surviving animals has been

reported in a colony of DeBrazza's monkeys (*Cercopithecus neglectus*) [109]. In early experiments performed during the initial characterization of BV, Sabin and Wright [101] demonstrated virus infection and fatal disease in rabbits inoculated intracerebrally with tissue homogenates from the first infected human. In contrast, rabbits inoculated intraperitoneally did not succumb to disease. In similar experiments, mice, guinea pigs and dogs were resistant to both intracerebral and intraperitoneal inoculation[101].

Saimiriine herpesvirus 1

Saimiriine herpesvirus 1 (SaHV-1), also known as *Herpesvirus saimiri 1*, *Herpesvirus tamarinus*, Herpes T, Marmoset herpesvirus, and *Herpesvirus platyrrhinae* is a simian alphaherpesvirus first isolated from aberrantly infected marmosets and tamarins. This virus is less well characterized than BV, but has similarly has been reported to cause severe disease in spontaneously infected aberrant hosts. A single description of presumptive human disease associated with SaHV-1 was reported in a research psychologist who, after contact with squirrel monkeys, developed non-fatal encephalitis [105]. Virus isolation was not attempted, but a rising antibody titer to SaHV-1 was demonstrated.

SaHV-1 was first isolated and independently characterized in 1963 by Holmes *et al.*[45, 46] and Melnick *et al.* [81]. Melnick *et al.* isolated the virus from the lungs and kidneys of marmosets or tamarins (*Saguinus nigricollis*) that died suddenly after shipment [81]. Holmes *et al.* isolated the virus from the lung, heart, kidney, liver, spleen and salivary gland tissue of black-mantle tamarins (*S. nigricollis*) and cotton-topped tamarins (*S. oedipus*), which died suddenly within the two weeks following the arrival of

new animals to the colony [45, 46]. Both laboratories found that the agent grew readily in a variety of cell cultures and produced cytopathic effect very similar to that of HSV. Based on the chemical, physical, biological and immunological properties of the agent, it was classified as a member of the alpha herpesvirus group [45, 46, 81].

SaHV-1 has also been isolated from another spontaneously infected New World species, the owl monkey (*Aotus trivirgatus*) [32, 52]. Similar to the cases in tamarins, SaHV-1 was isolated from owl monkeys that became ill and died after shipment or following the arrival of new animals to the colony. It is important to note that during this time period, this particular owl monkey colony was housed in the same quarters in which a squirrel monkey (*Saimiri sciureus*) colony was maintained. No squirrel monkeys exhibited signs of disease and there was no direct contact between the owl monkey and the squirrel monkey colonies [52]. Another report details the isolation of SaHV-1 from the brain, liver and tongue of one owl monkey from a pet shop in which several monkeys became ill with signs of pruritis shortly before dying [32].

Given the highly virulent nature of SaHV-1 in marmosets, tamarins and owl monkeys, it was considered unlikely that any of these species were the natural hosts of the virus. In 1966, Holmes *et al.* reported a serological survey of monkeys for exposure to SaHV-1 and noted that significant numbers of squirrel monkeys (*Saimiri* spp.), spider monkeys (*Ateles* spp.), and white-fronted capuchin monkeys (*Cebus albifrons*) had antibodies against SaHV-1 while few marmosets and tamarins were immune [47]. In a serological study of monkeys from a pet shop in which several deaths had occurred two months earlier, significant titers of antibody against SaHV-1 were noted in the majority of squirrel monkeys (17 of 19) but no antibody was present in the other simian species

examined [32]. In Holmes' study [47], it was also noted that significant antibody titers to SaHV-1 were more common in adults of *Saimiri sp.*, *Ateles sp.* and *C. albifrons*. On the contrary, the percentage of marmoset adults with antibody titers was slightly lower than the percentage of seropositive juveniles. The higher percentage of immune adults as compared to juveniles for squirrel, spider, and cinnamon ringtail monkeys reflects what would be expected in an endemic, non-fatal infection. In contrast, the relatively even distribution in young and old marmosets is consistent with an infection at some common time point that is not age related [47].

SaHV-1 Infection in Squirrel Monkeys

Aside from the serological data described above, the indigenous nature of SaHV-1 in the squirrel monkey is suggested by the isolation of the virus from apparently healthy, latently infected individuals. Throat and anal swabs from 10 squirrel monkeys collected every other day over 15 days provided an isolate of SaHV-1 from the throat swab of one monkey on the third day and an isolate from the anal swab of the same monkey on the fifth day [80]. In addition, SaHV-1 has been isolated from the salivary gland and tongue of young, naturally infected squirrel monkeys exhibiting mild clinical disease consisting of small, scab covered ulcers or necrotic plaques on the lips and mucous membranes of the tongue and hard palate [22, 58]. The nature and distribution of lesions as well as reported shedding of virus and development of lesions in young animals at the time of shipment or other stress mimic HSV infection in humans [47]. It has been proposed that SaHV-1 is analogous to HSV in humans and would be an excellent model for HSV study [58, 80].

SaHV-1 Disease in Owl Monkeys, Marmosets and Tamarins

Lesions produced by spontaneous SaHV-1 infection in owl monkeys were well described by Hunt and Melendez in 1966 and by Emmons *et al.* in 1968 [32, 52]. Necrotizing ulcerative stomatitis that sometimes extended throughout the length of the esophagus was commonly observed [32, 52]. Microscopically, the oral and esophageal lesions consisted of zones of partial to complete necrosis with several multinucleate giant cells present. Inclusion bodies (described below) were present in many of the giant cells and epithelial cells [32, 52]. Intestinal lesions consisted of coagulative necrosis involving both the epithelium and its supporting tissues with intranuclear inclusions present in the remaining epithelial cells [52]. Similar multiple foci of necrosis were present in nasal mucosa[52], liver, spleen, and lymph nodes [32, 52]. In the skin, the entire epidermal layer was necrotic with a minimal number of neutrophils infiltrating the dermis and subcutis [52]. No nervous system lesions were reported by Hunt and Melendez [52]. However, in the owl monkey described by Emmons *et al.* [32], bilateral trigeminal ganglioneuritis with neuronal necrosis and intranuclear inclusions in neurons, satellite cells and Schwann cells was observed. In addition, a unilateral focus of acute inflammation with glial and neuronal necrosis and intranuclear inclusions was seen in the medulla oblongata adjacent to the sensory nucleus of the trigeminal nerve [32].

Lesions described in spontaneously infected marmosets and tamarins from which the virus was first isolated were similar to those observed in owl monkeys, consisting of multifocal necrosis in a variety of organs [45, 46]. Regarding lesions in the nervous system, Morita *et al.* [82] described severe degeneration and necrosis with intranuclear

inclusion bodies in ganglionic plexi of the digestive tract as well as sympathetic ganglia within the abdominal cavity. In 1963, prior to the isolation of SaHV-1, a case of “inclusion body hepatitis” was described in marmosets. Lesions included multiple sublobular foci of swollen or necrotic hepatocytes, some of which were multinucleated and contained intranuclear inclusion bodies. An attempt was made to demonstrate the presence of BV via intradermal and subcutaneous inoculation into rabbits, but no detectable clinical symptoms were noted [104]. No other virus isolation was attempted, but due to the similarity of the observed lesions in the marmoset, it seems likely that this was a case of SaHV-1 infection. In 1971, Murphy *et al.* [85] reported the isolation of SaHV-1 from throat swabs of an apparently healthy black-mantle tamarin (*S. nigricollis*), suggesting that a small proportion of tamarins survive infection with SaHV-1 and become asymptomatic carriers of the virus. It is possible that these animals serve as a reservoir for virus resulting in spontaneous outbreaks of disease in stabilized tamarin or marmoset colonies [85].

Experimentally infected tamarins (*S. nigricollis* and *S. oedipus*) invariably developed multiple foci of necrosis: the route of infection determined the distribution and severity of lesions in various organ systems. For example, intranasal infection resulted in extensive necrotizing pneumonia while animals fed by gavage exhibited multifocal necrosis of the small intestine [46]. Intradermal inoculation led to a hemorrhagic lesion at the injection site within two days that steadily enlarged until 4 and 7 days p.i., when the animals became weak and died. Extensive bilateral adrenal hemorrhage was present in the intradermally inoculated animals and was observed to a lesser extent in animals infected by other routes [46]. Following the identification of healthy tamarins (*S.*

nigricollis) carrying SaHV-1, experimental inoculations demonstrated a species difference in SaHV-1 susceptibility, with greater resistance to disease in black-chested mustached tamarins (*S. mystax*) than in black mantle tamarins (*S. nigricollis*)[85].

In an attempt to transmit the virus to marmoset monkeys via exposure to infected squirrel monkeys, two marmosets (species not reported) were caged for a period of thirty days with two squirrel monkeys from which virus had been isolated. At the end of the thirty days, neither marmoset exhibited detectable clinical signs or antibody production for SaHV-1. In another experiment, one marmoset was inoculated intradermally with SaHV-1 and kept in the same cage as another uninoculated marmoset. After seven days, the inoculated monkey became ill and died on the eighth day. The uninoculated marmoset developed oral lesions five days after the death of the first marmoset and died two days following the development of oral lesions. SaHV-1 was isolated from serum. This raises questions as to how the virus is transmitted and may suggest that larger quantities of virus are shed from infected aberrant hosts or perhaps readily infectious doses of virus are only shed from overtly diseased animals [22].

SaHV-1 in Infant Mice

To further characterize the pathogenicity of SaHV-1, rodent inoculation studies were performed. Intraperitoneal and intracerebral inoculation of infant mice has been reported to result in generalized disease and death in 3 to 5 days [22, 45, 56]. In infant mice inoculated intracerebrally, a severe meningoencephalomyelitis with numerous prominent intranuclear inclusion bodies in meningeal macrophages, ependymal cells, glial cells, and the choroid plexus was present 30 hours p.i. These mice exhibited multifocal coagulative

necrosis in the liver with intranuclear inclusion bodies in hepatocytes surrounding these foci. At 60 hours p.i., the hepatic lesions were more severe than at 30 hours, but the severity of the CNS lesions was not appreciably greater. Other organs affected included the lungs, spleen and thymus, which all exhibited the necrosis and inclusion bodies typical of herpesvirus infections. Infant mice inoculated intraperitoneally exhibited multifocal subcapsular necrosis and intranuclear inclusion bodies in the liver and spleen and other organs at 36 hours p.i., which progressed to massive coagulative necrosis in the spleen, liver, mediastinal lymph nodes, and thymus by 48 to 72 hours p.i. Mice infected intraperitoneally did not develop the CNS lesions observed in mice inoculated intracerebrally [56].

In the study of experimental infection of infant mice with SaHV-1 by Jones *et al.*, [56] direct fluorescent antibody staining was used to detect viral antigen in tissue sections. Specific fluorescence occurred in the cytoplasm of cells in the leptomeninges, choroid plexus and ependyma 24 hours after intracerebral inoculation. At 42 hours, specific fluorescence outside the CNS was seen in the liver, lungs, pancreas and spleen. Maximal intensity of antigen staining occurred at 42 and 48 hours, while maximal distribution of specific staining in different organs was observed at 48 and 60 hours. In mice inoculated intraperitoneally, specific fluorescence was visible in the cytoplasm of the cells in the mesentery, intestinal serosa, parietal peritoneum, and liver capsule at 24 hours p.i. At 48 hours, staining was observed in the lungs, pleura, mediastinal lymph nodes, thymus, and spinal meninges. Maximal intensity and distribution of specific staining occurred at 60 and 72 hours. The areas of specific fluorescence were associated with histologic lesions; in foci of extensive coagulative necrosis, fluorescence was

generally observed only at the periphery. This seems plausible, since the virus would already have been released from necrotic cells [56].

SaHV-1 in Other Species

As part of the initial description of SaHV-1, experimental inoculations of other mammalian species were performed to characterize the pathogenicity of the virus. In rabbits, adult mice, and guinea pigs, disease was similar between species for each route of inoculation. Intradermal inoculation of rabbits and guinea pigs resulted in local, ulcerative skin lesions that resolved without progression to systemic disease [22, 46]. Meningoencephalitis leading to death occurred in rabbits and adult mice following intracerebral inoculation [46]. Corneal infection of rabbits resulted in conjunctivitis that resolved with scarring and retraction of the inoculated eyeball [22]. No infection or disease was seen following intraperitoneal inoculation of rabbits, adult mice or guinea pigs [46].

Plaque assay studies of the SaHV-1 isolate acquired from latently infected squirrel monkeys [80] yielded a large plaque variant (LPV) and small plaque variant (SPV) of SaHV-1 [23]. Animal inoculation studies in rabbits, hamsters and mice demonstrated different pathogenicity between variant types. The LPV was always fatal in weaned and adult mice via IC route, had 70% mortality in weaned mice inoculated IM and 40% mortality via IP route in weaned mice [24]. Weaned and adult mice inoculated IM developed skin ulcers at the site of inoculation that healed by scarring in surviving mice [24]. In contrast, the SPV was fatal only to infant mice via IC inoculation and resulted in no disease in older groups by any inoculation route [24]. In hamsters, the

LVP given IC was lethal in infants and weaned animals but was not lethal by SC, IP or IM routes [24]. The SPV was lethal only in infant hamsters, with weaned animals surviving IC inoculation [24]. The LPV given to rabbits via corneal scarification resulted in acute conjunctivitis and keratitis that resolved in 3-4 weeks, depending on the dose of inoculum [24]. The SPV did not cause ocular lesions in rabbits, even with an 8-fold increase in inoculated dose [24]. No disease was induced by either variant in rabbits inoculated IP [24].

SaHV-1 as an animal model of human disease

Several years after the initial isolation and characterization of SaHV-1, researchers used various isolates of the virus for the study of herpesvirus encephalitis [66] as well as the study of latency and reactivation as a model of herpes zoster [53, 54, 70, 110]. These viruses were isolated from four temporally distinct outbreaks of fatal disease in owl monkeys between 1968 and 1971 [71] and were demonstrated to be similar to each other and to reference strains of SaHV-1 by growth kinetics, restriction endonuclease analysis, kinetic neutralization tests, and SDS-PAGE analysis of viral peptides [65]. The four isolates were shown to have variable virulence in rabbits when inoculated intradermally, ranging from rapidly fatal encephalitis associated with the KM91 strain [66] to localized skin lesions with ganglioneuritis, latency and experimentally induced reactivation following inoculation with isolate KM322 [53, 54, 70, 110].

Rabbits inoculated intradermally (in the flank) with the KM91 strain of SaHV-1 developed erythematous papules at the inoculation site 2-3 days p.i. which continued to enlarge until 4-6 days p.i. By 6-7 days p.i., animals became lethargic and developed head-swaying followed by flaccid posterior paralysis at 8-9 days p.i., and coma and death

by 10-14 days p.i. [66]. In this model, virus replicated in the inoculated skin, appeared in the ipsilateral DRG at day 5 p.i. and the contralateral DRG at day 8 p.i. By day 10, brainstem, cerebellum and cerebral hemispheres were infected [66]. Characterization of microscopic lesions was not the focus of these experiments, but pathologic changes were briefly described. Histopathologic lesions in these rabbits consisted of inflammation and neuronal destruction in DRGs serving the dermatomes of inoculated skin, inflammation and necrosis in spinal cord segments at the level of affected DRGs, and occasional focal microgliosis and perivascular cuffing in cerebral hemispheres [66].

Intradermal inoculation of rabbits with KM322 resulted in the development of an erythematous papule at the site of inoculation by day 2 p.i. that progressed to central necrosis by day 4 and healed by 14 days p.i. [110]. Ganglioneuritis, evidenced by severe local irritation in the region of the visibly unchanged skin lesion at the inoculation site, occurred at 5-6 days p.i. and progressed by 6-8 days to loss of sensation in skin adjacent to the lesion and extending to involve the entire dermatome [110]. Brief descriptions of histologic lesions include foci of necrosis with mixed neutrophilic and mononuclear inflammation of the inoculated skin and edema and neuronal destruction in DRGs accompanied by mixed inflammatory infiltrate [110]. Virus isolation was demonstrated from skin and DRG within the first week, and then only via DRG culture for up to 550 days [110]. Recovery of virus only from regional DRGs demonstrated limited spread of virus up and down the cord and ganglion chain or to ganglia of the contralateral side [110]. Reactivation of virus in latently infected rabbits was achieved by subcutaneous cortisone injection after intervals of a few weeks to 2 years following recovery from primary skin lesions [70].

In 1990 Illanes *et al.* reported detailed light and electron microscopic and morphometric studies on cutaneous spinal nerves of rabbits intradermally inoculated with isolate KM322 of SaHV-1 to provide insight into the pathology of herpetic neuropathy [53, 54]. Light microscopy of lateral cutaneous branches of spinal nerves in rabbits 17-45 days p.i. revealed reduced density of myelinated fibers and Schwann cell proliferation with fiber degeneration, foamy macrophages and myelin debris [54]. Reduction in the density of myelinated and unmyelinated fibers was clearly evident at 45 days p.i. via electron microscopy with a high proportion of regenerating axons composed of unmyelinated fibers [54]. By two years p.i., a marked reduction in the density of unmyelinated axons was evident [54], and in morphometric studies, the reductions in total number per nerve and density estimates of unmyelinated fibers were shown to be statistically highly significant, suggesting unmyelinated axons are more severely affected in cutaneous infection with SaHV-1 [53].

Relatedness of SaHV-1 to other alphaherpesviruses

Characterization of SaHV-1 confirms antigenic and genetic relatedness to HSV [4, 26] as well as other primate alphaherpesviruses, including BV, SA8 and AtHV-1 [27, 28, 44]. Virion DNA of SaHV-1 cross-hybridized with virion DNA of HSV-1 by approximately 16% [26]. Using similar methods, DNAs of HSV-1 and HSV-2 cross-hybridize by approximately 60% and SA8 DNA cross-hybridizes with HSV-1 DNA by 31% [26]. In addition to genetic cross-hybridization described above, slight cross-reactivity of antigenic proteins was detected between HSV-1 and SaHV-1 by cross-neutralization tests [4] and immunoprecipitation [26, 27, 44]. Shared antigenic determinants have been

demonstrated among several primate alphaherpesviruses, including HSV-1, HSV-2, SA8, BV, SaHV-1 and AtHV-1 [27, 44]. Analysis of viral polypeptide cross-reactivity and genome cross-hybridization reveal that HSV-1, HSV-2, SA8 and BV are antigenically and genetically closely related [27, 44]. SaHV-1 and AtHV-1, both platyrrhine monkey viruses, are closely related to each other and are more distantly related to human and catarrhine monkey viruses [27, 44].

Biological properties of SaHV-1 have several similarities with those of other alphaherpesviruses. SaHV-1 replicates rapidly and efficiently in tissue culture, releasing free infectious virions at a rate similar to HSV-1 and SA8 [84]. In infected cells, SaHV-1 rapidly shuts off host cell protein synthesis and induces the production of viral proteins in a kinetically regulated manner [84]. Similar to other alphaherpesviruses, SaHV-1 infection of cells results in the production of over 30 virus-specific polypeptides [84]. The amino acid sequence of gB, a glycoprotein that has been shown to be highly conserved among herpesviruses, demonstrates sub-grouping of primate alphaherpesviruses distinct from other alphaherpesviruses [28]. Alignment of the gB glycoprotein sequences of primate alphaherpesviruses identifies conserved regions that probably impart similar structural features, as well as divergent regions to which most of the non-conserved amino acid substitutions can be localized [28]. Much like broader antigenic and genetic comparisons, sequence analysis and complementation studies of gB reveal further division of the primate alphaherpesviruses into platyrrhine primate viruses (SaHV-1, AtHV-1) and catarrhine primate viruses (HSV-1, HSV-2, SA8, BV) [28, 30].

Summary of Background Significance

As a whole, antigenic, genetic and biological characterizations of SaHV-1 support the likelihood that SaHV-1 is to squirrel monkeys the viral equivalent of HSV to humans. Numerous similarities to HSV and an analogous host relationship to a commonly used laboratory species make SaHV-1 a suitable virus for the study of a primate alphaherpesvirus pathogenesis. Viral pathogenesis studies in both experimental rodent hosts and the natural primate host would be useful in elucidating details of alphaherpesvirus neurovirulence and could prove valuable in comparative studies of viruses such as HSV or BV, where experimental inoculation of natural hosts is either not possible or creates great risk to researchers and animal handlers. In addition, trans-species transmission of SaHV-1 commonly results in fatal disease in marmosets, a primate species that also succumbs to BV infection. While the disease manifestations of the two viruses differ, link of a common susceptible primate host lends importance to the use of SaHV-1 as a comparative model for the investigation of more significant alphaherpesviruses.

References

1. Anonymous (1973) Editorial: Provisional labels for herpesviruses. *J Gen Virol* 20: 417-419
2. Bak IJ, Markham CH, Cook ML, Stevens JG (1977) Intraaxonal transport of Herpes simplex virus in the rat central nervous system. *Brain Res* 136: 415-429
3. Benson PM, Malane SL, Banks R, Hicks CB, Hilliard J (1989) B virus (*Herpesvirus simiae*) and human infection. *Arch Dermatol* 125: 1247-1248
4. Blue WT, Plummer G (1973) Antigenic relationships among four herpesviruses. *Infect Immun* 7: 1000-1002
5. Brack M (1977) Morphological and Epidemiological Aspects of Simian Herpesvirus Infections. Verlag Paul Parey, Berlin & Hamburg
6. Broseta E, Osca JM, Morera J, Martinez-Agullo E, Jimenez-Cruz JF (1993) Urological manifestations of herpes zoster. *Eur Urol* 24: 244-247
7. Card JP, Rinaman L, Schwaber JS, Miselis RR, Whealy ME, Robbins AK, Enquist LW (1990) Neurotropic properties of pseudorabies virus: uptake and transneuronal passage in the rat central nervous system. *J Neurosci* 10: 1974-1994
8. Card JP, Whealy ME, Robbins AK, Moore RY, Enquist LW (1991) Two alpha-herpesvirus strains are transported differentially in the rodent visual system. *Neuron* 6: 957-969
9. Card JP, Rinaman L, Lynn RB, Lee BH, Meade RP, Miselis RR, Enquist LW (1993) Pseudorabies virus infection of the rat central nervous system: ultrastructural characterization of viral replication, transport, and pathogenesis. *J Neurosci* 13: 2515-2539
10. Card JP, Enquist LW (1995) Neurovirulence of pseudorabies virus. *Crit Rev Neurobiol* 9: 137-162

11. Card JP (1998) Practical considerations for the use of pseudorabies virus in transneuronal studies of neural circuitry. *Neurosci Biobehav Rev* 22: 685-694
12. Carter SR, Pereira L, Paz P, LaVail JH (1992) A quantitative assay of retrograde transported HSV in the trigeminal ganglion. *Invest Ophthalmol Vis Sci* 33: 1934-1939
13. Center for Disease Control., Centers for Disease Control (U.S.), Centers for Disease Control and Prevention (U.S.) (1987) Morbidity and mortality weekly report : MMWR Epidemiologic notes and reports: B virus infection in humans-Pensacola, Florida. U.S. Dept. of Health Education and Welfare Public Health Service Center for Disease Control, Atlanta, Ga., vol 36, pp 289-290,295-296
14. Center for Disease Control., Centers for Disease Control (U.S.), Centers for Disease Control and Prevention (U.S.) (1987) Morbidity and mortality weekly report : MMWR Guidelines for prevention of Herpesvirus simiae (B virus) infection in monkey handlers. U.S. Dept. of Health Education and Welfare Public Health Service Center for Disease Control, Atlanta, Ga., vol 36, pp 680-682,687-689
15. Center for Disease Control., Centers for Disease Control (U.S.), Centers for Disease Control and Prevention (U.S.) (1989) Morbidity and mortality weekly report : MMWR Epidemiologic notes and reports: B virus infection in humans-Michigan. U.S. Dept. of Health Education and Welfare Public Health Service Center for Disease Control, Atlanta, Ga., vol 38, pp 453-454
16. Center for Disease Control., Centers for Disease Control (U.S.), Centers for Disease Control and Prevention (U.S.) (1998) Morbidity and mortality weekly report : MMWR Fatal Cercopithecine herpesvirus 1 (B virus) infection following a mucocutaneous exposure and interim recommendations for worker protection. U.S. Dept. of Health Education and Welfare Public Health Service Center for Disease Control, Atlanta, Ga., vol 47, pp 1073-1076,1083
17. Chen PH, Hsueh HF, Hong CZ (2002) Herpes zoster-associated voiding dysfunction: a retrospective study and literature review. *Arch Phys Med Rehabil* 83: 1624-1628
18. Constantian HM (1969) Herpes zoster causing bladder atony. *J Urol* 102: 689-692
19. Cook ML, Stevens JG (1973) Pathogenesis of herpetic neuritis and ganglionitis in mice: evidence for intra-axonal transport of infection. *Infect Immun* 7: 272-288

20. Corey L, Spear PG (1986) Infections with herpes simplex viruses (1). *N Engl J Med* 314: 686-691
21. Craig CP, Nahmias AJ (1973) Different patterns of neurologic involvement with herpes simplex virus types 1 and 2: isolation of herpes simplex virus type 2 from the buffy coat of two adults with meningitis. *J Infect Dis* 127: 365-372
22. Daniel MD, Karpas A, Melendez LV, King NW, Hunt RD (1967) Isolation of herpes-T virus from a spontaneous disease in squirrel monkeys (*Saimiri sciureus*). *Arch Gesamte Virusforsch* 22: 324-331
23. Daniel MD, Melendez LV (1968) Herpes T virus variants. Isolation and characterization. *Arch Gesamte Virusforsch* 25: 18-29
24. Daniel MD, Melendez LV (1970) Pathogenicity studies in rabbits, hamsters, mice and embryonated eggs with herpes T virus variants. *Arch Gesamte Virusforsch* 32: 45-52
25. DeHertogh DA, Brettman LR (1988) Hemorrhagic cystitis due to herpes simplex virus as a marker of disseminated herpes infection. *Am J Med* 84: 632-635
26. Desrosiers RC, Falk LA, Jr. (1981) Herpesvirus tamarinus and its relation to herpes simplex virus. *J Gen Virol* 56: 119-130
27. Eberle R, Black D, Hilliard JK (1989) Relatedness of glycoproteins expressed on the surface of simian herpes-virus virions and infected cells to specific HSV glycoproteins. *Arch Virol* 109: 233-252
28. Eberle R, Black D (1993) Sequence analysis of herpes simplex virus gB gene homologs of two platyrrhine monkey alpha-herpesviruses. *Arch Virol* 129: 167-182
29. Eberle R, Hilliard J (1995) The simian herpesviruses. *Infect Agents Dis* 4: 55-70
30. Eberle R, Tanamachi B, Black D, Blewett EL, Ali M, Openshaw H, Cantin EM (1997) Genetic and functional complementation of the HSV1 UL27 gene and gB glycoprotein by simian alpha-herpesvirus homologs. *Arch Virol* 142: 721-736

31. Elliott KJ (1994) Other neurological complications of herpes zoster and their management. *Ann Neurol* 35 Suppl: S57-61
32. Emmons RW, Gribble DH, Lennette EH (1968) Natural fatal infection of an owl monkey (*Aotus trivirgatus*) with Herpes T virus. *J Infect Dis* 118: 153-159
33. Engel JP, Madigan TC, Peterson GM (1997) The transneuronal spread phenotype of herpes simplex virus type 1 infection of the mouse hind footpad. *J Virol* 71: 2425-2435
34. Enquist LW, Husak PJ, Banfield BW, Smith GA (1998) Infection and spread of alphaherpesviruses in the nervous system. *Adv Virus Res* 51: 237-347
35. Gay FP, Holden M (1933) The herpes encephalitis problem, II. *J Infect Dis* 53: 287-303
36. Gerber SI, Cromie WJ (1996) Herpes simplex virus type 2 infection associated with urinary retention in the absence of genital lesions. *J Pediatr* 128: 250-251
37. Gesser RM, Valyi-Nagy T, Altschuler SM, Fraser NW (1994) Oral-oesophageal inoculation of mice with herpes simplex virus type 1 causes latent infection of the vagal sensory ganglia (nodose ganglia). *J Gen Virol* 75 (Pt 9): 2379-86
38. Gesser RM, Valyi-Nagy T, Fraser NW, Altschuler SM (1995) Oral inoculation of SCID mice with an attenuated herpes simplex virus-1 strain causes persistent enteric nervous system infection and gastric ulcers without direct mucosal infection. *Lab Invest* 73: 880-9
39. Gesser RM, Koo SC (1996) Oral inoculation with herpes simplex virus type 1 infects enteric neuron and mucosal nerve fibers within the gastrointestinal tract in mice. *J Virol* 70: 4097-4102
40. Goel N, Mao H, Rong Q, Docherty JJ, Zimmerman D, Rosenthal KS (2002) The ability of an HSV strain to initiate zosteriform spread correlates with its neuroinvasive disease potential. *Arch Virol* 147: 763-773
41. Goodpasture EW, Teague O (1923) Transmission of the virus of herpes febrilis along nerves in experimentally infected rabbits. *Journal of medical research* 44: 139-184

42. Greenstein A, Matzkin H, Kaver I, Braf Z (1988) Acute urinary retention in herpes genitalis infection. Urodynamic evaluation. *Urology* 31: 453-456
43. Herbaut AG, Nogueira MC, Wespes E (1990) Urinary retention due to sacral myeloradiculitis: a clinical and neurophysiological study. *J Urol* 144: 1206-1208
44. Hilliard JK, Black D, Eberle R (1989) Simian alphaherpesviruses and their relation to the human herpes simplex viruses. *Arch Virol* 109: 83-102
45. Holmes AW, Dedmon RE, Deinhardt F (1963) Isolation of a new herpes-like virus from south american marmosets. *Federation Proceedings* 22: 324
46. Holmes AW, Caldwell RG, Dedmon RE, Deinhardt F (1964) Isolation and characterization of a new herpes virus. *J Immunol* 92: 602-610
47. Holmes AW, Devine JA, Nowakowski E, Deinhardt F (1966) The epidemiology of a herpes virus infection of New World monkeys. *J Immunol* 96: 668-671
48. Holmes GP, Hilliard JK, Klontz KC, Rupert AH, Schindler CM, Parrish E, Griffin DG, Ward GS, Bernstein ND, Bean TW, et al. (1990) B virus (*Herpesvirus simiae*) infection in humans: epidemiologic investigation of a cluster. *Ann Intern Med* 112: 833-839
49. Holmes GP, Chapman LE, Stewart JA, Straus SE, Hilliard JK, Davenport DS (1995) Guidelines for the prevention and treatment of B-virus infections in exposed persons. The B virus Working Group. *Clin Infect Dis* 20: 421-439
50. Huard J, Feero WG, Watkins SC, Hoffman EP, Rosenblatt DJ, Glorioso JC (1996) The basal lamina is a physical barrier to herpes simplex virus-mediated gene delivery to mature muscle fibers. *J Virol* 70: 8117-8123
51. Hull RN (1973) The simian herpesviruses. In: Kaplan AS (ed) *The herpesviruses*. Academic Press, New York, pp 389-425
52. Hunt RD, Melendez LV (1966) Spontaneous herpes-T infection in the owl monkey (*Aotus trivirgatus*). *Pathol Vet* 3: 1-26

53. Illanes O, Mossman S, McCarthy K (1990) Alphaherpesvirus saimiri infection in rabbits. 2. Morphometric studies of cutaneous spinal nerves. *Acta Neuropathol (Berl)* 79: 558-565
54. Illanes O, Mossman S, McCarthy K (1990) Alphaherpesvirus saimiri infection in rabbits. 1. Light and electron microscopy study of cutaneous spinal nerves. *Acta Neuropathol (Berl)* 79: 551-557
55. International Committee on Taxonomy of Viruses., Van Regenmortel MHV, Fauquet CM, Bishop DHL, International Union of Microbiological Societies. Virology Division. (2000) Virus taxonomy : classification and nomenclature of viruses : seventh report of the International Committee on Taxonomy of Viruses. Academic Press, San Diego
56. Jones SR, Stair EL, Gleiser CA, Bridges CH (1971) Histopathologic changes and specific immunofluorescence in infant mice infected with *Herpesvirus tamarinus*. *Am J Vet Res* 32: 1143-1153
57. Kinchington PR (1999) Latency of varicella zoster virus; a persistently perplexing state. *Front Biosci* 4: 200-211
58. King NW, Hunt RD, Daniel MD, Melendez LV (1967) Overt herpes-T infection in squirrel monkeys (*Saimiri sciureus*). *Lab Anim Care* 17: 413-423
59. Krinke GJ, Dietrich FM (1990) Transneuronal spread of intraperitoneally administered herpes simplex virus type 1 from the abdomen via the vagus nerve to the brains of mice. *J Comp Pathol* 103: 301-306
60. Kristensson K (1970) Morphological studies of the neural spread of herpes simplex virus to the central nervous system. *Acta Neuropathol (Berl)* 16: 54-63
61. Kristensson K, Ghetti B, Wisniewski HM (1974) Study on the propagation of Herpes simplex virus (type 2) into the brain after intraocular injection. *Brain Res* 69: 189-201
62. Kristensson K, Nennesmo L, Persson L, Lycke E (1982) Neuron to neuron transmission of herpes simplex virus. Transport of virus from skin to brainstem nuclei. *J Neurol Sci* 54: 149-156

63. Kuypers HG, Ugolini G (1990) Viruses as transneuronal tracers. *Trends Neurosci* 13: 71-75
64. LaVail JH, Johnson WE, Spencer LC (1993) Immunohistochemical identification of trigeminal ganglion neurons that innervate the mouse cornea: relevance to intercellular spread of herpes simplex virus. *J Comp Neurol* 327: 133-140
65. Leib DA, Hart CA, McCarthy K (1987) Characterization of four herpesviruses isolated from owl monkeys and their comparison with Herpesvirus saimiri type 1 (*Herpesvirus tamarinus*) and herpes simplex virus type 1. *J Comp Pathol* 97: 159-169
66. Leib DA, Hart CA, McCarthy K (1988) Alphaherpesvirus saimiri in rabbits: a model for human encephalitis? *J Gen Virol* 69 (Pt 7): 1609-1615
67. Love FM, Jungherr E (1962) Occupational infection with virus B of monkeys. *Jama* 179: 804-806
68. Margolis TP, Dawson CR, LaVail JH (1992) Herpes simplex viral infection of the mouse trigeminal ganglion. Immunohistochemical analysis of cell populations. *Invest Ophthalmol Vis Sci* 33: 259-267
69. Martin X, Dolivo M (1983) Neuronal and transneuronal tracing in the trigeminal system of the rat using the herpes virus suis. *Brain Res* 273: 253-276
70. McCarthy K, Tosolini FA (1975) Hazards from simian herpes viruses: reactivation of skin lesions with virus shedding. *Lancet* 1: 649-650
71. McCarthy K, Tosolini FA (1975) A review of primate herpes viruses. *Proc R Soc Med* 68: 145-150
72. McClanahan C, Grimes MM, Callaghan E, Stewart J (1994) Hemorrhagic cystitis associated with herpes simplex virus. *J Urol* 151: 152-153
73. McGeoch DJ (1989) The genomes of the human herpesviruses: contents, relationships, and evolution. *Annu Rev Microbiol* 43: 235-265

74. McGeoch DJ, Cook S (1994) Molecular phylogeny of the alphaherpesvirinae subfamily and a proposed evolutionary timescale. *J Mol Biol* 238: 9-22
75. McGeoch DJ, Cook S, Dolan A, Jamieson FE, Telford EA (1995) Molecular phylogeny and evolutionary timescale for the family of mammalian herpesviruses. *J Mol Biol* 247: 443-458
76. McGeoch DJ, Davison AJ (1999) The molecular and evolutionary history of the herpesviruses. In: Webster RG (ed) *Origin and evolution of viruses*. Academic Press, San Diego, Calif., pp 441-446
77. McGeoch DJ, Dolan A, Ralph AC (2000) Toward a comprehensive phylogeny for mammalian and avian herpesviruses. *J Virol* 74: 10401-6
78. McLean JH, Shipley MT, Bernstein DI (1989) Golgi-like, transneuronal retrograde labelling with CNS injections of herpes simplex virus type 1. *Brain Res Bull* 22: 867-881
79. McSorley J, Shapiro L, Brownstein MH, Hsu KC (1974) Herpes simplex and varicella-zoster: comparative histopathology of 77 cases. *Int J Dermatol* 13: 69-75
80. Melendez LV, Hunt RD, Garcia FG, Trum BF (1966) A latent herpes-T infection in *Saimiri sciureus* (squirrel monkey). In: Fiennes RNT-W (ed) *Some Recent Developments in Comparative Medicine*. Academic Press, New York & London, pp 393-397
81. Melnick JL, Midulla M, Wimberly I, Barrera-Oro JG, Levy BM (1964) A new member of the herpesvirus group isolated from South American marmosets. *J Immunol* 92: 596-601
82. Morita M, Iida T, Tsuchiya Y, Aoyama Y (1979) Fatal herpesvirus tamarinus infection in cotton-topped marmosets (*Saguinus oedipus*). *Jikken Dobutsu* 28: 537-550
83. Moriyama K, Imayama S, Mohri S, Kurata T, Mori R (1992) Localization of herpes simplex virus type 1 in sebaceous glands of mice. *Arch Virol* 123: 13-27
84. Mou SW, Hilliard JK, Song CH, Eberle R (1986) Comparison of the primate alphaherpesviruses. I. Characterization of two herpesviruses from spider monkeys

and squirrel monkeys and viral polypeptides synthesized in infected cells. Arch Virol 91: 117-133

85. Murphy BL, Maynard JE, Krushak DH, Fields RM (1971) Occurrence of a carrier state for Herpesvirus tamarinus in marmosets. Appl Microbiol 21: 50-52
86. Nakajima H, Furutama D, Kimura F, Shinoda K, Ohsawa N, Nakagawa T, Shimizu A, Shoji H (1998) Herpes simplex virus myelitis: clinical manifestations and diagnosis by the polymerase chain reaction method. Eur Neurol 39: 163-167
87. Nguyen ML, Borochovit D, Thomas G, McClure T, Ruben FL (1992) Hemorrhagic cystitis with herpes simplex virus type 2 in the bladder mucosa. Clin Infect Dis 14: 767-768
88. Norgren RB, Jr., Lehman MN (1989) Retrograde transneuronal transport of herpes simplex virus in the retina after injection in the superior colliculus, hypothalamus and optic chiasm. Brain Res 479: 374-378
89. Norgren RB, Jr., Lehman MN (1998) Herpes simplex virus as a transneuronal tracer. Neurosci Biobehav Rev 22: 695-708
90. Oates JK, Greenhouse PR (1978) Retention of urine in anogenital herpetic infection. Lancet 1: 691-692
91. Olson LC, Buescher EL, Artenstein MS, Parkman PD (1967) Herpesvirus infections of the human central nervous system. N Engl J Med 277: 1271-1277
92. Ostrowski SR, Leslie MJ, Parrott T, Abelt S, Piercy PE (1998) B-virus from pet macaque monkeys: an emerging threat in the United States? Emerg Infect Dis 4: 117-121
93. Palmer AE (1987) B virus, *Herpesvirus simiae*: historical perspective. J Med Primatol 16: 99-130
94. Richmond W (1974) The genito-urinary manifestations of herpes zoster. Three case reports and a review of the literature. Br J Urol 46: 193-200

95. Roizman B (1979) The structure and isomerization of herpes simplex virus genomes. *Cell* 16: 481-494
96. Roizman B, Baines J (1991) The diversity and unity of *Herpesviridae*. *Comp Immunol Microbiol Infect Dis* 14: 63-79
97. Roizman B, Knipe DM (2001) Herpes simplex viruses and their replication. In: Fields BN, Knipe DM, Howley PM and Griffin DE (eds) *Fields Virology*. Lippincott Williams & Wilkins, Philadelphia, vol 2, pp 2399-2459
98. Roizman B, Pellet PE (2001) The Family *Herpesviridae*: A Brief Introduction. In: Fields BN, Knipe DM, Howley PM and Griffin DE (eds) *Fields Virology*. Lippincott Williams & Wilkins, Philadelphia, vol 2, pp 2381-2397
99. Roizmann B, Desrosiers RC, Fleckenstein B, Lopez C, Minson AC, Studdert MJ (1992) The family *Herpesviridae*: an update. The Herpesvirus Study Group of the International Committee on Taxonomy of Viruses. *Arch Virol* 123: 425-449
100. Rouiller EM, Capt M, Dolivo M, De Ribaupierre F (1989) Neuronal organization of the stapedius reflex pathways in the rat: a retrograde HRP and viral transneuronal tracing study. *Brain Res* 476: 21-28
101. Sabin AB, Wright AM (1934) Acute ascending myelitis following a monkey bite, with the isolation of a virus capable of reproducing the disease. *J Exp Med* 59: 115-136
102. Sakakibara R, Hattori T, Fukutake T, Mori M, Yamanishi T, Yasuda K (1998) Micturitional disturbance in herpetic brainstem encephalitis; contribution of the pontine micturition centre. *J Neurol Neurosurg Psychiatry* 64: 269-272
103. Sams JM, Jansen AS, Mettenleiter TC, Loewy AD (1995) Pseudorabies virus mutants as transneuronal markers. *Brain Res* 687: 182-190
104. Sauer RM, Bishop RW (1963) Inclusion body hepatitis in marmosets. *Lab Anim Care* 13: 790-792
105. Schrier A (1966) Editor's notes. *Laboratory Primate Newsletter* 5: ii

106. Simmons A, Nash AA (1984) Zosteriform spread of herpes simplex virus as a model of recrudescence and its use to investigate the role of immune cells in prevention of recurrent disease. *J Virol* 52: 816-821
107. Steinberg J, Rukstalis DB, Vickers MA, Jr. (1991) Acute urinary retention secondary to Herpes simplex meningitis. *J Urol* 145: 359-360
108. Sydiskis RJ, Schultz I (1965) Herpes simplex skin infection in mice. *J Infect Dis* 115: 237-246
109. Thompson SA, Hilliard JK, Kittel D, Lipper S, Giddens WE, Jr., Black DH, Eberle R (2000) Retrospective analysis of an outbreak of B virus infection in a colony of DeBrazza's monkeys (*Cercopithecus neglectus*). *Comp Med* 50: 649-657
110. Tosolini FA, McCarthy K, Baker BF (1982) Studies of herpes virus latency in the sensory spinal ganglia of rabbits. *J Hyg (Lond)* 89: 421-437
111. Ugolini G, Kuypers HG, Simmons A (1987) Retrograde transneuronal transfer of herpes simplex virus type 1 (HSV 1) from motoneurons. *Brain Res* 422: 242-256
112. Ugolini G, Kuypers HG, Strick PL (1989) Transneuronal transfer of herpes virus from peripheral nerves to cortex and brainstem. *Science* 243: 89-91
113. Ugolini G (1992) Transneuronal transfer of herpes simplex virus type 1 (HSV 1) from mixed limb nerves to the CNS. I. Sequence of transfer from sensory, motor, and sympathetic nerve fibres to the spinal cord. *J Comp Neurol* 326: 527-548
114. Vahlne A, Nystrom B, Sandberg M, Hamberger A, Lycke E (1978) Attachment of herpes simplex virus to neurons and glial cells. *J Gen Virol* 40: 359-371
115. Vahlne A, Svennerholm B, Sandberg M, Hamberger A, Lycke E (1980) Differences in attachment between herpes simplex type 1 and type 2 viruses to neurons and glial cells. *Infect Immun* 28: 675-680
116. Weeks BS, Ramchandran RS, Hopkins JJ, Friedman HM (2000) Herpes simplex virus type-1 and -2 pathogenesis is restricted by the epidermal basement membrane. *Arch Virol* 145: 385-396

117. Weigler BJ, Roberts JA, Hird DW, Lerche NW, Hilliard JK (1990) A cross sectional survey for B virus antibody in a colony of group housed rhesus macaques. *Lab Anim Sci* 40: 257-261
118. Weigler BJ (1992) Biology of B virus in macaque and human hosts: a review. *Clin Infect Dis* 14: 555-567
119. Wharton SB, Meyers NL, Nash AA (1995) Experimental herpes simplex virus type 1 (HSV-1) infection of the spinal cord and dorsal root ganglia. *Neuropathol Appl Neurobiol* 21: 228-237
120. Whitley RJ (1996) Herpes Simplex Viruses. In: Fields BN, Knipe DM and Howley PM (eds) *Fields Virology*. Lippincott-Raven Publishers, Philadelphia, vol 2, pp 2297-2342
121. Whitley RJ, Hilliard JK (2001) *Cercopithecine herpesvirus* (B Virus). In: Fields BN, Knipe DM, Howley PM and Griffin DE (eds) *Fields Virology*. Lippincott Williams & Wilkins, Philadelphia, vol 2, pp 2835-2848
122. Yamanishi T, Yasuda K, Sakakibara R, Hattori T, Uchiyama T, Minamide M, Ito H (1998) Urinary retention due to herpes virus infections. *Neurourol Urodyn* 17: 613-619
123. Zwartouw HT, Boulter EA (1984) Excretion of B virus in monkeys and evidence of genital infection. *Lab Anim* 18: 65-70
124. Zwartouw HT, MacArthur JA, Boulter EA, Seamer JH, Marston JH, Chamove AS (1984) Transmission of B virus infection between monkeys especially in relation to breeding colonies. *Lab Anim* 18: 125-130
125. Zwartouw HT, Humphreys CR, Collins P (1989) Oral chemotherapy of fatal B virus (*herpesvirus simiae*) infection. *Antiviral Res* 11: 275-283

CHAPTER III

CHARACTERIZATION OF GROSS AND HISTOLOGICAL LESIONS IN BALB/C MICE EXPERIMENTALLY INFECTED WITH *Saimiriine herpesvirus 1* (SaHV-1)

Summary

Accidental B virus (*Herpesvirus simiae*) infection of human beings working with macaques is frequently fatal. However, the pathogenic potential of other similar simian alphaherpesviruses, such as the squirrel monkey virus *Saimiriine herpesvirus* (SaHV-1), is virtually unknown. As part of an effort to develop a murine model for infections with these agents, Balb/c mice were inoculated intramuscularly in the left hindlimb with 10 to 10⁶ plaque forming units (PFU) of SaHV-1. After observation for clinical signs of infection for 21 days, mice were killed and specimens collected for serology and histopathology. Mice receiving 10³ PFU or greater of SaHV-1 exhibited severe, pruritic, ulcerative skin lesions near the site of inoculation and developed unilateral or bilateral hindlimb paralysis with severe muscle atrophy. Histological lesions were characterized by a necrotizing dermatitis and folliculitis. Spinal cord lesions consisted of a non-suppurative myelitis affecting primarily the ipsilateral dorsal horn of the thoracolumbar spinal cord with occasional extension to ventral and contralateral spinal cord regions. Immunohistochemical labelling confirmed the presence of viral antigen within the lesions, and anti-SaHV-1 IgG concentrations were related to the occurrence of disease.

SaHV-1 infection in some mice extended from the ipsilateral dorsal horn and funiculus into the ventral and contralateral grey and white matter, resulting in bilateral hindlimb paralysis. Thoracolumbar spinal cord lesions resolved without continued spread of the virus to cranial nervous system structures, i.e., cervical spinal cord and brain.

Introduction

Non-human primates are invaluable in many biomedical research programmes. Their anatomical, biochemical and physiological similarities to man make them excellent laboratory models for the investigation of some human diseases. However, these same similarities led to the risk of transfer of simian infections to animal attendants and research workers. Alphaherpesviruses are widespread among primates and are well known for interspecies transmissibility, often resulting in severe or fatal disease (Brack, 1977; Eberle and Hilliard, 1995). *Cercopithecine herpesvirus 1* or B virus of macaques is enzootic in monkeys of the genus *Macaca*, in which it seldom results in overt disease. When disease is evident, it usually consists of ulcerative or vesicular lesions of the oral and pharyngeal mucosa. Only in rare cases has systemic disease in macaques been reported (Weigler, 1992). The mild disease associated with B virus in the natural host contrasts with the severe and often fatal disease that occurs in other species, in which it readily invades the central nervous system (CNS) (Palmer, 1987; Weigler, 1992).

Saimiriine herpesvirus 1 (SaHV-1), an alphaherpesvirus related to B virus, is enzootic in squirrel monkey populations. Natural infection is typically symptomless or causes only mild disease characterized by ulcerative lesions of the oral mucosa, similar to those seen in macaques infected with B virus (Daniel *et al.*, 1969). SaHV-1 was

originally isolated from marmosets suffering severe, fatal infection (Holmes *et al.*, 1963, 1964; Melnick *et al.*, 1964). Disease associated with SaHV-1 infection in marmosets and owl monkeys was characterized by disseminated multifocal necrosis throughout visceral organs and occasional foci of necrosis within the CNS (Holmes *et al.*, 1963, 1964; Hunt and Melendez, 1966; Emmons *et al.*, 1968). Subsequent seroepidemiological studies indicated that squirrel monkeys are the natural reservoir for SaHV-1 (Holmes *et al.*, 1964). SaHV-1 has not been reported to cause disease in man; however, its pathogenicity has been only minimally investigated and, as a primate virus, it would seem to present a potential risk of cross-species infection.

In view of the close genetic relationship of monkey B virus to other simian alphaherpesviruses, such as SaHV-1, *Herpesvirus papio 2* (HVP2), and Simian agent 8 (SA8), the question arises as to why there is so much variation in the pathogenic properties of these agents. The establishment of a small animal model system would provide a “comparative pathology” approach to examining the neurovirulence of these simian viruses. In this study, adult mice were infected with SaHV-1 to investigate the possibility of establishing such a model in this species. This report describes the gross and histological lesions seen in mice after SaHV-1 infection and establishes a baseline for more sophisticated studies to investigate the role of viral and host determinants in the pathogenesis of simian alphaherpesvirus infections.

Materials and Methods

Virus, Cells and Antigen

The MV-5-4 strain of SaHV-1 was used for all experiments (Mou *et al.*, 1986). The virus was propagated in Vero cells grown in Dulbecco's modified Eagle medium (DMEM) containing fetal bovine serum (FBS) 10%, 200mM L-glutamine, penicillin 100 IU/ml and streptomycin 100 µg/ml. Viral stocks were prepared by infecting subconfluent Vero cell monolayers with SaHV-1 at a low multiplicity of infection (<0.01). Infected cell cultures were maintained at 37°C in DMEM supplemented with FBS 2% until a cytopathogenic effect (CPE) had spread throughout the entire monolayer. The culture flasks were freeze-thawed three times, and the contents pooled and centrifuged for 5 minutes at 1000 g to remove cell debris. The supernate was collected, titrated by standard methods, dispensed in small volumes and stored at -70°C.

To serve as ELISA antigen, pelleted cell debris was resuspended in 0.5% TX-100 (Biorad Laboratories, Richmond, California, USA) at a concentration of 10^7 cells/ml, incubated on ice for 15 min with occasional mixing, centrifuged at 14,000 g for 15 min and the supernate dispensed in small volumes and stored at -70°F (Ohsawa *et al.*, 1999). Uninfected cell cultures were prepared in the same manner for use as a negative control antigen.

Animals

Specific pathogen-free female Balb/c mice (The Jackson Laboratory, Bar Harbor, Maine, USA), aged four-weeks and weighing 14-16 g, were randomly divided into six groups of

eight animals, each group being housed in two cages (four mice per cage). Two mice served as controls. Animals were housed in an isolation rack in a biosafety level three (BSL3) facility and given unlimited access to food and water.

Mice were first anaesthetized by Metofane[®] (Schering-Plough Animal Health Corp., Union, New Jersey, USA) inhalation. After clipping the hair from the posterior aspect of the left thigh, the mice were inoculated intramuscularly in the semimembranosus/semitendinosus muscle group. Each animal received 20 µl of SaHV-1 viral stock diluted in phosphate-buffered saline (PBS) to contain 10^1 , 10^2 , 10^3 , 10^4 , 10^5 or 10^6 plaque-forming units (PFU), depending upon the group. Control mice (n=2) received 20 µl of PBS. Mice were observed twice daily for clinical signs of disease, and any markedly weak, depressed or moribund animals were killed by cardiac exsanguination after deep anaesthesia produced by Metofane[®] inhalation. All but three surviving mice were killed at 21 days post-inoculation (p.i.) and tissues were collected for histopathology. To observe the long-term changes in clinical disease and histological lesions, however, three mice were not killed until 60 days p.i. Two of these mice were from the group inoculated with 10^4 PFU and had active skin lesions at the site of injection. The third mouse, which was from the 10^5 PFU inoculation group, was paralysed in the left hindlimb but remained active and alert.

Necropsy and Histopathology

All mice received a full post-mortem examination after euthanasia. Tissue samples from visceral organs, skin, skeletal muscle and brain were fixed in 10% buffered formalin, embedded in paraffin wax, sectioned at 5 µm and stained with haematoxylin and eosin

(H&E). The vertebral columns with spinal cords *in situ* were fixed in 10% buffered formalin and decalcified in formic acid before being divided into anatomical regions (cervical, thoracic and lumbar), sectioned at 5 µm and stained with H&E.

Immunohistochemistry

Formalin-fixed, paraffin wax-embedded tissue samples were dewaxed and rehydrated before heat treatment under pressure for epitope retrieval (Miller and Estran, 1995). Staining was performed on an automated stainer. Endogenous peroxidase activity was blocked by flooding sections with 3% hydrogen peroxide for 10 min. Non-specific immunoreactivity was blocked with 10% normal goat serum for 20 min before addition of the primary antibody. This was a polyclonal hyperimmune rabbit serum raised against SaHV-1-infected RK 13 cells (Hilliard *et al.*, 1989); it was applied at a dilution of 1 in 1000 for 1 h. The secondary antibody, which consisted of biotinylated goat anti-rabbit (Zymed Laboratories, San Francisco, California, USA), was applied at a dilution of 1 in 500 for 20 min. The horseradish peroxidase-streptavidin conjugate was applied for 20 min at a 1 in 1000 dilution and the stain developed with aminoethyl carbazole (AEC) substrate (Zymed Laboratories, San Francisco, California, USA). Sections were counterstained with Mayer's haematoxylin.

Serology

Bleeding from the tail was performed on one-half of each group at 16 days p.i. and individual serum samples were pooled within each dosage group. Surviving animals were exsanguinated at the time of euthanasia (21 days) and sera pooled for each dosage

group. ELISA for SaHV-1 specific antibody in serum pools was performed as previously described (Ohsawa *et al.*, 1999).

Results

Clinical Disease and Gross Lesions

The effects of the virus were almost entirely confined to animals that received at least 10^3 PFU (Table 1). Several mice (23/32) in the 10^3 - 10^6 PFU inoculation groups developed discrete, pruritic skin lesions at the site of inoculation beginning on day 5 p.i. These early skin lesions were characterized by alopecia and intense hyperaemia. During the next 4-5 days, similar discrete skin lesions developed in the caudo- to caudolateral region of the upper part of the left hindlimb, separate from the original lesion at the site of inoculation. Ultimately (by day 12 p.i.), these multifocal, discrete skin lesions coalesced to form well-circumscribed, moist, shallow ulcers that covered most of the caudolateral region of the upper left hindlimb. In most animals, the development of a thin crust (scab) and loss of the intense hyperaemia indicated that the lesions had begun to heal by day 16 p.i. In addition to the skin lesions, the mice also had lymphadenomegaly of the ipsilateral popliteal lymph node.

From 6-16 days p.i., 12/32 mice in the higher dosage groups (10^3 - 10^6 PFU) developed either flaccid or spastic paralysis of the left hindlimb. In two of these mice, the paralysis progressed to affect both hindlimbs. No discernable pattern for the development of spastic versus flaccid paralysis was noted. Also, the hindlimbs of mice with initial spastic paralysis did not progress to flaccidity, but remained rigid until euthanasia. All paralysed mice exhibited a rapidly progressive loss of muscle mass in the

affected hindlimbs, which was consistent with denervation muscle atrophy. This was particularly conspicuous in the two mice with bilateral hindlimb paralysis, in which the atrophy of the hindlimbs was accompanied by severe atrophy of the epaxial musculature. In four of the 12 mice with hindlimb paralysis, urinary incontinence was indicated by urine staining of the haircoat of the perineum and hindlimbs. Over the course of the experiment, nine of the 12 mice with hindlimb paralysis became weak and depressed, at which time they were killed. The three remaining mice were still alert and active but had not regained the use of the paralysed limb by day 21 p.i.

The mice that developed paralysis usually had skin lesions (9/12), but the severity of the skin lesions did not appear to be related to the development of paralysis. Three of the 12 mice with hindlimb paralysis at no time had grossly observable skin lesions. Fourteen of the 32 mice developed skin lesions but did not display clinical signs of neuromuscular involvement.

All but three mice were killed at the termination of the experiment (day 21 p.i.). Other than the previously described skin lesions and muscle atrophy, gross lesions were not seen in any organ system. The three remaining mice were maintained and examined daily until day 60 p.i. Two of these mice had persistent, non-healing skin lesions that remained active up to day 60, but they showed no hindlimb paralysis. The skin lesion from the third mouse had healed by day 60, but the hindlimb paralysis had neither progressed nor abated.

Histological lesions

Significant lesions were present only in the skin (in the region of inoculation) and spinal cord of diseased mice (Table 2). The skin lesions consisted of an ulcerative and necrotizing dermatitis and folliculitis (Fig.1). There was partial to full thickness necrosis of the epidermal and follicular epithelial cells and occasional areas of necrosis of the sebaceous epithelium. The inflammatory infiltrate (dermatitis) was confined to the superficial dermis and periadnexal regions. The infiltrate consisted primarily of macrophages and lymphocytes; however, significant numbers of neutrophils were present, particularly in regions of full thickness necrosis, ulceration, and crusting. Intranuclear inclusion bodies consistent with herpesvirus were occasionally seen, primarily in follicular epithelial cells of mice killed before day 14; they were not seen, however, in the skin of mice killed later.

Lesions in the spinal cord varied widely in severity. In lumbar spinal cord segments, lesions consisted of mild to severe rarefaction and inflammation of the dorsal root, dorsal funiculus and dorsal gray horn (Fig.2). The inflammatory cell component consisted almost entirely of lymphocytes and microglia (Fig.3). The lesions at the lumbar level were always ipsilateral (left) to the site of inoculation. The lesions appeared to be more severe in paralysed mice; however, they remained localized to the unilateral dorsal region of the spinal cord, and involvement of contralateral or ventral (motor) regions was not evident. There was an occasional, mild to moderate, mononuclear infiltration of the unilateral and bilateral dorsal root ganglia (DRG) at the level of the lumbar cord (Fig.4). In the thoracic cord segments, lesions in mice that were not

clinically paralysed were similar to those seen in lumbar segments. In mice that had either unilateral or bilateral hindlimb paralysis, the thoracic spinal cord segments were characterized by unilateral or contralateral (or both) dorsal and ventral involvement of the white and grey matter (Fig.5). The white matter was dominated by mild to severe rarefaction and the grey matter by necrosis of neuronal and glial elements. Inflammation ranged from mild to severe, was primarily mononuclear and in bilaterally paralysed mice, showed greater dissemination throughout the spinal cord. Occasional intranuclear viral inclusion bodies were seen in neurons and glial cells and, as in the skin, were present only in samples collected before day 14 p.i. In the paralysed mouse kept until day 60 p.i., the lumbar cord was characterized by marked asymmetry, secondary to destruction and loss of the left dorsal portion of the cord (Fig.6). Lesions were not seen in the cervical cord, brain or other neural structures, including autonomic ganglia, or in visceral tissues.

Immunohistochemistry

Viral antigen was detected in the spinal cord and skin lesions of animals that were killed early (up to 14 days p.i.) but was not in animals killed later (21 or 60 days p.i.). In skin lesions, viral antigen was most intense in follicular epithelial cells, but was also present in the epidermis and sebaceous glands (Fig. 7). The distribution of viral antigen in the spinal cord accorded with the distribution of lesions seen on H&E-stained sections; antigen was detected in both neurons and glial cells (Fig. 8).

Serology

Sera were tested by ELISA for the presence of anti-SaHV-1 IgG. Pooled sera from the animals in the higher dosage groups (10^3 - 10^6 PFU) were positive at both day 16 and day 21 (Fig. 9). Sera of mice inoculated with 10 or 10^2 PFU were negative at day 16 p.i. While mice inoculated at 10^2 PFU were also negative at 21 days p.i., those inoculated with 10 PFU were positive at 21 days.

Discussion

As a simian alphaherpesvirus, SaHV-1 is related to monkey B virus and may therefore be useful in comparative pathogenesis and virulence studies. Disease due to spontaneous SaHV-1 infection has been described previously in marmosets (Holmes *et al.*, 1964) and owl monkeys (Hunt and Melendez, 1966; Emmons *et al.*, 1968). These animals generally exhibited a necrotizing stomatitis accompanied by multifocal necrosis in the liver, spleen and lymph nodes, with minimal involvement of the central nervous system (Holmes *et al.*, 1964; Hunt and Melendez, 1966; Emmons *et al.*, 1968). Experimental infection of rabbits, guinea-pigs (Holmes *et al.*, 1964; Daniel *et al.*, 1969) and neonatal mice (Jones *et al.*, 1971) has also been documented. As an initial step in the development of a murine model for simian alphaherpesvirus infections, this study showed that mice can be infected with SaHV-1 and that infection results in clinical disease accompanied by gross and histological lesions.

The disease produced in adult mice was accompanied by lesions comparable to those reported in other mammalian species inoculated via similar routes. For example, the lesions in the skin and spinal cord of SaHV-1-infected mice were comparable to those

described in rabbits inoculated with SaHV-1 by either intradermal, intramuscular or subcutaneous routes (Tosolini *et al.*, 1982). SaHV-1-associated disease in other species differs according to the route of inoculation. Experimental infection of marmosets with SaHV-1 invariably resulted in focal necrosis of organ systems associated with the route of infection (Holmes *et al.*, 1964). Similarly, multifocal necrosis was a common feature in neonatal mice inoculated via the intracerebral or intraperitoneal route (Jones *et al.*, 1971); in addition, intracerebrally inoculated mice developed a severe meningoencephalitis, which was neither present in mice inoculated intraperitoneally. Meningoencephalitis did not occur in intramuscularly inoculated mice in the present study.

Mice in the higher dosage groups (10^3 - 10^6 PFU) developed ulcerative skin lesions similar to those produced by intradermal SaHV-1 inoculation in marmosets (Holmes *et al.*, 1964), rabbits and guinea-pigs (Tosolini *et al.*, 1982). In rabbits, intramuscular inoculation did not produce skin lesions (Tosolini *et al.*, 1982), but inoculation by this route has not been reported in other species. It is possible that the cutaneous lesions seen in our mouse experiments may have resulted from secondary skin inoculation occurring at the time of intramuscular injection. However, we hypothesize that the skin lesions were a result of virus traversing a neural circuit from the site of inoculation up to the sensory ganglia and then down the cutaneous afferent nerves to emerge and infect the regional epithelium. This mechanism would explain the progression from focal to regional skin lesions, the latter often beginning as small, multifocal lesions and ultimately coalescing to form a single large lesion. Furthermore, the development of skin lesions coincided temporally with the development of neurological signs rather than preceding

them, indicating that the virus was already present within the CNS by the time skin lesions appeared.

Although it was not the primary purpose of this study to investigate neural pathways or to undertake detailed mapping of transneuronal viral spread, the relationship between the occurrence of spinal cord lesions and clinical signs proved interesting. The unilateral and occasionally bilateral paralysis seen in animals in the higher dosage groups (10^3 - 10^6 PFU), as well as the urinary incontinence that occasionally accompanied the paralysis, indicated the involvement of the motor portion of the spinal cord or interruption of the corticospinal tract. As no lesions were seen in the ventral horns of the lumbar segments, we speculate that SaHV-1-induced paralysis is a result of involvement of motor neurons or proprioceptive pathways in the more cranial regions of the spinal cord. This was supported by the often diffuse and severe lesions within the thoracic white and grey matter of paralysed mice. Ventral motor portions of the thoracic spinal cord of paralysed mice often contained detectable viral antigen. It is possible for virus to reach these ventral motor neurons or contralateral regions of the grey matter via transsynaptic spread from the sensory regions of the cord through interneurons. Another possible explanation for the hindlimb paralysis is damage to the corticospinal tract in the lumbar or thoracic segments. This mode of paralysis has been postulated in transneuronal spread studies of herpes simplex virus 1 in mice (Engel *et al.*, 1997) and seems to be the likely cause of paralysis in some mice infected with SaHV-1. For example, the unilaterally paralysed mouse maintained until 60 days p.i. did not exhibit lesions in the ventral portion of the thoracic cord but showed almost complete destruction

of the ipsilateral posterior column of lumbar white matter containing the corticospinal tract.

Alphaherpesviruses traverse ascending sensory pathways from infected epithelium via retrograde axonal transport (Cook and Stevens, 1973). It is interesting to note that in SaHV-1-infected mice, virus-associated lesions appear in non-sensory portions of the spinal cord. Alphaherpesviruses can also undergo retrograde axonal transport in motor neurons (Ugolini *et al.*, 1987). It is possible that intramuscular inoculation with high doses of virus provides a viral load sufficient for retrograde axonal transport of virions within motor neurons to the ventral or motor portion of the spinal cord; however, this probably did not occur in our study. All lesions present within the caudal lumbar segments of the spinal cord (corresponding to the nerve supply to the caudal thigh) were within the dorsal (sensory) region of the cord. From this area, virus appears to have travelled cranially within the spinal cord to involve the thoracic segments, extending to the motor regions, both ipsilateral and contralateral. To show that time was not a limiting factor in the cranial spread of virus and development of subsequent encephalomyelitis, we maintained a unilaterally paralysed mouse until day 60 p.i. In this animal, the infection progressed locally and resulted in dramatic scarring of the lumbar and thoracic cord; it did not, however, progress in a cranial direction. This is reminiscent of other species, such as the rabbit, in which peripheral inoculation results in a limited ascending infection that does not reach the brain (Tosolini *et al.*, 1982).

Viral antigen was demonstrated immunohistochemically in lesions at 14 days p.i. but not at later time points, possibly because by day 21 p.i. viral antigen expression in lesions was contained by the host's immune system. ELISA results on pooled serum

samples collected at days 16 and 21 accorded well with the presence of lesions and clinical disease. Serum from animals in the higher dosage groups (10^3 - 10^6 PFU) had high concentrations of anti-SaHV-1 IgG on days 16 and 21. Pooled serum from the lower dosage groups did not have detectable levels of anti-viral IgG at day 16 p.i. It should be pointed out, however, that detectable concentrations were found in pooled sera from the 10 PFU group on day 21. It is important to note that only half of the animals in each group were bled on day 16, while the 21-day sample included serum from every animal. The single animal in the 10 PFU group that exhibited a skin lesion was not included in the 16-day serum pool. It seems probable that this one animal was responsible for the anti-SaHV-1 IgG in the 21-day sample of the 10 group.

From this study, we conclude that inoculation of adult mice with SaHV-1 virus results in active infection characterized by seroconversion with skin and CNS lesions, the severity and frequency of which are related to the dose of virus. SaHV-1 ascends the spinal cord but, unlike B virus in man and other animals, not far enough to produce an encephalomyelitis. Thus, SaHV-1 injected intramuscularly into mice ascends only as far as the thoracic and lumbar spinal cord segments, resulting in regional limb paralysis. This report of SaHV-1 infection in mice and previous reports of B virus infection in mice (Goszotonyi *et al.*, 1992) suggest the suitability of mice for comparative studies on the pathogenesis of simian alphaherpesvirus infections. In addition, mice may prove useful for studies on new anti-viral drugs, potential vaccines, and the role of various viral genes or proteins in determining the pathogenic properties of alphaherpesviruses.

Acknowledgements

This work is supported by a grant (no. NCRR RO1 RR07849) from the National Institutes of Health to one of the authors (R.E.). The first author (M.A.B.) is a Howard Hughes Medical Institute Predoctoral Fellow. We thank Dr R.J. Panciera for assistance with the histomicrographs and Dr J.T. Saliki for critical appraisal of the manuscript.

References

- Brack, M. (1977). Morphological and Epidemiological Aspects of Simian Herpesvirus Infections Verlag Paul Parey, Berlin and Hamburg, pp. 6-63.
- Cook, M.L. and Stevens, J.G. (1973). Pathogenesis of herpetic neuritis and ganglionitis in mice: evidence for intra-axonal transport of infection. *Infection and Immunity*, **7**, 272-288.
- Daniel, M.D., Karpas, A., Melendez, L.V., King, N.W. and Hunt, R.D. (1969). Isolation of herpes-T virus from a spontaneous disease in squirrel monkeys (*Saimiri sciureus*). *Archiv für die Gesamte Virusforschung*, **22**, 324-331.
- Eberle, R. and Hilliard, J. (1995). Review: the simian herpesviruses. *Infectious Agents and Disease*, **4**, 55-70.
- Emmons, R.W., Gribble, D.H. and Lennette, E.H. (1968). Natural fatal infection of an owl monkey (*Aotus trivirgatus*) with herpes T virus. *Journal of Infectious Disease*, **118**, 153-159.
- Engel, J.P., Madigan, T.C. and Peterson, G.M. (1997). The transneuronal spread phenotype of herpes simplex virus type 1 infection of the mouse hind footpad. *Journal of Virology*, **71**, 2425-2435.
- Gosztonyi G., Falke, D. and Ludwig, H. (1992). Axonal and transsynaptic (transneuronal) spread of *Herpesvirus simiae* (B virus) in experimentally infected mice. *Histology and Histopathology*; **7**:63-74.
- Hilliard, J.K., Black, D. and Eberle, R. (1989). Simian alphaherpesviruses and their relation to the human herpes simplex viruses. *Archives of Virology*, **109**, 83-102.

- Holmes, A.W., Caldwell, R.G., Dedmon, R.E. and Deinhardt, F. (1964) Isolation and characterization of a new herpes virus. *Journal of Immunology*, **92**, 602-610.
- Holmes, A.W., Dedmon, R.E. and Deinhardt, F. (1963). Isolation of a new herpes-like virus from South American marmosets. *Federation Proceedings*, **22**, 324.
- Hunt, R.D. and Melendez, L.V. (1966). Spontaneous herpes-T infection in the owl monkey (*Aotus trivirgatus*). *Pathologica Veterinaria*, **3**, 1-26.
- Jones, S.R., Stair, E.L., Gleiser, C.A. and Bridges, C.H. (1971). Histopathologic changes and specific immunofluorescence in infant mice infected with *Herpesvirus tamarinus*. *American Journal of Veterinary Research*, **32**, 1143-1153.
- Melnick, J.L., Midulla, M., Wimberly, I., Barrera-Oro, J.G. and Levy, B.M. (1964). A new member of the herpesvirus group isolated from South American marmosets. *Journal of Immunology*, **92**, 596-601.
- Miller, R.T. and Estran, C. (1995). Heat-induced epitope retrieval with a pressure cooker. *Applied Immunohistochemistry*, **3**, 190-193.
- Mou, S.W., Hilliard, J.K., Song, C.H. and Eberle, R. (1986). Comparison of the primate alphaherpesviruses. I. Characterization of two herpesviruses from spider monkeys and squirrel monkeys and viral polypeptides synthesized in infected cells. *Archives of Virology*, **91**, 117-133.
- Ohsawa, K., Lehenbauer, T.W. and Eberle, R. (1999). *Herpesvirus papio 2*: alternative antigen for use in monkey B virus diagnostic assays. *Laboratory Animal Science*, **49**, 605-616.
- Palmer, A.E. (1987). B virus, *Herpesvirus simiae*: historical perspective. *Journal of Medical Primatology*, **16**, 99-130.

- Tosolini, F.A., McCarthy, K. and Baker, B.F. (1982). Studies of herpes virus latency in the sensory spinal ganglia of rabbits. *Journal of Hygiene*, **89**, 421-437.
- Ugolini, G., Kuypers, H.G.J.M. and Simmons, A. (1987). Retrograde transneuronal transfer of herpes simplex virus type 1 (HSV1) from motorneurons. *Brain Research*, **422**, 242-256.
- Weigler, B.J. (1992). Biology of B virus in macaque and human hosts: a review. *Clinical Infectious Disease*, **14**, 555-567.

Table 1

Clinical signs and gross lesions

Viral dose (PFU)	Number of mice affected in groups of eight				
	Skin lesion	Paralysis/ paresis		Urinary incontinence	Early euthanasia
		Unilateral	Bilateral		
10 ⁶	7	4	0	0	3
10 ⁵	7	3	1	2	2*
10 ⁴	5	2	0	0	2
10 ³	4	1	1	2	2
10 ²	0	0	0	0	0
10	1	0	0	0	0
0 (controls)	0†	0†	0†	0†	0†

* One mouse found dead

† Group of two mice

Table 2

Microscopical lesions

Dosage group (PFU)	Tissues	Lesions
10, 10 ³ , 10 ⁴ , 10 ⁵ , 10 ⁶	Skin	Ulcerative necrotizing dermatitis and folliculitis
10 ³ to 10 ⁶	Thoracic spinal cord	Focal rarefaction of left dorsal funiculus and horn to diffuse vacuolation and necrosis of grey matter
10 ³ to 10 ⁶	Lumbar spinal cord	Mild to severe unilateral rarefaction of dorsal funiculus and horn with microgliosis and mononuclear inflammation
10 to 10 ⁶	Brain and cervical spinal cord	No lesions seen
10 to 10 ⁶	Various organs: spleen, liver, kidney, lung, heart, thymus, sciatic nerve	No lesions seen

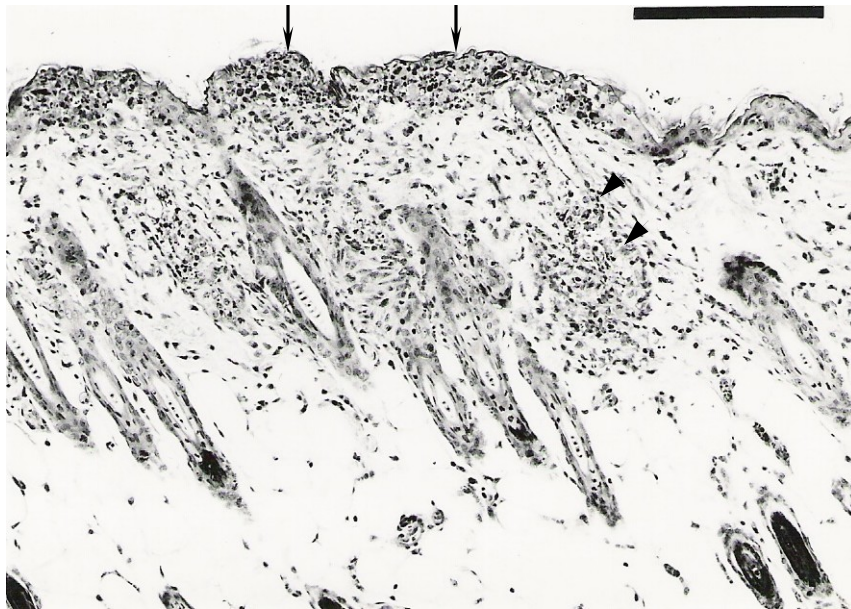


Fig. 1. Typical skin lesion, characterized by foci of necrosis in the epidermis (arrows) and hair follicles (arrowheads) accompanied by an inflammatory infiltrate. H&E. Bar, 200 μm .

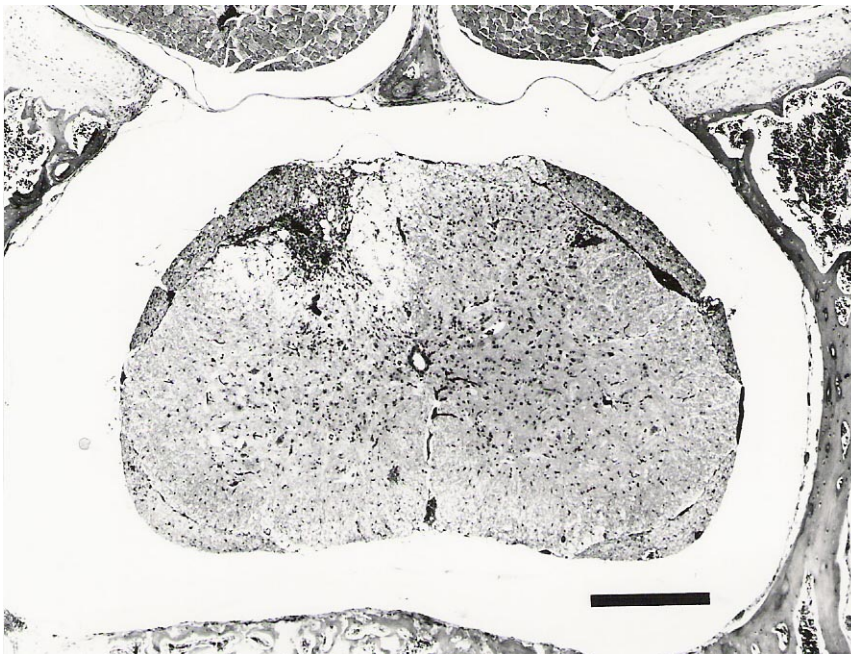


Fig. 2. Lumbar spinal cord segment from a mouse given 10^3 PFU. This animal appeared neurologically normal but had a skin lesion on the left hindlimb and was killed at day 21 p.i. In the left dorsal funiculus and horn there is a focus of intense mononuclear infiltrate and microglial proliferation surrounded by rarefaction. H&E. Bar, 300 μm .

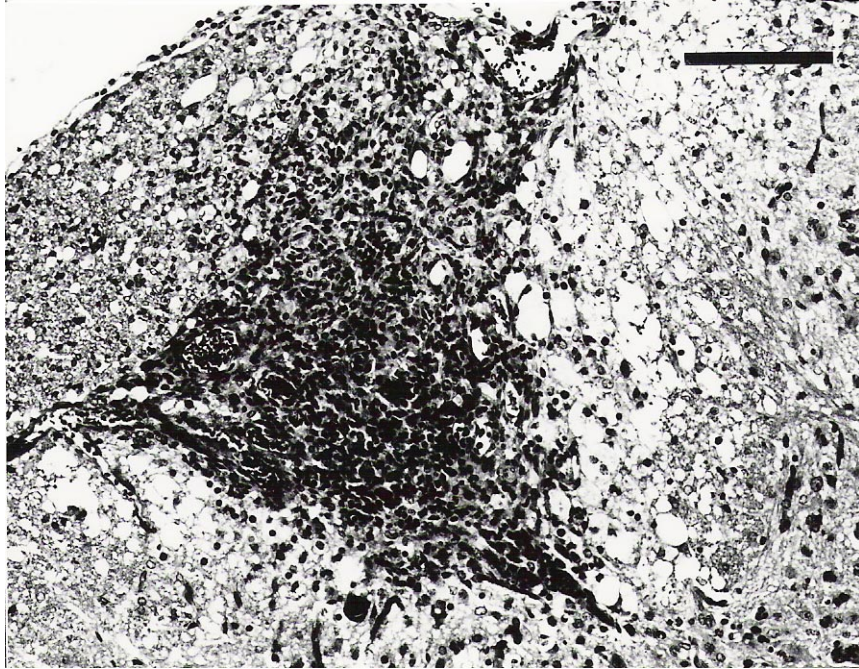


Fig. 3. Higher magnification of mononuclear infiltrate and microglial proliferation in the dorsal funiculus shown in Fig. 2. H&E. Bar, 200 μ m.

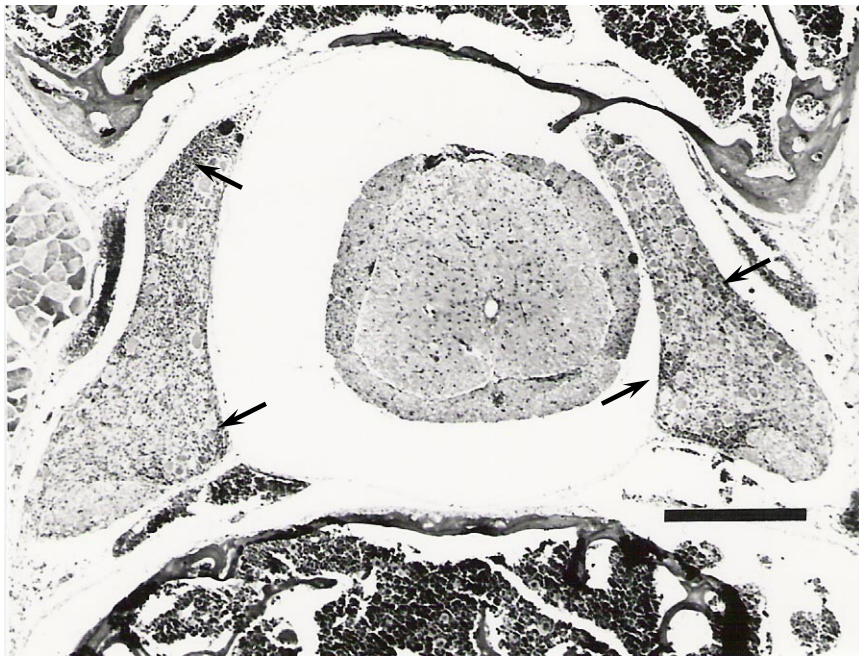


Fig. 4. More distal lumbar spinal cord segment from the animal shown in as Figs. 2 and 3. A mononuclear infiltrate between neuronal cell bodies is present bilaterally in the dorsal root ganglia (arrows). H&E. Bar, 300 μ m.

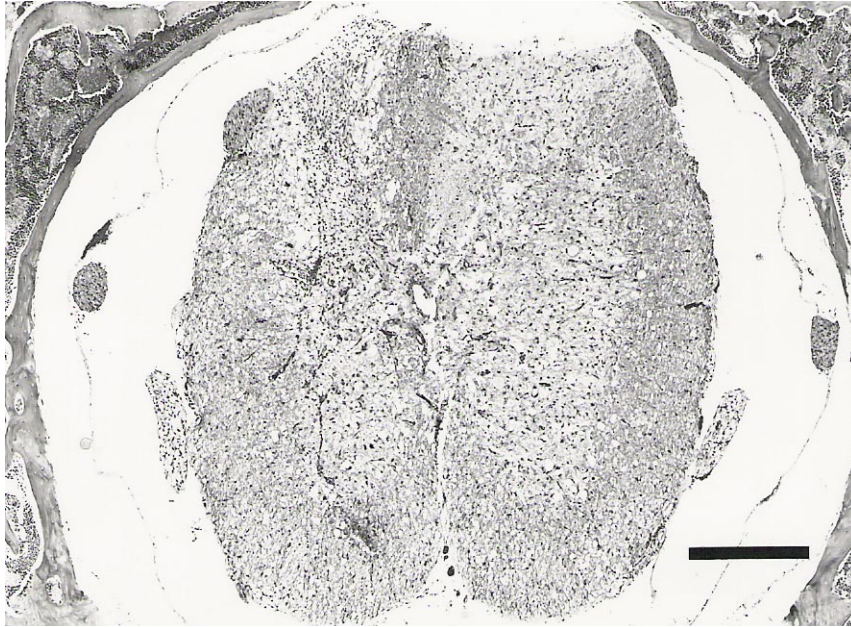


Fig. 5. Thoracic spinal cord segment from a mouse in the 10^6 PFU group, with unilateral hindlimb paralysis. This animal was killed at day 6 p.i. Note the severe, diffuse vacuolation in the grey matter. On higher magnification, necrosis of neurons and glial cells was evident, as well as a mild mononuclear infiltrate. H&E. Bar, 300 μ m.

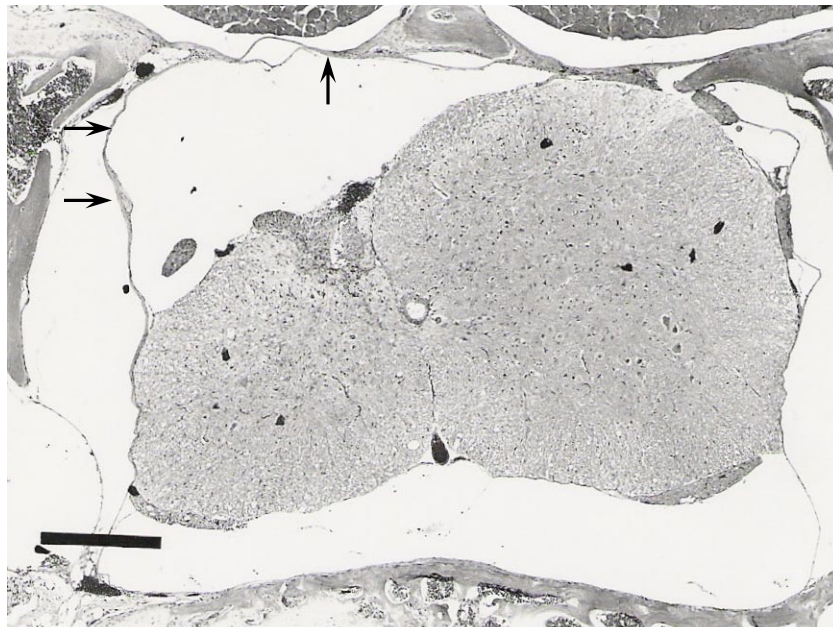


Fig. 6. Lumbar spinal cord from mouse that received 10^5 PFU. The animal developed unilateral hindlimb paralysis and was killed at day 60 p.i. There is marked asymmetry of the cord secondary to loss of the unilateral dorsal horn and funiculus. Meninges indicated by arrows. H&E. Bar, 300 μ m.

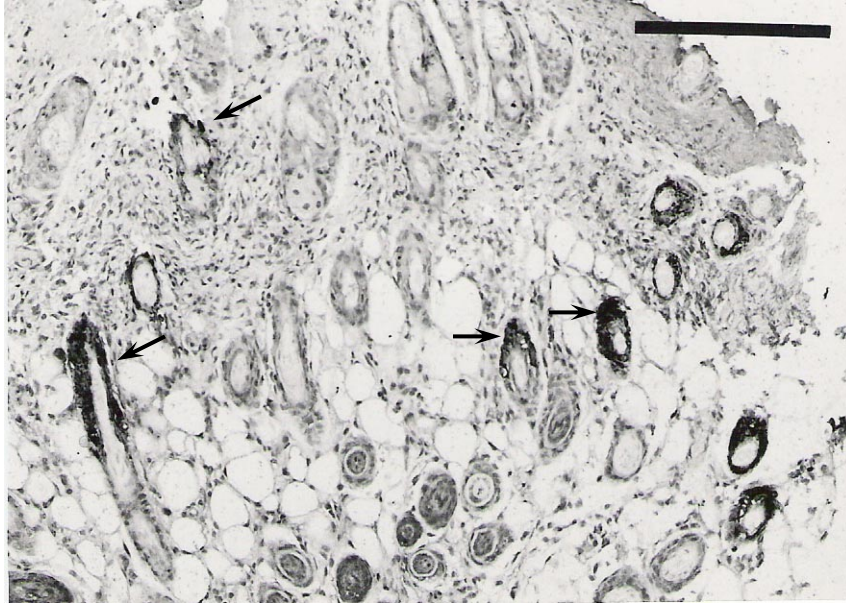


Fig. 7. Immunohistochemical labelling of skin lesion from mouse shown in Fig. 1. Intense labelling of viral antigen is present in the follicular epithelium (arrows). Mayer's hematoxylin counterstain. Bar, 200 μm .

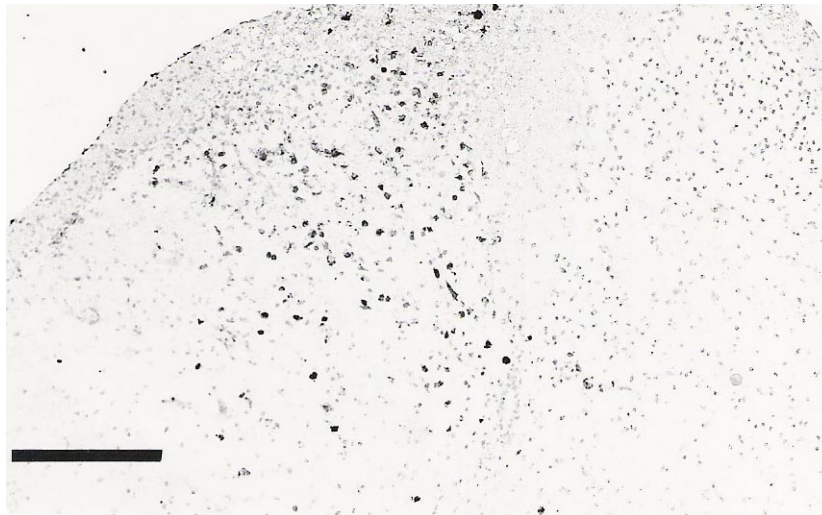


Fig. 8. Immunohistochemical labeling of lumbar spinal cord from a mouse that received 10^6 PFU. Note the intense viral signal in the left dorsal horn and funiculus. Viral signal is present in both neurons and surrounding glial cells. Mayer's hematoxylin counterstain. Bar, 200 μm .

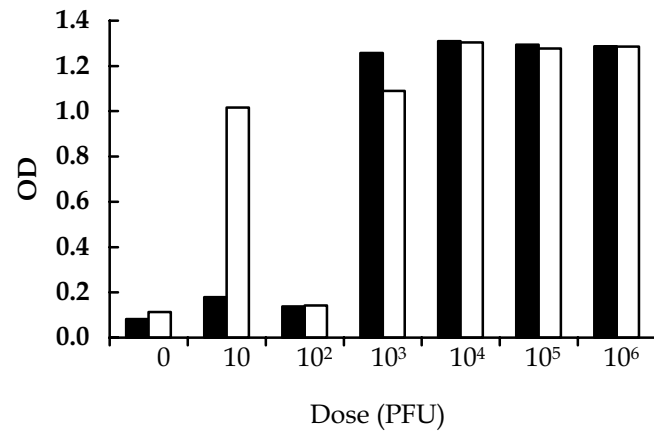


Fig. 9. ELISA results for HVS1-specific IgG at 16 (■) and 21 (□) days p.i. The various mouse groups are indicated by the dose (PFU) of virus administered (“0 PFU” indicates controls). OD, optical density.

CHAPTER IV

CONSTRUCTION AND *IN VIVO* DETECTION OF AN ENHANCED GREEN FLUORESCENT PROTEIN-EXPRESSING STRAIN OF *Saimiriine herpesvirus 1* (SaHV-1)

Summary

Saimiriine herpesvirus 1 (SaHV-1) is an α -herpesvirus of squirrel monkeys used in mice to study neural pathogenesis of herpesviruses. To trace dissemination of virus from a peripheral site of inoculation to the central nervous system tissues, a recombinant strain of SaHV-1 expressing enhanced green fluorescent protein (GFP) was constructed by site-specific insertion of a GFP expression cassette into a transcriptionally null point in the SaHV-1 genome. PCR and Southern blot confirmed insertion of a single GFP expression cassette into the target site of the SaHV-1 genome. The recombinant virus was shown to produce strong fluorescence in the cytoplasm of infected cells *in vitro*. Growth kinetic experiments demonstrated no differences between recombinant and wild type SaHV-1 in producing infectious progeny virions. The recombinant virus was comparable to wild type SaHV-1 in development of clinical disease, microscopic lesions and induction of an antibody response in mice following intramuscular inoculation. Using confocal microscopy, GFP expression was easily observed in formalin fixed, paraffin-embedded tissues of mice infected with the recombinant SaHV-1. This simple specimen processing technique preserves tissue morphology and allows detection of viral replication within various tissues of experimentally infected animals.

Introduction

Non-human primates are invaluable biomedical research subjects due to their anatomical, biochemical and physiological similarities to humans. These same similarities, however, increase the risk of trans-species transfer of infectious agents from non-human primates to their human handlers. Alpha-herpesviruses are important infectious agents in this regard because they are widespread in primate populations and interspecies transmission often results in severe or fatal disease [1, 12]. *Cercopithecine herpesvirus 1* or B virus (BV) of macaques is enzootic in monkeys of the genus *Macaca*. In its natural host, BV infections are usually asymptomatic but occasionally present as mild disease consisting of oral, lingual, pharyngeal and/or genital vesicles and ulcers. Severe systemic disease in the natural host is rare [32]. In contrast, humans or other species infected with BV develop a severe, often fatal encephalomyelitis [27, 32].

Saimirine herpesvirus 1 (SaHV-1) is an α -herpesvirus enzootic in squirrel monkey populations that is genetically related to BV and human herpes simplex virus [6, 11, 16, 21]. Infection of the natural host is usually clinically inapparent, but occasionally results in ulcerative oral lesions [3]. In aberrant hosts such as the marmoset and owl monkey, SaHV-1 causes a severe, fatal infection characterized by disseminated, multifocal necrosis in visceral organs and occasionally the central nervous system (CNS) [14, 17-19]. SaHV-1 has not been definitively shown to cause disease in man, but has been presumptively associated with one case of encephalitis in a research psychologist who had contact with squirrel monkeys but no known bites or scratches [29]. Virus

isolation was not attempted, but the individual was shown to have a rising antibody titer to SaHV-1.

Human herpes simplex virus has been used as a model for α -herpesvirus neurovirulence and latency in small animals. Since it is a virus of human origin, the only possibility for *in vivo* studies is in xenogeneic experimental hosts. Conversely, SaHV-1 allows characterization of the disease in both the natural host and in xenogeneic experimental hosts, making comparative studies between viral neuropathogenesis in natural and aberrant hosts possible.

In an effort to establish a small animal model system for exploration of the pathogenesis of simian α -herpesviruses and comparison of the neurovirulence of these related viruses, gross and microscopic lesions of SaHV-1 infection in mice have been characterized [2]. To increase the utility of the mouse model system by more specifically tracing the neural route of the virus during infection, an enhanced green fluorescent protein (GFP)-expressing strain of SaHV-1 was constructed. While GFP-expressing viruses have been described previously, the microscopic detection of GFP expression in tissues other than brain has proven problematic. In this report we describe the construction and molecular characterization of the recombinant virus as well as a method for its microscopic detection in fixed tissues from experimentally infected mice.

Materials and Methods

Viruses and cells

The MV-5-4 strain of SaHV-1 [24] and the E90-136 strain of BVcy [30] were propagated and titered in Vero cells grown in Dulbecco's modified Eagle medium (DMEM)

containing 10% fetal bovine serum (FBS), 200 mM L-glutamine, 100 IU/ml penicillin and 100 µg/ml streptomycin. Vero cells were also used for growth kinetic assays, transfections, and preparation of antigens for immunoassays.

Viral growth kinetic assays were performed using subconfluent Vero cells grown in 12 well plates. Cells were inoculated with virus at an MOI of 5. Samples (one well/virus) were harvested by scraping cells into the medium at 3, 5, 8, 11, 14, 17, 24 and 30 hours post-inoculation (PI) and centrifuged at 14,000g for 1 min to pellet cells. Extracellular virus was quantitated by plaque assay of the supernatant. The cell pellet was freeze-thawed three times, debris removed by centrifugation and the supernatant assayed to quantitate cell-associated virus.

Construction of GFP expression cassette

A fragment of the BVcy genome (GenBank accession number AF501667) representing 710 bp 5' from the UL19 start codon was amplified by PCR (primers 5'-ATCTA**AAGCTT**GAAGCGGGCGTTGGTGTTTGCCTGGTC-3' and 5'-TCGGG**CATG**CCGCGCGGTCCTTCGGAGGGTGTG-3'; UL19 start codon underlined) and cloned into pUC19 using the restriction sites integrated into the primers (indicated in bold). Likewise, a 370 bp fragment extending 3' from the BV UL18 termination codon (primers 5'-ATACGGTACT**TCTAG**ACCCCCCCCCGACCCGCTCAG-3' and 5'-GACGA**ATT**CATGGTCGCCGTCATCATGGCCGTCTACC-3'; UL18 stop codon underlined) and the coding sequence of the GFP protein from the pEGFP vector (Epicentre, Madison, WI) (primers

5'-GGTCGCCAGC**ATG**CTGAGCAAGGGCGAGGAGCTGTTTAC-3' and 5'-ATGTGGTATGGCTGATTATGCT**CTAG**AGTCGCGGC-3'; EGFP start codon underlined) were amplified by PCR and cloned into pUC19 using restriction sites indicated (bold print). An expression cassette was constructed from these three fragments, with the GFP open reading frame (ORF) flanked 5' by the BV UL19 promoter and 3' by the BV UL18/19/20 poladenylation/ transcriptional termination elements as shown in Figure 1. Following assembly of this expression cassette, the *HindIII* restriction site at the 5' end of the BV UL19 promoter sequence was changed to an *EcoRI* site via PCR, thereby placing *EcoRI* sites on both ends of the expression cassette. The final construct was completely sequenced to ensure its fidelity.

Recombinant DNA and plasmids

A genomic DNA library of SaHV-1 was constructed in pUC19 by shotgun cloning of NaI gradient-purified viral DNA digested with *KpnI*. Cloned fragments were located on the genome map by end sequencing and BLAST search to identify homologous herpesvirus sequences in GenBank.

A 6 Kbp fragment designated pUQK3, spanning the region extending from the 3' portion of UL25 ORF to the 3' portion of UL27 ORF (Fig.1B) was subcloned and completely sequenced (GenBank accession number AY095366). Plasmid DNA was prepared for sequencing and transfection using a plasmid purification kit (Qiagen Inc., Valencia, CA). Sequence assembly and analysis was done using DNASTar and VectorNTI programs. The UL26.5- UL27 intergenic space was located within a 2 Kbp *BamHI-HindIII* fragment (pUQK3-BH) subcloned from pUQK3. An *EcoRI* restriction

site was inserted into this fragment via mutagenic PCR (primers 5'-TCCTGAATTCAGGCTTATCTCTCCTCTTCCGGTC-3' and 5'-TCCTGAATTCTCTACGGGACCCGCGTCTCTATCG-3'), yielding pUQK3-BHEcoRI. This clone was sequenced to verify the sequence integrity and location of the inserted *EcoRI* site. For recombination into SaHV-1, the GFP expression cassette construct was inserted into the *EcoRI* site of QK3-BHEcoRI, which was subsequently inserted into pUQK3 to yield pUQK3-GFP, providing approximately 3 Kbp of SaHV-1 flanking sequences on each side of the expression cassette to facilitate homologous recombination into the SaHV-1 genome.

Recombinant viruses

Recombinant SaHV-1 viruses SaHV-1rG1 and SaHV-1rG3 carrying the GFP expression cassette were generated by co-transfecting cells with purified SaHV-1 DNA and the pUQK3-GFP plasmid insert, which had been excised from the pUC vector and gel purified. Transfections were performed using subconfluent Vero cell cultures grown in 6 well plates. Viral DNA and recombinant constructs were co-transfected into cells using the calcium phosphate precipitation technique [15], modified as previously described [13]. Transfected cultures were monitored for fluorescent plaque formation using a Nikon Eclipse TE200 inverted microscope. Brightly fluorescent plaques were picked at 36-48 hours post-transfection. Two GFP-expressing isolates, designated SaHV-1rG1 or G3, were purified by repeated inoculation and selection of individual brightly fluorescent plaques until all developing plaques exhibited complete fluorescence (3-4 passages).

Animal inoculations

Specific-pathogen-free 13-15 gram female Balb/c mice (Charles River Laboratories, Inc., Wilmington, MA) were used in all experiments in accordance with the Institutional Animal Care and Use Committee (IACUC) guidelines. Animals were housed in an isolation room and given unlimited access to food and water. Mice were randomly divided into groups of eight animals to receive a selected dose of each virus strain. Mice were anesthetized by Metofane[®] (Schering-Plough Animal Health Corp., USA) inhalation and inoculated with virus intramuscularly in the semimembranosus/semitendinosus muscle group of the left hindlimb as described [2]. Individual mice were observed twice daily for clinical signs of disease. Any markedly weak, depressed or moribund mice were euthanized by Metofane[®] inhalation. All surviving mice were euthanized at 14 days PI. Sera and tissues were collected individually from all animals.

Immunoassays

ELISA for SaHV-1 specific IgG in individual serum samples was performed basically as described [25]. Briefly, antigen was prepared by TX-100 extraction of uninfected and SaHV-1-infected Vero cells. All sera were tested at a dilution of 1:100. Bound antibody was detected using a biotinylated secondary antibody (Vector Labs, Burlingame, CA) at a 1:5000 dilution followed by a complex of avidin/ biotinylated peroxidase and OPD/ peroxidase substrate.

For immunoblot antigen, Vero cell monolayers grown in 96-well plates were infected with virus. At 1, 3, 5, 7 and 9 hours PI medium was removed and individual

wells of infected cells were harvested by adding 30 μ l of SDS-PAGE sample buffer. Samples were denatured at 95°C for 5 min before proteins were separated by SDS-PAGE and blotted onto a nitrocellulose membrane [10]. The membrane was probed with polyclonal hyperimmune rabbit sera (1:1000 dilution) raised against purified SaHV-1 gB as described [9]. Biotinylated secondary antibody (1:3000) and a DAB detection kit (Vector Labs, Burlingame, CA) were used to detect bound antibody.

Southern blotting

DNA for Southern blots was prepared by phenol extraction of virus infected Vero cells. Infected cell DNA was digested with restriction enzymes for 1.5 hours, fragments separated by electrophoresis on agarose gels, transferred overnight to a GeneScreen™ nylon membrane (NEN® Life Science Products, Boston, MA) and then UV-crosslinked. Membranes were hybridized with a biotin-labeled probe (NEN® Life Science Products, Boston, MA) made from pUQK3 according to the manufacturer's instructions. The probe was detected via streptavidin-AP conjugate and CDP-Star Chemiluminescence Reagent (NEN® Life Science Products, Boston, MA) on Kodak X-OMAT Blue autoradiography film following protocols outlined in manufacturer's instructions.

Detection of GFP in tissue sections

Intact vertebral columns and skin lesions from the legs of mice inoculated with SaHV-1rG were collected and fixed in 10% buffered formalin for 9 to 18 hours before processing. Vertebral columns with spinal cord *in situ* were decalcified in a 0.5M EDTA solution in water, pH 8.0 for 4-5 days before trimming into multiple 3-4mm segments

within each anatomical region. Tissues were processed in an automated processor using a protocol similar to that described by Walter *et al.* [31] to detect GFP in tissue sections. Embedding solvents and times used were as follows: twice in 80% ethanol for 50 min each, twice in 95% ethanol for 50 min each, three times in 100% ethanol for 50 min each, twice in toluene for 50 min each at room temperature, three times each in Paraplast[®] tissue embedding medium (Sherwood Medical, St. Louis, MO) for 50 min at 60°C and finally embedding in Paraplast[®] at 59°C.

Tissues were sectioned at 5 µm, mounted on positively charged slides, deparaffinized in toluene, rehydrated in 100% ethanol twice for 1 min each, 95% ethanol twice for 1 min each and once in water for 2 min. After counterstaining with 132 µg/ml propidium iodide in PBS for 3 min, slides were coverslipped with fluorescent mounting medium (Dako, USA). Sections were examined on a Leica SP2 laser scanning confocal microscope using two-channel detection with an argon laser and the filter setting for FITC/ TRITC fluorescence.

Immunohistochemistry

Anti-GFP immunostaining was done using a monoclonal antibody against GFP (Clontech, Palo Alto, CA) with an M.O.M.[™] Immunodetection kit following manufacturer's instructions (Vector Labs, Burlingame, CA). Anti-SaHV-1 immunostaining was performed as previously reported [2] using a polyclonal hyperimmune rabbit serum raised against SaHV-1 infected RK 13 cells [16] at a 1:1000 dilution for 1 hour.

Results

Construction of the GFP-expressing recombinant virus

To construct a GFP expressing strain of SaHV-1 with minimal chance of affecting the structure or expression of other viral genes, the targeted insertion site of the GFP expression cassette was the middle of the 507 bp intergenic space located between the polyadenylation/mRNA termination sites of the UL24/25/26 and the UL27/28 transcriptional gene sets (specifically, between nucleotide 3230 and 3231 of GenBank accession number AY095366). To avoid spontaneous rearrangement or internal homologous recombination from occurring secondary to the insertion of additional viral DNA, the expression cassette construct was constructed using transcriptional elements from the related simian herpesvirus, BV. Although the BV and SaHV-1 sequences are homologous, there is virtually no sequence identity. To evaluate the ability of SaHV-1 to use BV transcriptional elements to express the GFP ORF, cells were transfected with the expression cassette and then infected with SaHV-1. By 12 hours PI, transfected cell cultures infected with SaHV-1 exhibited bright green fluorescence, confirming the ability of SaHV-1 to express GFP under regulation of BV promoter and termination sequences. Cultures transfected with the expression cassette but not infected with virus did not exhibit GFP fluorescence.

The 1.8 Kbp GFP expression cassette was then inserted into the *EcoRI* site engineered into the UL26.5-UL27 intergenic space of a 2.0 Kbp *BamHI-HindIII* fragment of the SaHV-1 genome (pUQK3-BH; Fig. 1B). This fragment was then inserted back into the 6 Kbp pUQK3 fragment to provide adequate SaHV-1 flanking sequence (~3 Kbp

on each side) for homologous recombination of the GFP expressing cassette into the SaHV-1 genome (Fig. 1). Co-transfection of Vero cell cultures with the 7.8 Kbp gel purified fragment and purified SaHV-1 genomic DNA generated multiple GFP expressing recombinant viruses. Several of these were repeatedly plaque purified, and two (designated SaHV-1rG1 and SaHV-1rG3) were chosen for further characterization.

In vitro characterization of SaHV-1rG1 and SaHV-1rG3

To verify that the 1.8 Kbp BV/GFP expression cassette was inserted in the desired intergenic space of the SaHV-1 genome, the two recombinant viruses, SaHV-1rG1 and SaHV-1rG3, were characterized by PCR and Southern blot. A PCR primer pair was designed to amplify the region of the SaHV-1 genome between the targeted insertion site and the 3' portion of the UL27 ORF (Fig. 2A&B). Amplification of DNA from cell cultures infected with wtSaHV-1 yielded a 2.5 Kbp product while PCR of SaHV-1rG1 or SaHV-1rG3 DNA yielded products of 4.3 Kbp, indicating the presence of an insert in the recombinants equivalent in size to the expression cassette (Fig. 2C). To confirm the genomic insertion site of the expression cassette more specifically, Southern blot of wtSaHV-1, SaHV-1rG1 and SaHV-1rG3 DNA digests were probed with pUQK3, the cloned 6 Kbp fragment spanning the region from UL25 to UL27 (Fig. 2D). In SaHV-1rG1 and SaHV-1rG3, *Hind*III, *Kpn*I and *Nco*I all generated a single band that was the anticipated 1.8 Kbp larger than in the wild type virus (*Nco*I digest of wtSaHV-1 yielded two fragments of 2.5 and 2.6 Kbp that co-migrate). In *Sph*I digests, the probe hybridized with two bands in the wild type, and three bands in the recombinant, all of expected sizes given the additional *Sph*I site located within the expression cassette. These experiments

also demonstrate that only a single expression cassette was present in the genome of both recombinants, and that their location was precisely at the UL26-UL27 intergenic point intended.

To ascertain if insertion of the expression cassette affected the ability of the virus to replicate, growth kinetic assays were performed. Growth curves of wtSaHV-1 and recombinants SaHV-1rG1 and SaHV-1rG3 were essentially the same for production of both intracellular and extracellular virus (Fig. 3). In addition, virus-induced cytopathic effect characterized by rounding and botryoidal clustering of infected cells developed at the same rate and was indistinguishable between wild type and recombinant viruses. In cultures inoculated with the recombinant viruses, detectable fluorescence was first observed in individual cells at about 5 hrs PI that gradually expanded to become large plaques by 30 hours post-inoculation. This time-course is consistent with expression of the UL19 gene (the promoter driving GFP expression).

Insertion of foreign genes or expression cassettes has been shown to alter expression of adjacent viral genes [5]. Lacking specific reagents to detect any SaHV-1 gene products of nearby genes other than the gB glycoprotein (UL27 gene product), we could only examine the kinetics of expression of this one gene. Using western blot, the time of synthesis and level of expression of the gB glycoprotein was identical in the wild type and recombinant viruses (not shown), indicating that the BV/GFP expression cassette insertion did not alter expression of the UL27 gene.

In vivo comparison of wtSaHV-1 to SaHV-1rG1 and SaHV-1rG3

To determine if insertion of the GFP expression cassette or expression of GFP in infected cells altered the pathogenic behavior of the virus *in vivo*, Balb/c mice were experimentally infected with wild-type and recombinant viruses. As previously reported, mice inoculated with $\geq 10^3$ PFU of wtSaHV-1 routinely exhibit pruritic, ulcerative skin lesions near the site of inoculation and often developed unilateral and occasionally bilateral hindlimb paresis or paralysis [2]. SaHV-1rG1, SaHV-1rG3 or wtSaHV-1 all exhibited a similar progression of clinical disease and development of gross lesions (Table 1). Mice inoculated with 10^5 or 10^6 PFU of either wild type or recombinant virus began at day 5 PI to develop pruritic, ulcerative skin lesions that increased in size and severity until approximately day 12 PI. A few mice in lower dosage groups of all viral strains developed similar skin lesions 2-3 days after mice receiving higher doses of virus. Beginning on day 7 or 8 and through day 12 PI, mice receiving 10^5 or 10^6 PFU of wild type or recombinant virus exhibited unilateral and occasionally bilateral abnormal hindlimb posture, paresis or paralysis that sometimes increased in severity until euthanasia was deemed necessary. Sporadically, mice receiving lower doses of virus also developed abnormal hindlimb posture, paresis or rarely paralysis in much the same time frame as those in higher dosage groups. ELISA on individual sera indicated the production of anti-SaHV-1 IgG in all animals receiving 10^5 or 10^6 PFU of wild type or recombinant SaHV-1, in the majority of animals receiving 10^3 and 10^4 PFU of virus, and in roughly half of the animals receiving 10^2 PFU. Probit regression was used to calculate the 50% infectious dose (ID_{50}) as well as the dose needed to cause CNS disease in 50% of animals ($CNSD_{50}$) for each of the viruses. ID_{50} values were found to not be

significantly different ($10^{2.24}$ for wtSaHV-1, $10^{1.89}$ for SaHV-1rG1 and $10^{2.31}$ for SaHV-1rG3). CNSD₅₀ values of wtSaHV-1 and SaHV-1rG1 were not significantly different between wtSaHV-1 ($10^{5.01}$) and SaHV-1rG1 ($10^{4.95}$), while the CNSD₅₀ of SaHV-1rG3 was slightly lower ($10^{4.21}$) than either the wtSaHV-1 or SaHV-1rG1.

Microscopic lesions seen in mice inoculated with wild type or recombinant SaHV-1 were indistinguishable. In all but three mice, significant lesions were restricted to the skin and CNS. Typical skin lesions consisted of a necrotizing, ulcerative dermatitis and folliculitis at the site of inoculation. Lesions in the CNS were restricted to the thoracic and lumbar spinal cord, including dorsal root ganglia in these regions. The most frequent lesion present in animals inoculated with either wild type or recombinant virus was mild to severe microglial and lymphocytic inflammation in the ipsilateral dorsal horn with rarefaction of the dorsal funiculus in the thoracic and lumbar segments. These lesions were typically present in mice exhibiting abnormal unilateral hindlimb posture or paresis. Non-suppurative inflammation in the dorsal root ganglia was also fairly common in these mice. Mice sporadically demonstrating acute, severe bilateral paresis/paralysis exhibited a diffuse, severe necrotizing myelitis in thoracic spinal cord regions. Sporadic lesions present in tissues other than skin or CNS included multifocal adrenal gland necrosis in one mouse given 10^4 PFU of wild type virus and one mouse given 10^6 PFU of the SaHV-1rG3 recombinant strain as well as non-suppurative ganglioneuritis in the colonic myenteric plexus of one mouse given 10^6 PFU of the SaHV-1rG1 recombinant virus. Lesions at these locations have not previously been reported.

Microscopic detection of GFP in tissues from experimentally infected mice

Since the recombinant viruses express GFP during their replication, GFP should be detectable in tissues where the virus is actively replicating. Several techniques were tested in attempts to prepare sections of skin and spinal cord for microscopic detection of GFP, including paraformaldehyde fixation with sucrose/OCT infiltration as well as snap-freezing of fresh tissue, both for cryosectioning. Neither of these techniques preserved tissue morphology or allowed visualization of a strong fluorescent signal. Furthermore, background fluorescence was problematic, particularly in neural tissue. The only fixation technique that allowed detection of GFP while also preserving tissue morphology was brief formalin fixation followed by paraffin embedding as described in Materials and Methods.

Using scanning confocal microscopy, skin lesions exhibited bright and specific green fluorescence within individual keratinocytes in the epidermis (Fig. 4G). In sections of thoracic and lumbar spinal cords from these same mice, the dorsal horn of gray matter ipsilateral to the site of injection contained individual neurons with fluorescent cytoplasm (Fig.4H). The fluorescence in both the skin and spinal cord corresponded with microscopic lesions visible on serial sections stained with H&E (Fig.4A,B), although fluorescence within the section of skin examined involved a smaller area than the lesion visible on H&E. Tissue sections were also immunohistochemically stained to unequivocally identify SaHV-1 viral antigen as well as GFP. Foci of cells positive for viral antigen or GFP corresponded with fluorescence detected by confocal microscopy and focal lesions seen in H&E stained sections of both skin (Fig.4A,C,E,G) and spinal cord (Fig.4B,D,F,H). Again, the area of skin exhibiting fluorescence was smaller than

the areas staining positive for GFP or SaHV-1 antigen. These results demonstrate that the observed fluorescence is co-localized with the presence of GFP, viral antigen and microscopic lesions, thereby validating the specificity of green fluorescence for viral replication in tissue sections.

Discussion

Construction of GFP-expressing viral mutants has been described by many investigators using a number of viruses. Most commonly, the GFP coding sequence is inserted in the viral genome either fused to or in place of an existing viral gene. These approaches not only disrupt expression of the targeted viral gene, but can also affect the expression of adjacent genes within the same multi-gene transcriptional set [5]. In this study, we sought to produce a GFP-expressing virus that expressed all genes the same as wt virus so as to minimize if not eliminate any changes to the pathogenesis of the virus *in vivo*.

In vitro characterization of two recombinant SaHV-1 viruses by PCR and Southern blot unequivocally demonstrated the desired placement of a single copy of the BV/GFP expression cassette into the UL26/UL 26.5 – UL 27 intergenic space of the viral genome. The appearance of bright and complete fluorescence in cells infected with recombinant virus clearly indicates that SaHV-1 is able to recognize and utilize the UL19 transcriptional elements of BV to express GFP beginning at about 5 hours PI and increasing with time. Neither the insertion of the GFP expression cassette nor production of GFP in infected cells was found to alter the CPE produced by the virus, the rate or

efficiency of virus replication, or expression of the UL27 gene located adjacent to the inserted expression cassette.

The *in vivo* experimental results demonstrated that there were minimal differences in the severity or progression of disease caused by recombinant SaHV-1 as compared to wtSaHV-1. The host antibody response was similar for wild type and recombinant viruses, and both gross and microscopic lesions were essentially identical between animals receiving equivalent doses of either virus. It has been suggested that GFP expression may be toxic to mammalian cells [22]; and therefore, recombinant viruses expressing GFP could be either more or less pathogenic than a wild type virus. We did not detect any such differences. As shown in Table 1, one recombinant (SaHV-1rG1) was no different from wtSaHV-1 in any parameter measured, and the other recombinant (SaHV-1rG3) exhibited minor differences that were randomly distributed through clinical signs and dosage groups. In fact, the statistical analysis of CNS disease occurrence argues that the variability in disease severity is not associated with GFP expression, since the CNSD₅₀ of wtSaHV-1 and SaHV-1rG1 are not significantly different and the CNSD₅₀ of SaHV-1rG3 alone is slightly lower. Rather, this minor increase in pathogenicity is likely secondary to a slight difference in viral dose titration combined with individual variation among animals. Given the lack of detectable differences in the *in vitro* and *in vivo* behavior of SaHV-1rG1 or SaHV-1rG3 as compared to wtSaHV-1 (other than the expression of GFP), the recombinant virus should prove useful for further development of a small animal α -herpesvirus model.

The use of a GFP-expressing recombinant virus in pathogenesis studies will allow specific and sensitive detection of viral replication within individual cells without

precluding the use of immunohistochemical stains for host cell type identification or characterization of an infiltrating inflammatory cell population. The increased area of positive immunostaining signal within skin lesions compared to GFP fluorescence at these sites might indicate a lower sensitivity of GFP detection. However, the smaller focus of fluorescence (Fig. 4G) in the skin compared with immunostaining for SaHV-1 antigen or GFP (Fig. 4C,E) is likely due to variability in the actual size of the lesion present in each tissue section, since these lesions are small and tissues photographed are not adjacent sections from the same block, but are several 5 μ m sections apart or are from a similar lesion in a different tissue block (Fig. 4C). Also, the extent of positive signal in immunohistochemical stains for SaHV-1 antigen or GFP within spinal cord (Fig. 4D,F) corresponds exactly with fluorescence (Fig. 4H) in sections from the same tissue block. Therefore, the apparent variability of GFP fluorescence compared to GFP or SaHV-1 antigen detection in the skin is not likely to be a function of decreased sensitivity of GFP detection, but rather represents an artifact of plane of section in the skin samples used. GFP expression specifically indicates viral replication, and not merely the presence of viral antigen as does IHC. This provides a tool for tracing the route of virus from the site of inoculation to the CNS via identification of specific host cells that support active replication of the virus. The specificity of GFP expression to infected cells combined with the concurrent use of IHC to characterize the cellular host response to infection should throw light on finer details of the neuropathogenesis of SaHV-1 as a model of simian α -herpesviruses.

In previously reported studies using GFP as a marker of viral replication, GFP fluorescence was detected in fresh sections of brain maintained in medium [8] or

paraformaldehyde fixed cryosections of brain [4, 20]. Other investigators have indirectly detected GFP in tissues by immunohistochemistry [4, 20]. Given that tissues of primary interest in our study were spinal cord and skin, the previously described GFP detection methods (aside from the more laborious immunohistochemistry) were not optimal for use in detailed studies of viral neuropathogenesis. Furthermore, tissues prepared by these methods are not easily archived, nor are they suitable for subsequent procedures such as immunohistochemical staining for the identification of various cell types. Thus, detection of GFP in tissue sections was challenging, particularly in the spinal cord where certain fixation techniques contributed to substantial non-specific autofluorescence. Using the described tissue processing technique, tissue morphology as well as GFP fluorescence is well preserved. Aside from the abbreviated formalin fixation period and EDTA decalcification, tissue processing techniques are essentially identical to those used for routine histopathological specimen processing. Fortunately, enhanced GFP maintains fluorescence through the high temperatures and solvent clearing steps of paraffin embedding. Importantly, this allows paraffin embedded tissues to be archived and available for GFP detection, routine H&E staining, and selected special stains from the same tissue block, thus negating the need for duplicate tissue specimens processed by different techniques.

The successful construction of a GFP expressing strain of SaHV-1 without altering the ability of the virus to grow in culture or spread and cause disease in experimentally infected mice, combined with the demonstrated utility of GFP as a readily detectable signal in histological tissue specimens opens the door to many exciting possibilities for future neuropathogenesis studies. This recombinant virus, used in

conjunction with simple microscopic detection, will be a powerful tool in elucidating the specific neural route of SaHV-1 from the inoculation site to the CNS and in illuminating its transneuronal spread within the spinal cord of infected animals.

Acknowledgements

This work is supported by PHS grants R01 RR07849 and P40 RR12317. The first author (M.A.B.) is a Howard Hughes Medical Institute Predoctoral Fellow. We gratefully acknowledge Dr. Mark Payton for assistance with the statistical analysis of data.

We also gratefully acknowledge Ms. Sandra Horton and Ms. Monica Mattmuller at North Carolina State University for technical assistance with immunohistochemical staining and the Electron Microscopy Lab at Oklahoma State University for assistance with confocal microscopy.

References

1. Brack M (1977) Morphological and Epidemiological Aspects of Simian Herpesvirus Infections. Verlag Paul Parey, Berlin & Hamburg
2. Breshears MA, Eberle R, Ritchey JW (2001) Characterization of gross and histological lesions in Balb/c mice experimentally infected with *Herpesvirus saimiri 1* (HVS1). J Comp Pathol 125: 25-33
3. Daniel MD, Karpas A, Melendez LV, King NW, Hunt RD (1967) Isolation of herpes-T virus from a spontaneous disease in squirrel monkeys (*Saimiri sciureus*). Arch Gesamte Virusforsch 22: 324-331
4. DeFalco J, Tomishima M, Liu H, Zhao C, Cai X, Marth JD, Enquist L, Friedman JM (2001) Virus-assisted mapping of neural inputs to a feeding center in the hypothalamus. Science 291: 2608-13
5. Demmin GL, Clase AC, Randall JA, Enquist LW, Banfield BW (2001) Insertions in the gG gene of pseudorabies virus reduce expression of the upstream Us3 protein and inhibit cell-to-cell spread of virus infection. J Virol 75: 10856-69
6. Desrosiers RC, Falk LA, Jr. (1981) Herpesvirus tamarinus and its relation to herpes simplex virus. J Gen Virol 56: 119-130
7. Dolan A, Jamieson FE, Cunningham C, Barnett BC, McGeoch DJ (1998) The genome sequence of herpes simplex virus type 2. J Virol 72: 2010-21
8. Duprex WP, McQuaid S, Roscic-Mrkic B, Cattaneo R, McCallister C, Rima BK (2000) In vitro and in vivo infection of neural cells by a recombinant measles virus expressing enhanced green fluorescent protein. J Virol 74: 7972-9
9. Eberle R, Courtney RJ (1980) Preparation and characterization of specific antisera to individual glycoprotein antigens comprising the major glycoprotein region of herpes simplex virus type 1. J Virol 35: 902-17

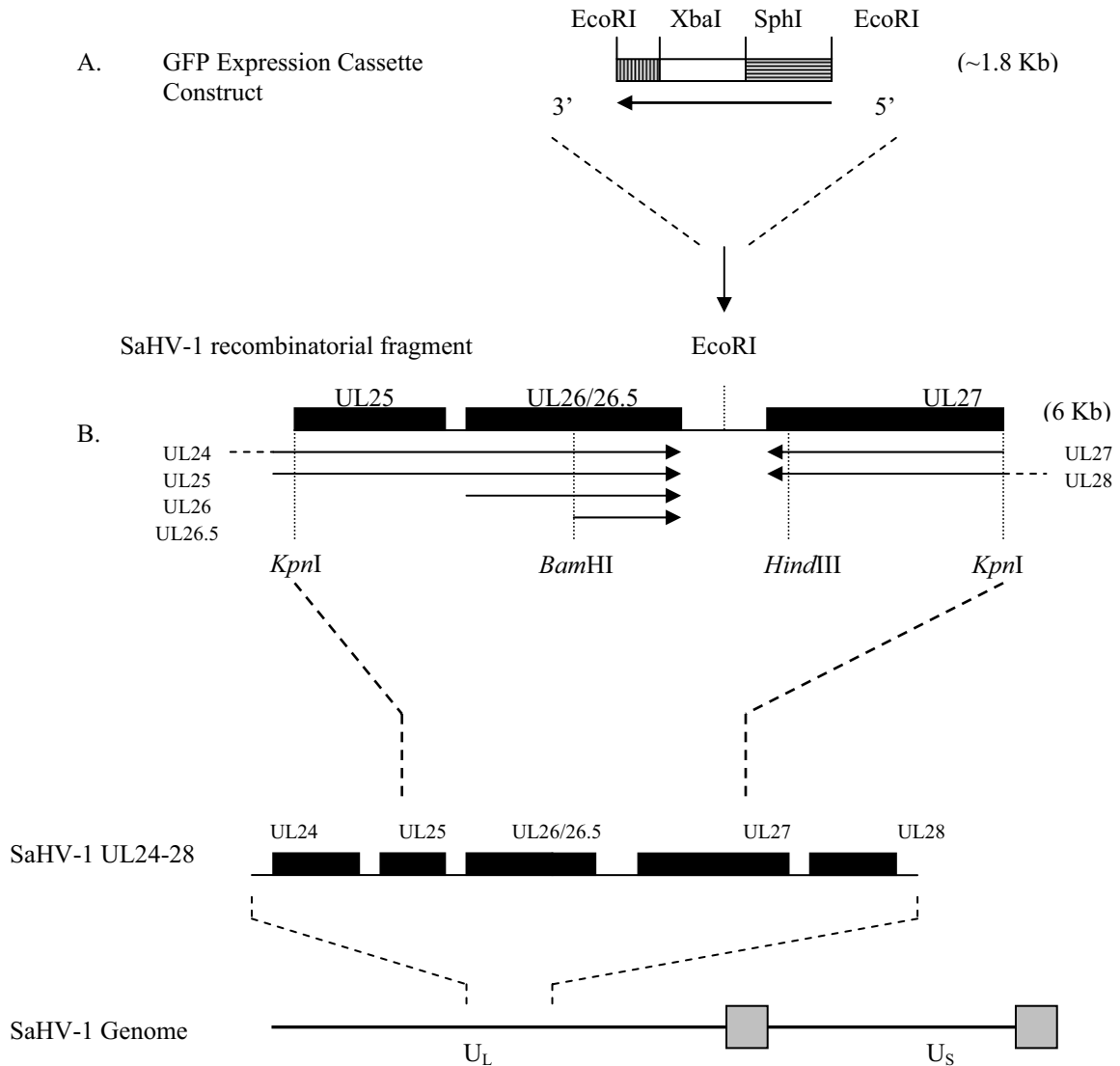
10. Eberle R, Mou SW, Zaia JA (1985) The immune response to herpes simplex virus: comparison of the specificity and relative titers of serum antibodies directed against viral polypeptides following primary herpes simplex virus type 1 infections. *J Med Virol* 16: 147-62
11. Eberle R, Black D, Hilliard JK (1989) Relatedness of glycoproteins expressed on the surface of simian herpes-virus virions and infected cells to specific HSV glycoproteins. *Arch Virol* 109: 233-252
12. Eberle R, Hilliard J (1995) The simian herpesviruses. *Infect Agents Dis* 4: 55-70
13. Eberle R, Tanamachi B, Black D, Blewett EL, Ali M, Openshaw H, Cantin EM (1997) Genetic and functional complementation of the HSV1 UL27 gene and gB glycoprotein by simian alpha-herpesvirus homologs. *Arch Virol* 142: 721-736
14. Emmons RW, Gribble DH, Lennette EH (1968) Natural fatal infection of an owl monkey (*Aotus trivirgatus*) with Herpes T virus. *J Infect Dis* 118: 153-159
15. Graham FL, van der Eb AJ (1973) A new technique for the assay of infectivity of human adenovirus 5 DNA. *Virology* 52: 456-67
16. Hilliard JK, Black D, Eberle R (1989) Simian alphaherpesviruses and their relation to the human herpes simplex viruses. *Arch Virol* 109: 83-102
17. Holmes AW, Dedmon RE, Deinhardt F (1963) Isolation of a new herpes-like virus from south american marmosets. *Federation Proceedings* 22: 324
18. Holmes AW, Caldwell RG, Dedmon RE, Deinhardt F (1964) Isolation and characterization of a new herpes virus. *J Immunol* 92: 602-610
19. Hunt RD, Melendez LV (1966) Spontaneous herpes-T infection in the owl monkey (*Aotus trivirgatus*). *Pathol Vet* 3: 1-26
20. Irnaten M, Neff RA, Wang J, Loewy AD, Mettenleiter TC, Mendelowitz D (2001) Activity of cardiorespiratory networks revealed by transsynaptic virus expressing GFP. *J Neurophysiol* 85: 435-8

21. Leib DA, Hart CA, McCarthy K (1987) Characterization of four herpesviruses isolated from owl monkeys and their comparison with *Herpesvirus saimiri* type 1 (*Herpesvirus tamarinus*) and herpes simplex virus type 1. *J Comp Pathol* 97: 159-169
22. Liu HS, Jan MS, Chou CK, Chen PH, Ke NJ (1999) Is green fluorescent protein toxic to the living cells? *Biochem Biophys Res Commun* 260: 712-7
23. McGeoch DJ, Dalrymple MA, Davison AJ, Dolan A, Frame MC, McNab D, Perry LJ, Scott JE, Taylor P (1988) The complete DNA sequence of the long unique region in the genome of herpes simplex virus type 1. *J Gen Virol* 69 (Pt 7): 1531-74
24. Mou SW, Hilliard JK, Song CH, Eberle R (1986) Comparison of the primate alphaherpesviruses. I. Characterization of two herpesviruses from spider monkeys and squirrel monkeys and viral polypeptides synthesized in infected cells. *Arch Virol* 91: 117-133
25. Ohsawa K, Lehenbauer TW, Eberle R (1999) *Herpesvirus papio 2*: alternative antigen for use in monkey B virus diagnostic assays. *Lab Anim Sci* 49: 605-16
26. Ohsawa K, Black DH, Sato H, Rogers K, Eberle R (2003) Sequence and genetic arrangement of the UL region of the monkey B virus (*Cercopithecine herpesvirus 1*) genome and comparison with the UL region of other primate herpesviruses. *Arch Virol* 148: 989-97
27. Palmer AE (1987) B virus, *Herpesvirus simiae*: historical perspective. *J Med Primatol* 16: 99-130
28. Perelygina L, Zhu L, Zurkuhlen H, Mills R, Borodovsky M, Hilliard JK (2003) Complete sequence and comparative analysis of the genome of herpes B virus (*Cercopithecine herpesvirus 1*) from a rhesus monkey. *J Virol* 77: 6167-77
29. Schrier A (1966) Editor's notes. *Laboratory Primate Newsletter* 5: ii
30. Simon MA, Daniel MD, Lee-Parritz D, King NW, Ringler DJ (1993) Disseminated B virus infection in a cynomolgus monkey. *Lab Anim Sci* 43: 545-50

31. Walter I, Fleischmann M, Klein D, Muller M, Salmons B, Gunzburg WH, Renner M, Gelbman W (2000) Rapid and sensitive detection of enhanced green fluorescent protein expression in paraffin sections by confocal laser scanning microscopy. *Histochem J* 32: 99-103

32. Weigler BJ (1992) Biology of B virus in macaque and human hosts: a review. *Clin Infect Dis* 14: 555-567

Fig. 1. Insertion of GFP expression cassette into the SaHV-1 genome. The GFP expression cassette was constructed by flanking the GFP ORF (□) with BV UL19 promoter (▨) and UL18/19/20 transcriptional termination sequences (▧) (A). The GFP expression cassette was inserted into an *EcoRI* restriction site inserted by mutagenic PCR between juxtaposed polyadenylation/mRNA termination sequences within the SaHV-1 UL26-UL27 intergenic space (B). The viral ORFs (■) and mRNA transcripts shown below by arrows are based on that of HSV1 (McGeoch *et al.*, 1988; Dolan *et al.*, 1998) and BV (Ohsawa *et al.*, 2003; Pereylygina *et al.*, 2003), and are consistent with available SaHV-1 sequence data. The reassembled 6 Kbp *KpnI* fragment was excised from the vector, gel-purified and co-transfected with genomic SaHV-1 DNA in Vero cells to generate recombinant virus.



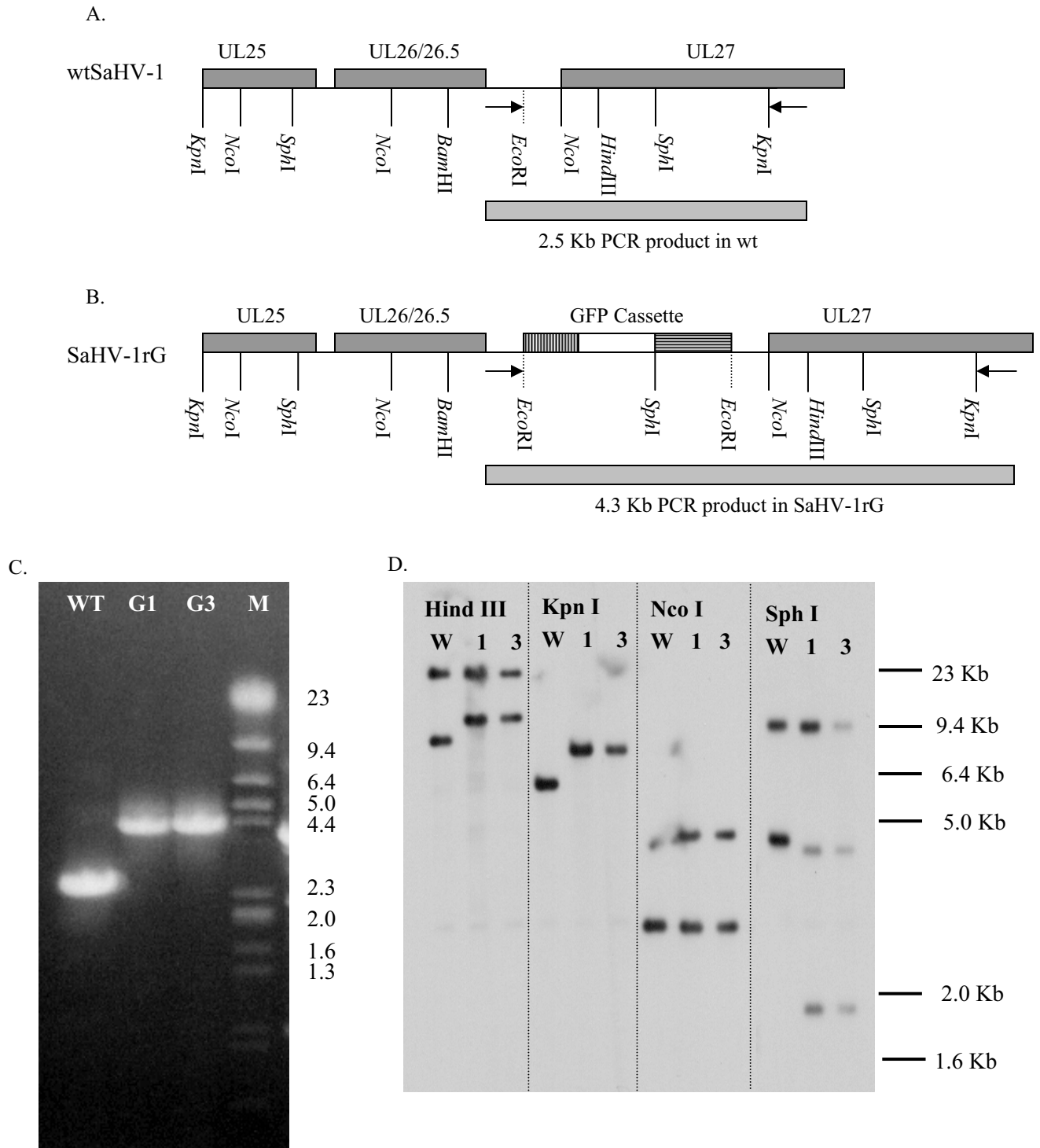


Fig. 2. Characterization of wtHVS1, HVS1rG1 and HVS1rG3. Restriction maps for the region of the genome in wtHVS1 based on sequence data (A) and predicted for the recombinant viruses (B) are shown. The location of PCR primers and their products as described in the text are shown beneath the maps. Actual PCR products amplified are shown in (C). A Southern blot using the 6 Kbp fragment (pUQK3) from wtHVS1 as probe is shown in (D) and is described in the text.

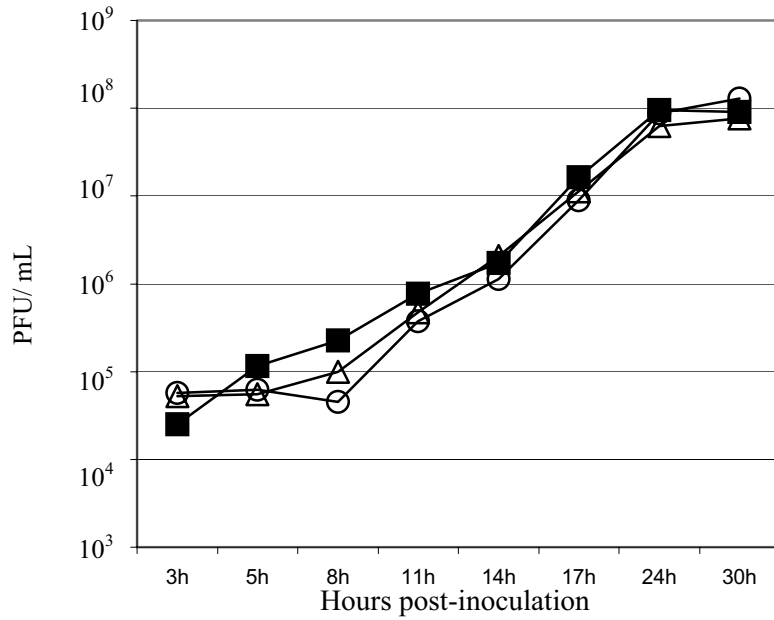
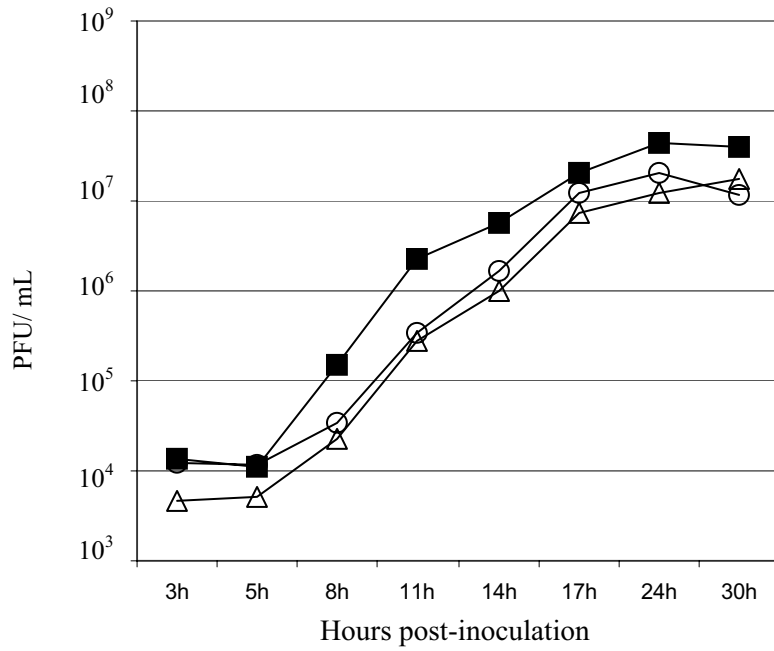


Fig. 3. Time course of replication of wild-type and recombinant HVS1. Cell associated virus (top) and extracellular virus (bottom) are indicated as follows: wtHVS1, (■); HVS1rG1, (△); HVS1rG3, (○).

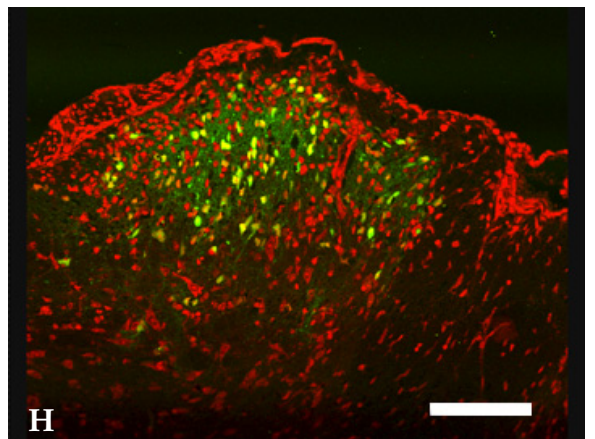
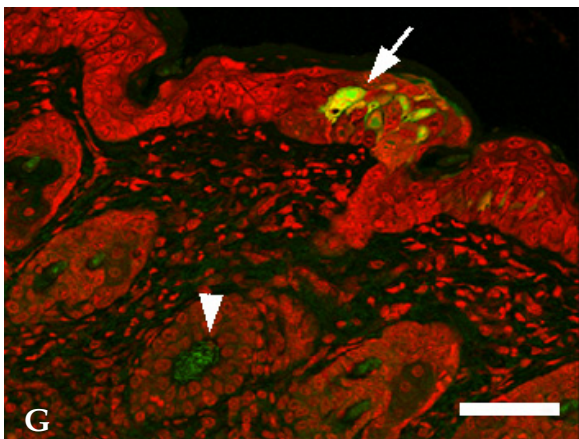
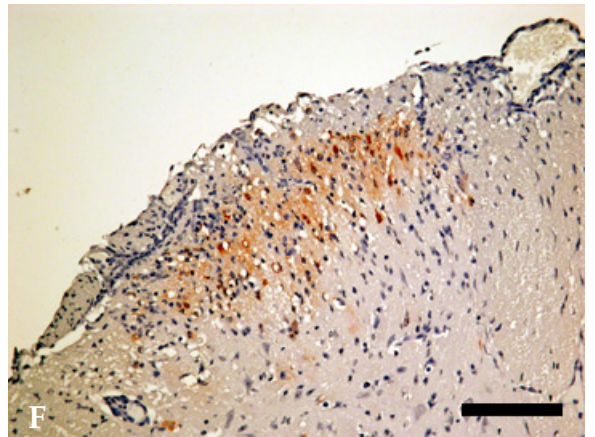
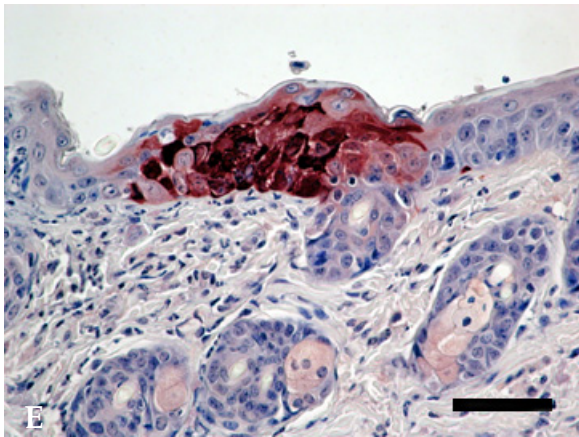
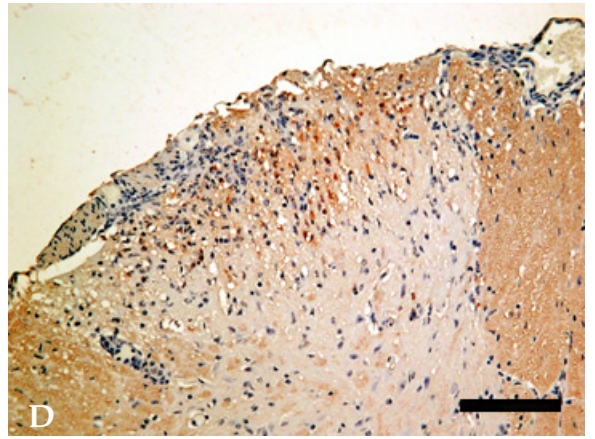
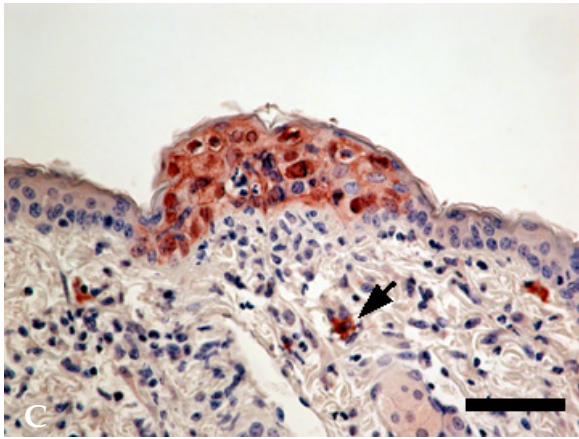
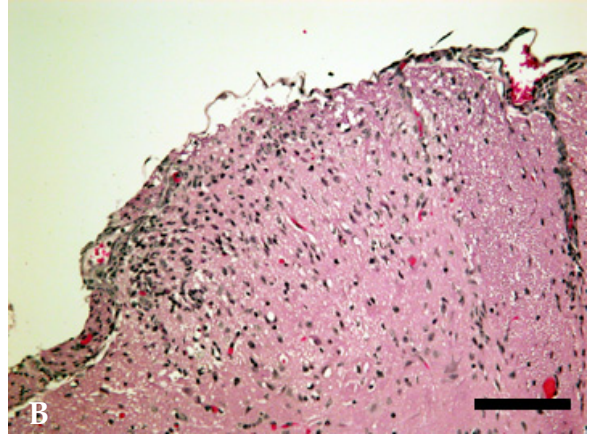
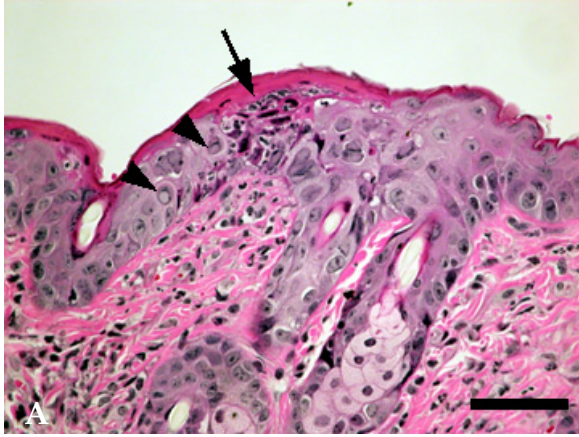


Fig. 4 (previous page). Skin and spinal cord lesions in mice given 10^6 PFU SAHV-1rG, 6 days p.i. Sections of skin (A,E,G) were cut from the same tissue block; skin section C is from a similar lesion in a different animal. In the H&E stained section of skin (A), necrotic keratinocytes (arrow) are surrounded by keratinocytes with intranuclear inclusions (arrowheads). Immunostaining with anti-SAHV-1 antibody (C) and with anti-GFP antibody (E) demonstrates the presence of viral antigen (C) and GFP (E) within skin lesions. In (C), mast cells (arrow) stain non-specifically with the anti-SAHV-1 polyclonal antibody. Confocal microscopy (G) reveals a focus of green fluorescence (arrow) that corresponds with the same lesion in (A) and (E); hairshafts exhibit autofluorescence (arrowhead). Sections of thoracic spinal cord (B,D,F,H) were cut from the same tissue block. In the H&E stained section (B), inflammatory cells consisting primarily of neutrophils infiltrate the ipsilateral dorsal grey horn. The anti HVS-1 immunostain (D) and the anti-GFP immunostain (F) demonstrate the presence of SAHV-1 antigen and GFP, respectively. Viral antigen and GFP are localized primarily within neurons of this region. Confocal microscopy reveals corresponding green fluorescence (H). Bar markers in skin photos (A,C,E,G) equal 50 μm . Bar markers in spinal cord photos (B,D,F,H) equal 125 μm .

Table 1 -Clinical Signs and Seropositivity

Clinical Signs	Virus	Virus dose ^a				
		10 ²	10 ³	10 ⁴	10 ⁵	10 ⁶
Skin Lesion	wtSaHV-1	2 ^b	1	1	5	6
	SaHV-1rG1	1	2	2	7	7
	SaHV-1rG3	1	2	1	6	8
Paresis/ Paralysis	wtSaHV-1	0	1	1	1	4
	SaHV-1rG1	0	0	0	3	3
	SaHV-1rG3	0	1	0	3	4
Early Euthanasia	wtSaHV-1	0	1	1	0	4
	SaHV-1rG1	0	0	0	1	3
	SaHV-1rG3	0	0	0	3	3
Anti-SaHV-1 Serum IgG	wtSaHV-1	5	3	8	8	8
	SaHV-1rG1	5	5	7	8	8
	SaHV-1rG3	2	8	7	8	8

^aGroups of 8 mice given virus in 20 µl volume

^bNumber represents the total number of mice in each group developing signs by 14 days PI.

CHAPTER V

TEMPORAL PROGRESSION OF VIRAL REPLICATION AND GROSS AND HISTOLOGICAL LESIONS IN BALB/C MICE EPIDERMALLY INOCULATED WITH *Saimiriine herpesvirus 1* (SaHV-1)

Summary

Saimiriine herpesvirus 1 (SaHV-1) is an alphaherpesvirus enzootic in squirrel monkeys that is genetically related to monkey B virus (BV) and human herpes simplex virus (HSV). To study the temporal progression of viral spread and associated lesions, Balb/c mice were epidermally inoculated with a green fluorescent protein (GFP)-expressing recombinant strain of SaHV-1 and sacrificed at sequential time points. Viral infection was initially recognized as pinpoint ulcerative lesions in the inoculated epidermis and progressed over a few days to result in unilateral or bilateral hindlimb paresis/paralysis, urinary and fecal incontinence, abdominal distension, hunched posture and eventual depression warranting euthanasia. Viral replication was present within epidermal keratinocytes, neurons of the dorsal root ganglia and thoracolumbar spinal cord, regional autonomic ganglia, lower urinary tract epithelium and colonic myenteric plexuses as indicated by histological lesions and GFP expression. All but one mouse inoculated with 10^5 or 10^6 PFU SaHV-1 developed severe, rapidly progressive disease. Two of eight mice inoculated with 10^4 PFU virus developed disease while no mice receiving less than 10^4 PFU virus developed evidence of infection. All mice that showed no clinical signs of

disease following inoculation also failed to develop an antiviral IgG response, indicating that an active viral infection was not established in these animals. For SaHV-1 inoculated epidermally, the ID₅₀, CNSD₅₀ and LD₅₀ values are identical (10^{4.38}), indicating that infection by this route invariably results in lethal CNS disease. Consistently severe disease in all infected animals with regionally extensive distribution of viral replication differs markedly from the disease process that occurs in mice inoculated intramuscularly with SaHV-1.

Introduction

Saimiriine herpesvirus 1 (SaHV-1) is an alphaherpesvirus that is enzootic in squirrel monkey populations and is genetically related to *Cercopithecine herpesvirus 1* or monkey B virus (BV) and human herpes simplex virus (HSV) (Desrosiers and Falk, 1981; Eberle *et al.*, 1989; Hilliard *et al.*, 1989; Leib *et al.*, 1987). Similar to BV in macaques, SaHV-1 infection in the natural host is usually clinically inapparent but occasionally results in ulcerative oral lesions (Daniel *et al.*, 1967). Also similar to BV, SaHV-1 infection of aberrant hosts such as marmosets and owl monkeys results in the development of severe fatal disease with disseminated, multifocal necrosis of visceral organs that occasionally involves the central nervous system (CNS) (Emmons *et al.*, 1968; Holmes *et al.*, 1964; Holmes *et al.*, 1963; Hunt and Melendez, 1966). While not documented to cause disease in humans, SaHV-1 has been presumptively associated with one case of encephalitis in a research psychologist having contact with squirrel monkeys, but with no known bites or scratches (Schrier, 1966). SaHV-1 was implicated because the researcher exhibited a

rising antibody titer to SaHV-1. Virus isolation was not attempted to confirm the infection.

HSV has long been used as a model of alphaherpesvirus neurovirulence and pathogenesis in laboratory animals and has been investigated in mice using several routes of inoculation. The route of virus exposure has a significant effect on the severity of disease caused by HSV infection (Irie *et al.*, 1992; McDermott *et al.*, 1984; Richards *et al.*, 1981; Rooney *et al.*, 1989; Wharton *et al.*, 1995). The skin scarification model of HSV infection closely mimics the typical process of an alphaherpesvirus infection, beginning with viral replication in keratinocytes at the site of inoculation followed by spread into free, unmyelinated nerve endings within the epidermis. Upon gaining access to peripheral afferent nerves, the virus travels via retrograde intra-axonal transport to dorsal root ganglia (DRG) where it replicates, and then travels back down sensory nerves by anterograde transport to infect epidermal epithelium in a broader region of the dermatome (Blyth *et al.*, 1984; Simmons and Nash, 1984; Sydiskis and Schultz, 1965). The epidermal basement membrane has been shown to restrict the pathogenesis of HSV by preventing intradermally or subcutaneously injected virus from reaching free nerve endings in the epidermis (Weeks *et al.*, 2000), which provide an efficient route of virus entry into the peripheral nervous system. Thus, viral replication within epidermal cells or the inoculation of infectious virus in quantities adequate to directly enter nerve endings is essential for neuronal infection.

Free, unmyelinated nerve endings within the cutaneous epithelium make up the largest group of nociceptive neurons, or sensory fibers that signal noxious events (Best *et al.*, 1991). Some of these fibers have low conduction velocities in the C-fiber range, are

not surrounded by protective lamina (Best *et al.*, 1991) and are characterized by their sensitivity to capsaicin, which excites and subsequently desensitizes the afferents (Holzer, 1991). It has been reported that mice treated with capsaicin exhibit degeneration of type C sensory neurons and subsequent decreased mortality of HSV-1 infection (Ljungdahl *et al.*, 1986). Similarly, guinea pigs treated with capsaicin prior to cutaneous inoculation with HSV-2 had reduced zosteriform spread of herpetic lesions, demonstrating that capsaicin-sensitive nerve fibers play a significant role in herpesvirus pathogenesis (Stanberry *et al.*, 1992). Likewise, humans affected by familial dysautonomia, an autosomal disorder in which patients are deficient in type C fibers, are better protected from HSV-1 infection than neurologically normal individuals (Maayan *et al.*, 1998). These observations, which associate decreased unmyelinated type C nerve fibers with increased resistance to HSV infection and spread, suggest that the port of viral entry from epithelium into the nervous system is the unmyelinated type C nerve fiber (Maayan *et al.*, 1998). While the type of nerve fiber involved in neural uptake of simian alphaherpesviruses has not been determined, it has been demonstrated that unmyelinated axons are most severely affected by SaHV-1 infection in intradermally inoculated rabbits (Illanes *et al.*, 1990a; Illanes *et al.*, 1990b). This observation supports similarities in the neuronal uptake of HSV and SaHV-1, and lends importance to the investigation of SaHV-1 infection via epidermal inoculation as a potential comparative model for HSV neuropathogenesis.

Given that HSV is a virus of human origin, all *in vivo* studies must be performed in xenogeneic experimental hosts. In contrast, for a non-human virus like SaHV-1, it is possible to characterize the disease and compare viral neuropathogenesis in both natural

and model host systems. In an effort to establish a small animal model system for exploration of simian alphaherpesvirus pathogenesis and comparison of neurovirulence of related viruses, gross and microscopic lesions of SaHV-1 in mice inoculated intramuscularly have been characterized (Breshears *et al.*, 2001). In addition, a green fluorescent protein (GFP)-expressing strain of SaHV-1 was constructed and shown to behave similar to the wild-type virus *in vitro* and *in vivo*, thus allowing microscopic detection of virus replication in tissues of experimentally infected mice (Breshears *et al.*, 2003). In this report, we describe the progression of viral replication and formation of associated lesions in mice following epidermal inoculation with a GFP-expressing recombinant strain of SaHV-1.

Materials and Methods

Virus and Cells

A GFP-expressing recombinant virus strain designated SaHV-1rG (Breshears *et al.*, 2003), was used for all experiments. The virus was propagated in Vero cells grown in Dulbecco's modified Eagle medium (DMEM) containing fetal bovine serum (FBS) 10%, 200mM L-glutamine, penicillin 100 IU/ml and streptomycin 100 µg/ml. Viral stocks were prepared by infecting subconfluent Vero cell monolayers with SaHV-1rG at a low multiplicity of infection (<0.01). Infected cell cultures were maintained at 37°C in DMEM supplemented with FBS 2% until cytopathic effect (CPE) had spread throughout the entire monolayer. The culture flasks were freeze-thawed three times, the contents pooled and centrifuged for 5 min at 1000g to remove cell debris. The supernatant was

collected, titrated by standard methods, dispensed in small volumes and stored at -70°C (Breshears *et al.*, 2001)

Animals

Specific-pathogen free, 13-15 gram female Balb/c mice (Charles River Laboratories, Inc., Wilmington, Massachusetts, USA) were used for all experiments. For skin inoculation, mice were anaesthetized by Metofane[®] (Schering-Plough Animal Health Corp., Union, New Jersey, USA) inhalation and hair removed from the posterior and lateral aspects of the left hip and thigh using Nair[®] depilatory cream (Carter-Wallace, Inc., New York, New York, USA) followed by a water rinse. One to two days following hair removal, mice were again anaesthetized and inoculated by epidermal scarification on the depilated skin overlying the left caudo-lateral hip region. The epidermis was lightly scarified with the point of a 22ga hypodermic needle to form a grid of 0.5 cm lines, 3 in each direction, virus (20 μl) was applied to the site, spread briefly with the needle shaft, and then scarified 5 more times over the inoculum in each direction. Scarification was performed so that the superficial epidermis was interrupted without inducing hemorrhage. Control mice were depilated, scarified and mock-inoculated with 20 μl of sterile PBS.

The 50% infectious dose (ID_{50}) was calculated using the appearance of an anti-viral IgG response as evidence of active viral infection. In addition, animals that developed clinical signs of disease but were killed prior to development of a detectable anti-viral IgG response were included in calculation of the ID_{50} . The ID_{50} , the 50% lethal dose (LD_{50}) and the dose needed to cause central nervous system (CNS) disease in 50 % of animals (CNSD_{50}) were determined using groups of eight mice inoculated with 10-fold

dilutions of virus ranging from 10^1 to 10^6 plaque forming units (PFU). Mice were observed twice daily for clinical signs of disease, and any markedly weak, depressed or moribund animals or those with extensive skin lesions were killed by carbon dioxide asphyxiation. All surviving mice were killed at 14 days post-inoculation (p.i.). To achieve consistent disease in all mice for temporal studies, mice were inoculated with 10^6 PFU of virus, a dose determined by the 10-fold dose inoculation study to result in disease in 100% of mice. Groups of 5 mice were sacrificed on sequential days from 1 day to 9 days p.i. Severely depressed or moribund animals from all groups were sacrificed early as necessary and animals from a pool of ten extra mice were randomly substituted to allow the sacrifice of 5 mice for each time point. Nevertheless, only two mice remained for sacrifice by day 9 p.i. All mice were exsanguinated via intracardiac puncture immediately following euthanasia and individual sera were stored at -70°C .

Necropsy and Histopathology

All mice with clinical signs of disease were subjected to a comprehensive post-mortem examination. Tissue samples from visceral organs and brain were fixed in 10% neutral buffered formalin for 18-24 hours and processed for histopathology and GFP detection as previously described (Breshears et al., 2003; Walter *et al.*, 2000). The vertebral columns with spinal cords, ureters, urinary bladder, uterus and distal colon/rectum in situ and disarticulated left hindlimbs were fixed whole in 10% buffered formalin for approximately 24 hours. Following fixation, tissues were decalcified in a 0.5 M EDTA solution in water, pH 8.0 for 4-5 days before trimming into multiple 3-4 mm segments for processing and embedding.

For GFP detection, tissues were sectioned at 5 μm , mounted on positively charged slides, deparaffinized, rehydrated and counterstained with 132 $\mu\text{g/ml}$ propidium iodide in PBS for 3 min and coverslipped with fluorescent mounting media as described (Breshears *et al.*, 2003). Sections were screened for GFP fluorescence on a Nikon Eclipse TE200 inverted microscope and examined in more detail with a Leica SP2 laser scanning confocal microscope using two-channel detection with an argon laser and the filter setting for FITC/TRITC fluorescence. Routine histopathological examination was conducted on tissues sectioned at 5 μm and stained with haematoxylin and eosin (H&E).

ELISA was used for detection of anti-SaHV-1 IgG in serum samples as previously described (Breshears *et al.*, 2003). Seropositivity was defined as an optical density (OD) of greater than 0.1 and at least 2x control (negative) serum values (Table 1).

Statistical Evaluation

Probit regression was used to calculate the ID_{50} , LD_{50} and CNSD_{50} values for mice inoculated by epidermal scarification. Using methods developed for effective dosages (Robertson and Preisler, 1992), these values were compared to values for mice inoculated intramuscularly with the same virus in Table 2 (Breshears *et al.*, 2003).

Results

Clinical Disease and Gross Lesions

Although the skin scarification/ epidermal inoculation model has been used for HSV, it has not been described for other primate alphaherpesviruses. To determine if SaHV-1

behaves similarly to HSV, we performed an experiment utilizing skin scarification as the route of inoculation. The clinical findings following epidermal inoculation of ten-fold dilutions of SaHV-1 are summarized in Table 1. Overt clinical disease was recognized only in animals that were inoculated with at least 10^4 PFU of SaHV-1. All mice that exhibited clinical disease followed the same general progression of lesions and corresponding clinical signs. At 2 days p.i., 8/8 mice receiving 10^6 PFU and 3/8 mice receiving 10^5 PFU had early focal ulceration or roughening of the skin at the site of inoculation. All animals that would eventually develop overt clinical disease had detectable skin lesions at the inoculation site by 5 or 6 days p.i. Lesions typically began as focal or multifocal pinpoint erosions or ulcers in the scarified epidermis. By 4 days p.i., multiple individual ulcers radiating distally in a roughly linear fashion from the site of inoculation began to coalesce. Over the next 1-2 days, these ulcers progressed to involve a wider zone of skin on the lateral hip and leg, consistent with zosteriform spread (Blyth *et al.*, 1984; Goodpasture and Teague, 1923; Sydiskis and Schultz, 1965). Mice with skin lesions began to exhibit various degrees of abnormal splaying of the left hindlimb by day 5 p.i., which progressed to paresis or paralysis by 6 days p.i. with occasional paresis of the right hindlimb by 7 days p.i. Mice often became depressed with a ruffled haircoat and hunched posture. Urinary incontinence, characterized by urine staining of the perineal region, developed in some mice by 7 to 8 days p.i. Abdominal distension and flaccidity of the external anal orifice were also seen in a few animals. The severity of clinical disease dictated that all mice exhibiting lesions be killed on or before 9 days p.i. The average survival time for mice receiving 10^6 PFU was approximately 1.5

days shorter than for mice that developed clinical signs following inoculation with 10^5 or 10^4 PFU.

At necropsy, the majority of mice with overt clinical disease had grossly evident hydronephrosis of the ipsilateral kidney. Several mice also had marked cecal and colonic distension and occasional distension of the urinary bladder. The only other gross lesions observed at necropsy were the skin lesions at the site of inoculation described above. Mice not exhibiting epidermal lesions at the inoculation site by 6 days p.i. remained clinically normal for the duration of the experiment. In these animals as well as mock-inoculated controls, the inoculated sites were completely healed by day 14 p.i.

Sera from individual mice were tested by ELISA for anti-SaHV-1 IgG. All but four mice with clinical disease were positive for SaHV-1 IgG at the time of euthanasia (6-9 days p.i.) with OD values ranging from 0.18 to 0.66 (Table 1). Four mice with clinical disease that were euthanized at day 6 and 8 p.i. had OD values less than 0.1. Since IgG responses are not readily detected less than 9 days p.i., it was assumed that these mice would have developed an IgG response had they lived longer and so were included in the seropositive group for calculation of the ID_{50} . Epidermally inoculated mice that did not develop clinical disease remained seronegative, indicating absence of an active viral infection in all animals that failed to develop disease.

Establishment of an active SaHV-1 infection via the epidermal route invariably resulted in fatal CNS disease. Rather than some animals developing intermediate levels of disease severity, all mice that became infected by the virus developed severe disease similar to that seen in high dose groups. No mice developed moderate, non-fatal disease or became seropositive without manifesting clinical disease. The consistent relationships

between active viral infection, CNS disease and death are statistically demonstrated by the identical ID₅₀, LD₅₀ and CNSD₅₀ values. (Table 2)

Temporal Progression of Histological Lesions

A time course experiment was performed to follow the progression of SaHV-1 infection and the development of microscopic lesions in epidermally inoculated mice. Mice were inoculated epidermally with 10⁶ PFU SaHV-1 and groups of 5 mice were sacrificed daily for 9 days and tissues were examined for microscopic lesions as well as the presence of viral replication indicated by GFP expression. Results are briefly summarized in Table 3.

Microscopic lesions in the skin at the inoculation site were present as early as 24 hours p.i. and consisted of small foci of edema or spongiosis in the epidermis with intranuclear inclusion bodies in keratinocytes, early necrosis, and an associated mild neutrophilic dermatitis [Fig. 1A]. Control mice had a few discrete foci of superficial epidermal necrosis with no change in deeper epidermis and no inflammatory response. By 2 days p.i., skin lesions were characterized by multifocal epidermal and superficial dermal necrosis with suppurative dermatitis; intranuclear inclusion bodies were present within epithelium of the epidermis, hair follicles and rarely sebaceous glands. Foci of epidermal and dermal necrosis were overlain by a serocellular crust by 3 days p.i. Skin lesions progressed from multifocal to regionally extensive with deeper dermal necrosis and mild neutrophilic and mononuclear subcutaneous inflammation and edema by 4 days p.i. Aside from an increase in the intensity of the subcutaneous inflammation, skin lesions remained similar through day 8 p.i.

At 3 and 4 days p.i., 2/5 and 4/5 mice respectively had small foci to larger regions of necrotic neurons with intranuclear inclusion bodies in ipsilateral DRG. By 5 days p.i. most mice had early but unequivocal neuronal necrosis in the unilateral dorsal gray horn with mild neutrophilic and lymphoplasmacytic inflammation and mild rarefaction of the unilateral dorsal funiculus in caudal thoracic and cranial lumbar spinal cord. In ipsilateral DRGs and sympathetic ganglia of the lumbar segments, necrotic neurons with intranuclear inclusion bodies were present in greater numbers by 5 days p.i. [Fig. 1B]. On day 6, the thoracolumbar myelitis was present in all mice and was characterized by moderate neuronal necrosis with inclusion bodies in the unilateral dorsal gray horn accompanied by moderate lymphocytic and neutrophilic inflammation, microgliosis and rarefaction of the neuropil [Fig. 1C]. The lesion extended to involve the ipsilateral intermediate gray horn and gray matter adjacent to the central canal and contralateral dorsal gray horn in some mice. In addition, neuronal necrosis was occasionally present in contralateral DRGs, especially in more caudal lumbar segments. By 7 days p.i., the distribution of the thoracolumbar myelitis had progressed to involve contralateral dorsal gray horns and frequently extended ventrally to the level of the central canal in ipsilateral gray matter. The intensity of the neutrophilic and lymphoplasmacytic thoracolumbar myelitis had increased from moderate to marked or severe by 7 and 8 days p.i. within the lumbar segments and also involving DRG and sympathetic ganglia. Additionally, by 7 and 8 days p.i., mice that exhibited complete unilateral or bilateral hindlimb paralysis had more widespread involvement of gray matter, especially within caudal thoracic segments. Occasionally, neurons within the ventral motor regions in these segments were necrotic.

Aside from the skin and CNS, microscopic lesions were often present in the kidneys, urinary bladder, urethra/ureters, and colon/rectum. Minimal to mild unilateral hydronephrosis was seen at 4 days p.i. Necrosis and intranuclear inclusion body formation in transitional epithelial cells of the urinary bladder and/or urethra accompanied by focal or multifocal moderate lymphoplasmacytic and neutrophilic inflammation in the submucosa was seen at 5 days p.i. In addition, mice had ureteral ectasia with occasional focal epithelial necrosis and mixed inflammation, [Fig. 1D] often accompanied by mild unilateral or bilateral hydronephrosis. By 7 days p.i., moderate unilateral hydronephrosis was accompanied by either unilateral or bilateral ureteritis or focal necrotizing cystitis. Often, diffuse moderate lymphoplasmacytic inflammation was present within the pelvic canal, involving multilocular adipose tissue and autonomic ganglia. Moderate unilateral hydronephrosis, accompanied by severe unilateral ureteritis, occasionally with complete obstruction of the lumen was present at 8 days p.i. Also, in most animals, multifocal lymphoplasmacytic and neutrophilic inflammation was present within the tunica muscularis of the colon, infiltrating and surrounding myenteric ganglia. Neurons within these ganglia were often necrotic with occasional degeneration of the adjacent smooth muscle [Fig. 1E]. Frequently, moderate to marked multifocal neutrophilic inflammation was present within the lamina propria and submucosa of the distal colon. In a few animals, crypts within the overlying mucosa were dilated and filled with serocellular debris.

Temporal Progression of Green Fluorescent Protein Expression

To confirm that virus played a role in lesion development, the temporal progression of SaHV-1 infection in the tissues of inoculated mice was evaluated by detecting GFP expression within the cytoplasm of infected cells. Results are summarized in Table 4. GFP was first detected at 24 hours p.i. in discrete foci of keratinocytes within the epidermis of the inoculation site, corresponding to the foci of spongiosis seen in H&E sections [Fig. 1F]. By day 2 p.i., GFP was more widespread within the epidermis and follicular epithelium of inoculated skin and was also visible in a few individual neurons in ipsilateral DRG of the lumbar spinal cord of 2/5 mice. Viral replication in neurons of the DRG increased such that by day 4 p.i., numerous neurons in unilateral DRG of the mid-lumbar segments of all mice were intensely fluorescent with GFP. By 5 days p.i., viral replication had spread to involve the ipsilateral dorsal gray horn of the caudal thoracic and lumbar spinal cord segments. Viral replication was present in sympathetic ganglia of the mid-lumbar region of all mice. Also at day 5, foci of urothelium within the urinary bladder of each mouse were intensely fluorescent [Fig. 1G]. Viral replication was present in neurons of right and left dorsal gray horns and DRGs in caudal thoracic and lumbar regions of the spinal cord in most mice by 6 days p.i. In addition, ependymal cells of the central canal and neurons within the surrounding gray matter within these spinal cord segments exhibited fluorescence. At 6 days p.i., GFP was also present in myenteric ganglia within the muscular tunic of the distal colon in most mice [Fig. 1H]. Although the distribution remained essentially the same, GFP expression became more diffuse within affected regions and less focally intense within individual neurons of

spinal cord gray matter, DRGs and sympathetic ganglia of the thoracolumbar segments by day 8 p.i.

Discussion

Epidermal scarification or the zosteriform model has long been used in mice to study HSV infection (Blyth *et al.*, 1984; Simmons and Nash, 1984; Sydiskis and Schultz, 1965). The ability of HSV to initiate zosteriform spread has been shown to correlate with the neuroinvasive potential of the virus (Goel *et al.*, 2002). Experimental inoculation of alphaherpesviruses by epidermal scarification provides a more “natural” progression of infection than intramuscular or footpad injection. In this study, we utilized a GFP-expressing recombinant strain of SaHV-1 to characterize the temporal progression of disease in mice inoculated epidermally on the haunch. GFP detection within infected neurons was more rapid and somewhat more sensitive than detection of morphologic changes in H&E stained sections. For example, viral replication was detected via GFP in individual neurons of lumbar DRG at 2 days p.i., while focal intranuclear inclusion body formation or early neuronal necrosis was first evident at 3 days p.i. on H&E sections. In addition, GFP expression in infected neurons confirmed equivocal or subtle morphologic changes seen in H&E sections that have previously only been associated with early viral replication. As viral replication progressed and infected neurons became necrotic, GFP became disseminated within the infected focus and visualization of discrete infected cells was no longer possible. This was most likely due to lysis of infected neurons and release of GFP into the surrounding neuropil.

While microscopic lesions were consistently present in the skin at the site of inoculation and in the thoracolumbar region of the spinal cord and associated sensory ganglia following both epidermal and intramuscular routes of inoculation, disease induced by epidermal scarification varied significantly from that occurring in mice given SaHV-1 intramuscularly (Breshears *et al.*, 2003; Breshears *et al.*, 2001). Compared to intramuscular inoculation, infection of mice with SaHV-1 via epidermal scarification consistently produced a more rapidly progressive, severe disease in high dose groups (10^5 and 10^6 PFU), causing death in all mice that developed any clinical signs of disease. This is supported statistically by the identical ID_{50} , $CNSD_{50}$ and LD_{50} values for epidermal scarification. While the $CNSD_{50}$ values for both routes do not differ significantly, the ID_{50} value for SaHV-1 given epidermally is roughly 100 times higher than the IM route, indicating the threshold dose of virus needed to elicit an antibody response via IM inoculation is much lower than that for the epidermal route.

It seems likely that the elicitation of a humoral immune response at a lower viral dose via intramuscular inoculation is a factor in less severe clinical disease or occasionally complete lack of clinical signs. An antibody response to virus given via epidermal inoculation, indicative of viral infection, is always accompanied by severe, ultimately fatal disease. This suggests that while a relatively high dose of virus is necessary to infect an animal by establishing viral replication in the epidermis, once established, the infection consistently progresses more rapidly than an effective immune response can be mounted and results in severe disease. The fulminant disease caused by epidermal scarification may be partially due to the epitheliotropic nature of the virus and/or its ability to efficiently enter type C unmyelinated nerve endings that innervate the

epidermis. When administered intramuscularly, the virus is deposited in a cell type in which it cannot replicate, evidenced by the lack of GFP expression within myocytes at the inoculation site in mice given virus IM (Breshears, unpublished observations). Also, virus injected into the muscle is separated from free epidermal nerve endings by physical barriers, including the basal lamina of muscle fibers and the epidermal basement membrane (Huard *et al.*, 1996; Weeks *et al.*, 2000). Furthermore, intramuscularly inoculated virus may be more exposed to the host immune system allowing immediate attempts at control by the innate arm of the immune system as well as initiation of a strong adaptive response.

It is probable that the more rapid disease progression in epidermally inoculated animals is a function of efficient viral replication in keratinocytes at the inoculation site and/or efficient viral uptake by free nerve endings within the epidermis, resulting in a marked increase in the viral load to which an animal is exposed prior to development of an immune response. Distribution of lesions within the spinal cord are similar for epidermal and IM inoculation, suggesting that virus likely follows a similar neural path to the CNS in both inoculation routes. Nonmyelinated (type C) fibers are reported to be major components of the afferent innervation of skeletal muscle (Mense, 1993), and may serve as the neural route of virus uptake in mice inoculated IM. Capsaicin-sensitive afferents, which are distributed in the fascia and connective tissue among skeletal muscle fibers have been shown to terminate within the superficial dorsal horn (Rexed's laminae I and II) of spinal cord gray matter (Della Torre *et al.*, 1996) and course through the dorsal funiculus (Ling *et al.*, 2003). Cutaneous C-fibers reportedly terminate within the same spinal cord laminae (Sugiura *et al.*, 1986; Sugiura *et al.*, 1989). The overlapping pattern

of spinal cord termination regions for C-fibers innervating both skeletal muscle and skin would explain the similar distribution of spinal cord lesions in mice inoculated in either skin or muscle of roughly the same anatomic region.

A unique feature of skin scarification is a necrotizing cystitis, urethritis and ureteritis as well as colonic ganglioneuritis. These lesions were not present in mice inoculated intramuscularly or had been observed only rarely (Breshears *et al.*, 2003). The cystitis seen in these mice is similar to cystitis described in humans associated with either HSV-2 or herpes zoster infections (Chen *et al.*, 2002; DeHertogh and Brettman, 1988; McClanahan *et al.*, 1994; Nguyen *et al.*, 1992). HSV-2 is an uncommon cause of cystitis in people, and has been reported in both disseminated infections (DeHertogh and Brettman, 1988) and in disease involving only the urinary bladder (McClanahan *et al.*, 1994; Nguyen *et al.*, 1992). Regarding VZV infection, it has been reported that over 25% of patients with herpes zoster involving lumbosacral dermatomes develop voiding dysfunction secondary to cystitis, neuritis or myelitis (Chen *et al.*, 2002). The colonic ganglioneuritis commonly seen in SaHV-1 infected mice is similar to that reported by Ritchey *et al.* (Ritchey *et al.*, 2002) in mice experimentally infected with HVP-2. The colonic lesion is also reminiscent of intestinal lesions described in porcine pseudorabies (Narita *et al.*, 1998).

In this study, mice developed lesions similar to those described in human patients with VZV-associated urine voiding dysfunction. Mice commonly had cystitis concurrent with ganglioneuritis and myelitis. Viral infection of sensory neurons in dorsal root ganglia at day 2 p.i. was followed by the development of zosteriform cutaneous lesions by 4 day p.i. Beginning at day 5 p.i., cystitis, ganglioneuritis of pelvic autonomic ganglia

and thoracolumbar myelitis was observed. Also, similar to reports of constipation and reduction or absence of sphincter reflexes in humans with neuritis-associated voiding dysfunction (Chen *et al.*, 2002), multiple mice exhibited flaccidity of the anal sphincter and megacolon beginning at day 7 p.i. Often, these mice exhibited multifocal colitis sometimes accompanied by serocellular debris within colonic crypts and lumen. Since GFP expression was not observed in mucosal epithelium in sections of colon, it is likely that mucosal lesions are not due to viral replication but rather are secondary to changes in autonomic neural regulation and associated obstipation.

Viral replication in sympathetic ganglia within the lumbar and pelvic regions was seen only in epidermally inoculated animals. We suspect that the virus reaches these ganglia as well as the organs they supply via visceral afferent nerves. It has been reported that capsaicin-sensitive sensory neurons, which are composed primarily of unmyelinated C-fibers, are scattered throughout the upper urinary tract of mammals and innervate adventitia, smooth muscle, blood vessels and epithelium (Ammons, 1992). There is evidence that these neurons play a role in maintaining contractility in the upper urinary tract (Lang *et al.*, 2002). Similarly, capsaicin-sensitive spinal afferents or nociceptors, which extend from dorsal root ganglia, are located in myenteric ganglia within the tunica muscularis and tunica mucosa of the gastrointestinal tract (Berthoud *et al.*, 2001; Cervero, 1988; Grundy, 2002; Ward *et al.*, 2003). We hypothesize that these unmyelinated fibers play a significant role in transfer of virus to urinary and gastrointestinal tracts. Afferent nerves supplying pelvic viscera have nerve cell bodies in the same dorsal root ganglia as do cutaneous afferents supplying skin in the region of inoculation. There is evidence suggesting that it is possible for alphaherpesviruses to

spread nonsynaptically within ganglia (Carter *et al.*, 1992; LaVail *et al.*, 1993; Margolis *et al.*, 1992). The more virulent the strain of virus, the more commonly nonsynaptic transfer occurs (Sams *et al.*, 1995). Thus, it is possible that virus ascending sensory nerves from the inoculated epidermis could laterally infect visceral afferent neurons within the DRG and travel via anterograde axonal transport to the regional autonomic ganglia and visceral organs. The initial detection of viral replication in thoracolumbar DRG followed by the synchronous appearance of virus in regional autonomic ganglia, urinary tract epithelium as well as spinal cord suggests nonsynaptic spread, likely occurring within the DRG.

Viral infection of urothelium within the urinary bladder, urethra and ureters could have resulted from direct spread of cutaneous lesions in the perineal region or from hematogenous dissemination, but are most likely the result of dissemination through a neural route. Neural spread of virus to the lower urinary tract is supported by viral replication in numerous ganglia within the pelvic region and by the lack of viral-associated lesions in other visceral organs as would be expected with hematogenous dissemination. Direct spread from regional skin lesions is unlikely since skin lesions did not extend caudal from the inoculation site to involve the perineal region, and oftentimes epithelial lesions were present in the urinary bladder or ureters without concurrent foci of viral infected epithelium in the urethra. Given the distribution of lesions within the pelvic autonomic nervous system and associated viscera following epidermal inoculation, this may prove a valuable model system with which to examine the mechanism of development of urinary retention, cystitis and constipation associated with HSV-2 or lumbosacral VZV infections in humans.

References

- Ammons, W. S. (1992). Bowditch Lecture. Renal afferent inputs to ascending spinal pathways. *Am J Physiol*, **262**, R165-176.
- Berthoud, H. R., Lynn, P. A. and Blackshaw, L. A. (2001). Vagal and spinal mechanosensors in the rat stomach and colon have multiple receptive fields. *Am J Physiol Regul Integr Comp Physiol*, **280**, R1371-1381.
- Best, C. H., Taylor, N. B. and West, J. B. (1991). *Best and Taylor's physiological basis of medical practice*. Williams & Wilkins, Baltimore.
- Blyth, W. A., Harbour, D. A. and Hill, T. J. (1984). Pathogenesis of zosteriform spread of herpes simplex virus in the mouse. *J Gen Virol*, **65 (Pt 9)**, 1477-1486.
- Breshears, M. A., Black, D. H., Ritchey, J. W. and Eberle, R. (2003). Construction and in vivo detection of an enhanced green fluorescent protein-expressing strain of *Saimiriine herpesvirus 1* (SaHV-1). *Arch Virol*, **148**, 311-327.
- Breshears, M. A., Eberle, R. and Ritchey, J. W. (2001). Characterization of gross and histological lesions in Balb/c mice experimentally infected with *Herpesvirus saimiri 1* (HVS1). *J Comp Pathol*, **125**, 25-33.
- Carter, S. R., Pereira, L., Paz, P. and LaVail, J. H. (1992). A quantitative assay of retrograde transported HSV in the trigeminal ganglion. *Invest Ophthalmol Vis Sci*, **33**, 1934-1939.
- Cervero, F. (1988). Neurophysiology of gastrointestinal pain. *Baillieres Clin Gastroenterol*, **2**, 183-199.
- Chen, P. H., Hsueh, H. F. and Hong, C. Z. (2002). Herpes zoster-associated voiding dysfunction: a retrospective study and literature review. *Arch Phys Med Rehabil*, **83**, 1624-1628.
- Daniel, M. D., Karpas, A., Melendez, L. V., King, N. W. and Hunt, R. D. (1967). Isolation of herpes-T virus from a spontaneous disease in squirrel monkeys (*Saimiri sciureus*). *Arch Gesamte Virusforsch*, **22**, 324-331.

- DeHertogh, D. A. and Brettman, L. R. (1988). Hemorrhagic cystitis due to herpes simplex virus as a marker of disseminated herpes infection. *Am J Med*, **84**, 632-635.
- Della Torre, G., Lucchi, M. L., Brunetti, O., Pettorossi, V. E., Clavenzani, P. and Bortolami, R. (1996). Central projections and entries of capsaicin-sensitive muscle afferents. *Brain Res*, **713**, 223-231.
- Desrosiers, R. C. and Falk, L. A., Jr. (1981). *Herpesvirus tamarinus* and its relation to herpes simplex virus. *J Gen Virol*, **56**, 119-130.
- Eberle, R., Black, D. and Hilliard, J. K. (1989). Relatedness of glycoproteins expressed on the surface of simian herpes-virus virions and infected cells to specific HSV glycoproteins. *Arch Virol*, **109**, 233-252.
- Emmons, R. W., Gribble, D. H. and Lennette, E. H. (1968). Natural fatal infection of an owl monkey (*Aotus trivirgatus*) with Herpes T virus. *J Infect Dis*, **118**, 153-159.
- Goel, N., Mao, H., Rong, Q., Docherty, J. J., Zimmerman, D. and Rosenthal, K. S. (2002). The ability of an HSV strain to initiate zosteriform spread correlates with its neuroinvasive disease potential. *Arch Virol*, **147**, 763-773.
- Goodpasture, E. W. and Teague, O. (1923). Transmission of the virus of herpes febrilis along nerves in experimentally infected rabbits. *J Med Res*, **44**, 139-184.
- Grundy, D. (2002). Neuroanatomy of visceral nociception: vagal and splanchnic afferent. *Gut*, **51 Suppl 1**, i2-5.
- Hilliard, J. K., Black, D. and Eberle, R. (1989). Simian alphaherpesviruses and their relation to the human herpes simplex viruses. *Arch Virol*, **109**, 83-102.
- Holmes, A. W., Caldwell, R. G., Dedmon, R. E. and Deinhardt, F. (1964). Isolation and characterization of a new herpes virus. *J Immunol*, **92**, 602-610.
- Holmes, A. W., Dedmon, R. E. and Deinhardt, F. (1963). Isolation of a new herpes-like virus from south american marmosets. *Fed Proc*, **22**, 324.

- Holzer, P. (1991). Capsaicin: cellular targets, mechanisms of action, and selectivity for thin sensory neurons. *Pharmacol Rev*, **43**, 143-201.
- Huard, J., Feero, W. G., Watkins, S. C., Hoffman, E. P., Rosenblatt, D. J. and Glorioso, J. C. (1996). The basal lamina is a physical barrier to herpes simplex virus-mediated gene delivery to mature muscle fibers. *J Virol*, **70**, 8117-8123.
- Hunt, R. D. and Melendez, L. V. (1966). Spontaneous herpes-T infection in the owl monkey (*Aotus trivirgatus*). *Pathol Vet*, **3**, 1-26.
- Illanes, O., Mossman, S. and McCarthy, K. (1990a). Alphaherpesvirus saimiri infection in rabbits. 1. Light and electron microscopy study of cutaneous spinal nerves. *Acta Neuropathol (Berl)*, **79**, 551-557.
- Illanes, O., Mossman, S. and McCarthy, K. (1990b). Alphaherpesvirus saimiri infection in rabbits. 2. Morphometric studies of cutaneous spinal nerves. *Acta Neuropathol (Berl)*, **79**, 558-565.
- Irie, H., Harada, Y., Kataoka, M., Nagamuta, M., Moriya, Y., Handa, M., Saito, M., Matsubara, S., Kojima, K. and Sugawara, Y. (1992). Efficacy of oral administration of live herpes simplex virus type 1 as a vaccine. *J Virol*, **66**, 2428-2434.
- Lang, R. J., Davidson, M. E. and Exintaris, B. (2002). Pyeloureteral motility and ureteral peristalsis: essential role of sensory nerves and endogenous prostaglandins. *Exp Physiol*, **87**, 129-146.
- LaVail, J. H., Johnson, W. E. and Spencer, L. C. (1993). Immunohistochemical identification of trigeminal ganglion neurons that innervate the mouse cornea: relevance to intercellular spread of herpes simplex virus. *J Comp Neurol*, **327**, 133-140.
- Leib, D. A., Hart, C. A. and McCarthy, K. (1987). Characterization of four herpesviruses isolated from owl monkeys and their comparison with *Herpesvirus saimiri* type 1 (*Herpesvirus tamarinus*) and herpes simplex virus type 1. *J Comp Pathol*, **97**, 159-169.
- Ling, L. J., Honda, T., Shimada, Y., Ozaki, N., Shiraishi, Y. and Sugiura, Y. (2003). Central projection of unmyelinated (C) primary afferent fibers from gastrocnemius muscle in the guinea pig. *J Comp Neurol*, **461**, 140-150.

- Ljungdahl, A., Kristensson, K., Lundberg, J. M., Lycke, E., Svennerholm, B. and Ziegler, R. (1986). Herpes simplex virus infection in capsaicin-treated mice. *J Neurol Sci*, **72**, 223-230.
- Maayan, C., Nimrod, A., Morag, A. and Becker, Y. (1998). Herpes simplex virus-1 and varicella virus infections in familial dysautonomia patients. *J Med Virol*, **54**, 158-161.
- Margolis, T. P., Dawson, C. R. and LaVail, J. H. (1992). Herpes simplex viral infection of the mouse trigeminal ganglion. Immunohistochemical analysis of cell populations. *Invest Ophthalmol Vis Sci*, **33**, 259-267.
- McClanahan, C., Grimes, M. M., Callaghan, E. and Stewart, J. (1994). Hemorrhagic cystitis associated with herpes simplex virus. *J Urol*, **151**, 152-153.
- McDermott, M. R., Smiley, J. R., Leslie, P., Brais, J., Rudzroga, H. E. and Bienenstock, J. (1984). Immunity in the female genital tract after intravaginal vaccination of mice with an attenuated strain of herpes simplex virus type 2. *J Virol*, **51**, 747-753.
- Mense, S. (1993). Nociception from skeletal muscle in relation to clinical muscle pain. *Pain*, **54**, 241-289.
- Narita, M., Zhao, Y. M., Kawashima, K., Arai, S., Hirose, H., Yamada, S. and Ezura, K. (1998). Enteric lesions induced by different pseudorabies (Aujeszky's disease) virus strains inoculated into closed intestinal loops of pigs. *Journal of Veterinary Diagnostic Investigation*, **10**, 36-42.
- Nguyen, M. L., Borochoviz, D., Thomas, G., McClure, T. and Ruben, F. L. (1992). Hemorrhagic cystitis with herpes simplex virus type 2 in the bladder mucosa. *Clin Infect Dis*, **14**, 767-768.
- Richards, J. T., Kern, E. R., Overall, J. C., Jr. and Glasgow, L. A. (1981). Differences in neurovirulence among isolates of herpes simplex virus types 1 and 2 in mice using four routes of infection. *J Infect Dis*, **144**, 464-471.
- Ritchey, J. W., Ealey, K. A., Payton, M. E. and Eberle, R. (2002). Comparative pathology of infections with baboon and African green monkey alpha-herpesviruses in mice. *J Comp Pathol*, **127**, 150-161.

- Robertson, J. L. and Preisler, H. K. (1992). *Pesticide bioassays with arthropods*. CRC Press, Boca Raton, pp. 127.
- Rooney, J. F., Wohlenberg, C., Cremer, K. J. and Notkins, A. L. (1989). Immunized mice challenged with herpes simplex virus by the intranasal route show protection against latent infection. *J Infect Dis*, **159**, 974-976.
- Sams, J. M., Jansen, A. S., Mettenleiter, T. C. and Loewy, A. D. (1995). Pseudorabies virus mutants as transneuronal markers. *Brain Res*, **687**, 182-190.
- Schrier, A. (1966). Editor's notes. *Laboratory Primate Newsletter*, **5**, ii.
- Simmons, A. and Nash, A. A. (1984). Zosteriform spread of herpes simplex virus as a model of recrudescence and its use to investigate the role of immune cells in prevention of recurrent disease. *J Virol*, **52**, 816-821.
- Stanberry, L. R., Bourne, N., Bravo, F. J. and Bernstein, D. I. (1992). Capsaicin-sensitive peptidergic neurons are involved in the zosteriform spread of herpes simplex virus infection. *J Med Virol*, **38**, 142-146.
- Sugiura, Y., Lee, C. L. and Perl, E. R. (1986). Central projections of identified, unmyelinated (C) afferent fibers innervating mammalian skin. *Science*, **234**, 358-361.
- Sugiura, Y., Terui, N. and Hosoya, Y. (1989). Difference in distribution of central terminals between visceral and somatic unmyelinated (C) primary afferent fibers. *J Neurophysiol*, **62**, 834-840.
- Sydiskis, R. J. and Schultz, I. (1965). Herpes simplex skin infection in mice. *J Infect Dis*, **115**, 237-246.
- Walter, I., Fleischmann, M., Klein, D., Muller, M., Salmons, B., Gunzburg, W. H., Renner, M. and Gelbman, W. (2000). Rapid and sensitive detection of enhanced green fluorescent protein expression in paraffin sections by confocal laser scanning microscopy. *Histochem J*, **32**, 99-103.
- Ward, S. M., Bayguinov, J., Won, K. J., Grundy, D. and Berthoud, H. R. (2003). Distribution of the vanilloid receptor (VR1) in the gastrointestinal tract. *J Comp Neurol*, **465**, 121-135.

Weeks, B. S., Ramchandran, R. S., Hopkins, J. J. and Friedman, H. M. (2000). Herpes simplex virus type-1 and -2 pathogenesis is restricted by the epidermal basement membrane. *Arch Virol*, **145**, 385-396.

Wharton, S. B., Meyers, N. L. and Nash, A. A. (1995). Experimental herpes simplex virus type 1 (HSV-1) infection of the spinal cord and dorsal root ganglia. *Neuropathol Appl Neurobiol*, **21**, 228-237.

Table 1
Clinical Signs and Gross Lesions

Viral dose (PFU)	Number of mice affected in groups of eight					
	Skin lesion	Paralysis/paresis		Urinary Incontinence	Early Euthanasia	Seropositive for IgG
		Unilateral	Bilateral			
10 ⁶	8	8	0	3	8	6*
10 ⁵	7	5	2	1	7	6*
10 ⁴	2	1	1	1	2	1*
10 ³	0	0	0	0	0	0
10 ²	0	0	0	0	0	0
10	0	0	0	0	0	0
0 (controls)	0	0	0	0	0	0

Mice that exhibited clinical signs of disease but were not positive (2 in 10⁶, 1 each in 10⁵ and 10⁴ groups) were euthanized at 6-8 days p.i. and before an IgG response was detectable.

Table 2
Comparison of ID₅₀, CNSD₅₀ and LD₅₀

	Epidermal scarification	Intramuscular inoculation ¹
ID ₅₀	10 ^{4.38 a}	10 ^{2.31 b}
CNSD ₅₀	10 ^{4.38 a}	10 ^{4.21 a}
LD ₅₀	10 ^{4.38 a}	>10 ⁶

Values with the same superscript letter (unlike those with different letters) do not differ significantly ($P > 0.05$) by methods of Robertson and Preisler (1992).

1). Values taken from (Breshears *et al.*, 2003)

Table 3
Temporal Development of Histological Lesions

Days P.I.	Number Affected	Tissues*	Lesions*
1	5/5	Skin	Focal epidermal spongiosis and necrosis
3	3/5	Lumbar DRG	Focal clusters of necrotic neurons with intranuclear inclusion bodies
5	4/5 5/5	Thoracic spinal cord Lumbar spinal cord	Neuronal necrosis with INIB and rarefaction of neuropil in unilateral dorsal horn
5	4/5	Urinary bladder/urethra/ureters	Focal lymphoplasmacytic and neutrophilic inflammation with epithelial necrosis
5	4/5	Lumbar/ pelvic autonomic ganglia	Neuronal necrosis with INIB
5	2/5	Kidneys	Unilateral or occasionally bilateral hydronephrosis
8	3/5	Colon/rectum	Intramural inflammation associated with myenteric ganglia

*Days on which virus was first detected in different tissues and/or lesions observed.

Table 4
Temporal Development of GFP Expression

Days P.I.	Number affected	Tissues	Location of GFP
1	5/5	Skin	Multifocal in keratinocytes of superficial epidermis
2	5/5	Skin	Multifocal in epidermis and follicular epithelium
2	2/5	Lumbar DRG	Individual neurons
5	5/5	Thoracolumbar spinal cord	Unilateral dorsal gray horn and sympathetic ganglia
5	5/5	Urinary bladder/ ureters	Multifocal in urothelium
5	5/5	Lumbar/ pelvic autonomic ganglia	Multifocal in neurons
6	3/5	Colon/rectum	Multifocal in myenteric ganglia

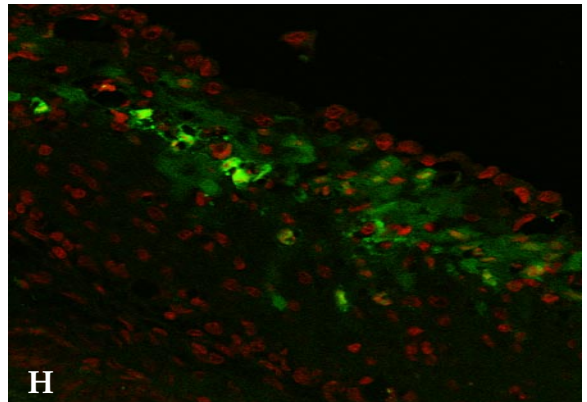
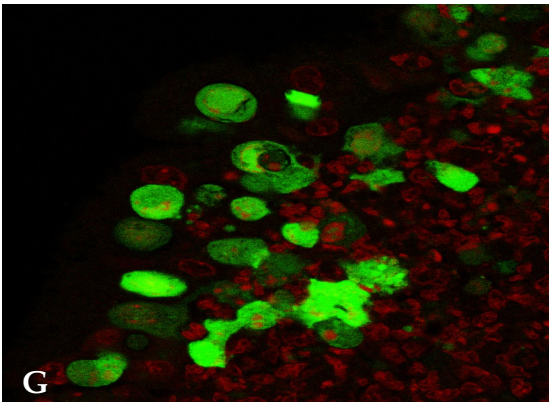
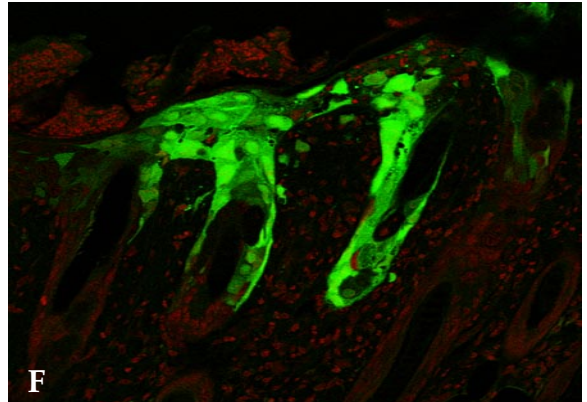
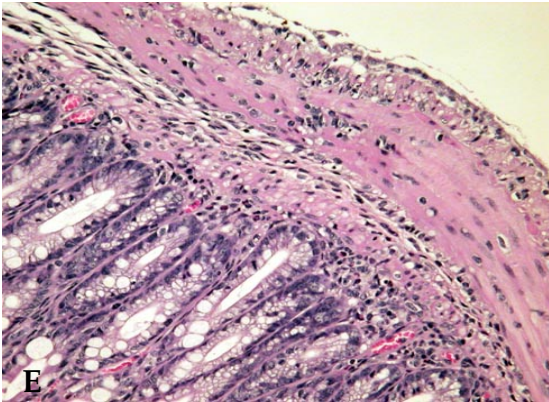
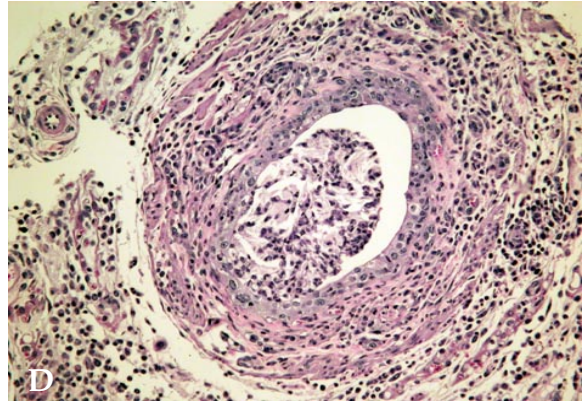
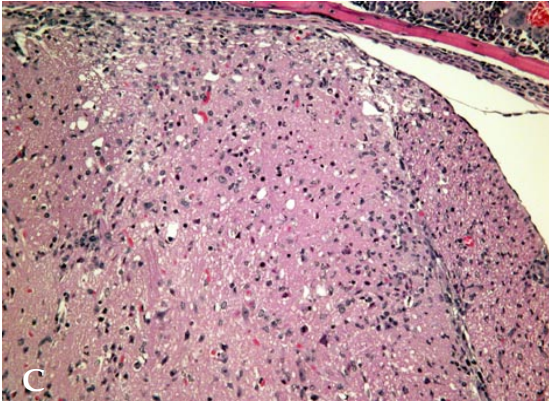
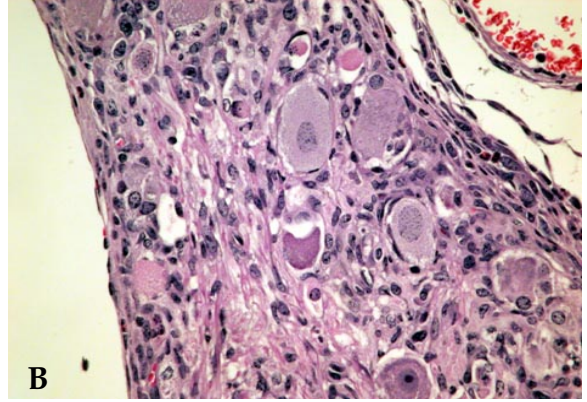
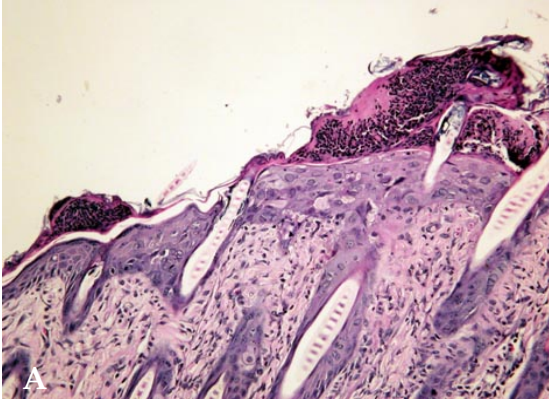


Figure 1. All tissues are from Balb/c mice epidermally inoculated with 10^6 PFU of SaHV-1rG.

A. Haired skin. Characteristic skin lesion at the inoculation site 24 hours p.i.

There is moderate swelling of epidermal keratinocytes, many of which have distinct intranuclear inclusion bodies. The underlying dermis contains a mild neutrophilic infiltrate and a fibrinosuppurative mat overlies the focus of infected epidermis. H&E.

B. Left dorsal root ganglion, lumbar region. Neuronal necrosis and loss is accompanied by a mild mononuclear inflammatory infiltrate at 6 days p.i. H&E.

C. Lumbar spinal cord. Typical lesion present in the lumbar spinal cord at 6 days p.i. The left dorsal grey horn exhibits regionally extensive neuronal necrosis accompanied by mild neutrophilic and lymphocytic inflammation and rarefaction of the left dorsal funiculus. At higher magnification, intranuclear inclusion bodies can be seen in scattered neurons of the left dorsal grey horn. H&E.

D. Ureter, 6 days p.i. There is marked ureteral ectasia with intense transmural and periureteral neutrophilic and lymphoplasmacytic inflammation. The lumen contains neutrophils admixed with fewer mononuclear cells in a fibrinous background. Ureteral epithelium is dysplastic and contains a small number of transmigrating inflammatory

cells but no discrete foci of viral infected cells. This mouse had grossly discernible unilateral hydronephrosis. H&E.

E. Colon. Characteristic colon lesion present at 8 days p.i. Neurons within the myenteric plexus are necrotic and myocytes of the adjacent smooth muscle tunics are moderately vacuolated. H&E.

F. Skin. Confocal image demonstrating GFP expression in SaHV-1 infected epidermal and follicular keratinocytes at 24 hours p.i. This tissue section is from the same lesion shown in A.

G. Urinary bladder. Confocal image of SaHV-1 infected focus of urinary bladder epithelium at 6 days p.i.

H. Colon. Confocal image of a colonic myenteric plexus, demonstrating viral replication within numerous neurons between the muscular tunics. This tissue section is from the same specimen as shown in E.

CHAPTER VI

SUMMARY AND CONCLUSIONS

The first experiment in which mice were inoculated IM with wild type SaHV-1 demonstrated that the virus produces an active infection in Balb/c mice, resulting in lesions of both the skin and thoracolumbar spinal cord. While infection did not always result in CNS disease, inoculation of dose groups with 10-fold dilutions of virus demonstrated a correlation between virus dose and severity of disease. Animals receiving $\geq 10^3$ or greater PFU of SaHV-1 developed an antiviral IgG response, often developed skin lesions at the site of inoculation, and less frequently exhibited paresis or paralysis. The incidence of both skin lesions and CNS disease increased in higher dosage groups. Skin lesions were often, but not always, present in mice with CNS disease; several mice had skin lesions but did not develop discernible neurological deficits.

Following inoculation of SaHV-1 in the semimembranosus/semitendinosus muscle group, skin lesions first appeared at day 5 p.i. and were grossly characterized as multifocal, shallow ulcers that ultimately coalesced to form larger ulcerative foci involving the caudolateral thigh. Histologically, cutaneous lesions were the result of partial to full thickness epidermal necrosis accompanied by a moderate superficial inflammatory infiltrate composed of lymphocytes and macrophages with intensely neutrophilic infiltrates adjacent to foci of full thickness epidermal necrosis. Intranuclear inclusion bodies were occasionally discernible, especially within follicular epithelium.

Spinal cord lesions following intramuscular inoculation varied widely in severity and also varied between thoracic and lumbar segments. In lumbar segments, lesions consisted of rarefaction accompanied by lymphocytic and microglial infiltrates within the dorsal root, dorsal funiculus and dorsal gray horn, all ipsilateral to the inoculation site. Neutrophilic infiltrates were prominent in more acute lesions. In lumbar segments, lesions in paralyzed mice were more severe than in non-paralyzed mice but remained restricted to the ipsilateral dorsal regions of the cord. Occasional moderate mononuclear infiltrates were present in unilateral or bilateral dorsal root ganglia in lumbar segments. In thoracic cord segments, lesions in non-paralyzed mice were similar to those described in lumbar segments. In mice with unilateral or bilateral paralysis, thoracic spinal cord segments were characterized by unilateral or bilateral rarefaction and widespread necrosis within both gray and white matter in dorsal and ventral regions of the cord. Inflammation composed of neutrophilic and mononuclear cell populations ranged from mild to severe and was widely disseminated throughout the thoracic segments. No lesions were seen in cervical segments of spinal cord, brain, autonomic ganglia or viscera.

Results from this initial mouse inoculation study supported the following conclusions: i.) IM inoculation of Balb/c mice with 10^3 - 10^6 PFUs of SaHV-1 often leads to active infection as indicated by seroconversion and development of lesions restricted to the skin in the region of inoculation and/or thoracolumbar spinal cord. ii.) Incidence and severity of disease increases with increasing virus dose. iii.) Development of skin lesions either briefly preceded or temporally coincided with the onset of neurological signs, suggesting the presence of virus within the CNS at the time skin lesions appeared. iv.) Virus replication within the CNS is confined to the thoracolumbar spinal cord and unlike

BV infection in humans, SaHV-1 infection in mice does not fully ascend the cord or result in encephalitis.

To detect viral replication within tissues of experimentally infected mice, the second major step in this dissertation project was the construction and characterization of a GFP-expressing SaHV-1 recombinant virus. To accomplish this without altering the *in vitro* or *in vivo* behavior of the virus, a GFP expression cassette was constructed using the BV UL19 promoter and transcriptional termination sequences and was inserted into a transcriptionally null site of the SaHV-1 genome. The intergenic space between termination sequences for the UL24/25/26 and the UL27/28 transcriptional gene sets was the target insertion site for the GFP expression cassette. PCR and Southern blot analysis confirmed insertion of a single copy of the expression cassette into the desired location, and virus replication in cell culture produced strong GFP fluorescence within the cytoplasm of infected cells. *In vitro* growth kinetics of wild type and recombinant viruses (SaHV-1rG1 and SaHV-1rG3) were shown to be similar; *in vivo* studies also revealed similarity in the development of clinical disease, humoral immune response and microscopic lesions in mice inoculated IM with wild type or recombinant virus. GFP expression in infected cells was easily detected by confocal microscopy in formalin-fixed, paraffin-embedded tissues (skin and spinal cord) of mice infected with recombinant SaHV-1.

Results of *in vitro* and *in vivo* characterization of the GFP-expressing recombinant strain of SaHV-1 support the following conclusions: i.) SaHV-1 is able to recognize and utilize BV transcriptional elements, as indicated by the expression of GFP in SaHV-1rG infected cells. ii.) Insertion of the GFP expression cassette and GFP-expression in

infected cells does not alter *in vitro* characteristics such as CPE, growth kinetics or kinetics of gB expression of recombinant SaHV-1. iii.) SaHV-1rG1 and SaHV-1 rG3 do not have significantly different ID₅₀ values than wtSaHV-1. iv.) CNSD₅₀ values for wtSaHV-1 and SaHV-1rG1 are not significantly different while the CNSD₅₀ value for SaHV-1rG3 was significantly lower. v.) Microscopic lesions associated with SaHV-1rG infection are similar to those reported for wtSaHV-1 in the initial study. vi.) GFP expression, which indicates viral replication, is easily detected in epidermal keratinocytes in the region of inoculation and in neurons of the ipsilateral dorsal gray horn of thoracolumbar spinal cord. vii.) GFP expression in skin and spinal cord of infected mice co-localizes with SaHV-1 antigen, as detected by IHC, and with early histological lesions visible on routine stains.

The final experiment was designed to more thoroughly study the neuropathogenesis of SaHV-1 in mice using the GFP-expressing recombinant virus strain. To mimic natural alphaherpesvirus infections, mice were inoculated with virus in the region of the left hip via epidermal scarification. Mice were sequentially sacrificed to investigate the temporal progression of infection and disease. While the pathogenesis of infection by different inoculation routes was not compared side-by-side in this experiment, interesting differences in the severity and progression of disease as well as lesion distribution were observed.

Following epidermal inoculation, SaHV-1 infection was initially manifested at 2 days p.i. as pinpoint ulcerative lesions in the inoculated epidermis. Skin lesions enlarged locally over the next 2-3 days, by which time mice began to exhibit abnormal hindlimb posture that progressed to unilateral paresis or paralysis by day 6 p.i. At 7 and 8 days

p.i., mice were depressed with hunched postures and abdominal distension, and often exhibited evidence of urinary and fecal incontinence. Disease severity dictated that all mice be humanely killed at or before 9 days p.i.

Gross lesions included unilateral or bilateral hydronephrosis, marked cecal and colonic distension and occasional urinary bladder distension. Histological lesions were present in skin, spinal cord, sympathetic ganglia, colonic myenteric plexuses, kidney and lower urinary tract. Skin lesions were characterized by epidermal and superficial dermal necrosis with suppurative dermatitis and intranuclear inclusion body formation. Lesions in the spinal cord were confined to the thoracolumbar region. In lumbar segments, lesions consisted of neuronal necrosis in dorsal root ganglia ipsilateral to the site of inoculation with progression to neuronal necrosis in the ipsilateral dorsal gray horn accompanied by moderate neutrophilic and lymphocytic inflammation, microgliosis and rarefaction of the dorsal funiculus. Distribution of lesions in the thoracic segments was widespread and similar to that seen in IM inoculated, paralyzed mice. Sympathetic ganglia in the pelvic region as well as myenteric plexuses within the colonic wall exhibited neuronal necrosis accompanied by lymphoplasmacytic and neutrophilic inflammation. Epithelial necrosis accompanied by local inflammation was often present in ureters, urinary bladder and/or urethra. In some cases, necrosis and destruction of the ureteral urothelium was so severe as to obstruct the ureteral lumen with fibrinonecrotic debris.

Viral replication, indicated by GFP expression, correlated with early lesions seen on H&E stained sections. GFP was first observed within the inoculated epidermis at 24 hours p.i. As early as 2 days p.i. GFP expression was present in individual neurons of

ipsilateral thoracolumbar DRG. As the infection progressed, viral replication became present in numerous DRG neurons by day 4 p.i. and neurons of the dorsal gray horn by 5 days p.i. At this time point, GFP expression was also seen in urothelium, lumbar and pelvic sympathetic ganglia. By 6 days p.i., viral replication was often present within neurons of colonic myenteric ganglia.

Lesions within the urinary tract, sympathetic ganglia and myenteric plexuses had either not previously been observed in mice inoculated IM with SaHV-1 or had been observed only rarely. Interestingly, in addition to the more widespread lesion distribution seen in epidermally inoculated mice, the rapidity of disease progression as well as disease severity was increased when compared to mice inoculated IM with similar doses of the virus. In fact, all mice that were infected via epidermal inoculation, (as indicated by seroconversion) developed severe disease that warranted euthanasia at or before day 9 p.i. Mice that were inoculated epidermally with lower doses of virus did not develop disease and failed to mount an antiviral antibody response, indicating an active viral infection was not established in these animals. Thus ID_{50} , $CNSD_{50}$ and LD_{50} values were all equal ($10^{4.38}$) for all mice inoculated epidermally with SaHV-1; active infection initiated by this route always resulted in CNS disease that was ultimately fatal. This varies significantly from IM inoculation experiments in which some mice injected with lower doses of virus seroconverted without exhibiting overt disease and in which other mice developed disease that did not consistently result in death. These features are supported by the median dose values for IM inoculation with SaHV-1 ($ID_{50} = 10^{2.31}$, $CNSD_{50} = 10^{4.21}$ and $LD_{50} > 10^6$).

Investigation of the temporal progression of disease in mice epidermally inoculated with a GFP-expressing SaHV-1 recombinant supports the following conclusions: i.) Infection with SaHV-1 via epidermal inoculation results in a rapidly progressive, severe disease with cutaneous lesions and regional involvement of the somatic and autonomic nervous systems. ii.) Viral infection of epithelium within the lower urinary tract is consistently present in mice inoculated epidermally with SaHV-1 and presumably occurs via neuronal transport through autonomic nerves. iii.) Spinal cord lesions in epidermally inoculated mice are comparable to those seen in mice inoculated intramuscularly. iv) The appearance of skin lesions in IM inoculated mice correlates temporally with zosteriform spread of cutaneous lesions in epidermally inoculated mice and follows viral replication within the DRG by about 2 days.

Taken together, the construction and characterization of a GFP-expressing recombinant strain of SaHV-1 and the series of mouse inoculation studies performed utilizing that virus demonstrate the limited neurovirulence of SaHV-1 in mice. Route of inoculation experiments illustrate the epitheliotropic nature of SaHV-1 and highlight its ability to enter the peripheral nerves following replication within epidermal epithelium. The restricted neurovirulence and neuroinvasiveness of SaHV-1 may limit its use in a model system for highly neurovirulent viruses such as monkey B virus. However, similarities in disease induced by epidermal inoculation and the cystitis associated with lumbosacral VZV infection in people are striking and are worthy of further investigation.

Appendix I

Selected Viruses of the Subfamily *Alphaherpesvirinae*

Genus *Simplexvirus*

Current Designation	Abbreviation	Synonyms
<i>Genus Simplexvirus</i>		
<i>Human herpesvirus 1</i>	HHV-1	Herpes simplex virus (HSV)
<i>Human herpesvirus 2</i>	HHV-2	Herpes simplex virus 2 (HSV-2)
<i>Cercopithecine herpesvirus 1</i>	CeHV-1	B virus (BV), Herpesvirus simiae
<i>Cercopithecine herpesvirus 2</i>	CeHV-2	Simian agent 8 (SA8)
<i>Cercopithecine herpesvirus 16</i>	CeHV-16	Herpesvirus papio 2, baboon herpesvirus
<i>Ateline herpesvirus 1</i>	AtHV-1	Spider monkey herpesvirus
<i>Saimiriine herpesvirus 1</i>	SaHV-1	Marmoset herpesvirus, herpes T, herpesvirus tamarinus,
<i>Genus Varicellovirus</i>		
<i>Human herpesvirus 3</i>	HHV-3	Varicella-zoster virus
<i>Suid herpesvirus 1</i>	SuHV-1	Pseudorabies virus, Aujeszky's disease
<i>Cercopithecine herpesvirus 9</i>	CeHV-9	Simian varicella herpesvirus

Appendix II

Taxonomy of Selected Non-human Primates

Infraorder: Catarrhini (“Old World Primates”)

Superfamily: Hominoidea (“Apes”) (include humans, chimpanzees, bonobos, gorillas, orangutans, gibbons and siamangs)

Superfamily: Cercopithecoidea (“Old World Monkeys”)

Family: Cercopithecidae (include macaques, baboons, guenons and mangabeys)

Macaca mulatta (rhesus monkey)

Papio spp. (baboons)

Cercopithecus neglectus (DeBrazza’s Monkey)

Family: Colobidae (include colobus, langurs, surelis, snub-nosed monkeys, doucs and proboscis monkeys)

Infraorder: Platyrrhini (“New World Monkeys”)

Superfamily: Ceboidea

Family: Cebidae (include capuchins, squirrel monkeys, spider monkeys, owl monkeys, howler monkeys and woolly monkeys)

Saimiri sciureus (South American squirrel monkey)

Aotus trivirgatus (owl monkey or northern night monkey)

Cebus albifrons (white-fronted capuchin)

Ateles spp. (spider monkeys)

Family: Callitrichidae (include marmosets and tamarins)

Genus: *Callithrix* (marmosets)

C. jacchus (common marmoset)

Genus: *Saguinus* (tamarins)

S. nigricollis (black-mantle tamarin)

S. mystax (black-chested mustached tamarin)

S. oedipus (cotton-top tamarin)

VITA

Melanie Ann Breshears

Candidate for the Degree of

Doctor of Philosophy

Thesis: INVESTIGATION OF THE PATHOGENESIS OF SAIMIRIINE
HERPESVIRUS 1 IN BALB/C MICE

Major Field: Veterinary Pathobiology

Biographical:

Personal Data: Born in Oklahoma City, Oklahoma on October 24, 1973, the daughter of Ronald and Patricia Breshears.

Education: Graduated from Mustang High School, Mustang, Oklahoma in May, 1991; received Bachelor of Science degree in Animal Science and a Doctor of Veterinary Medicine degree from Oklahoma State University, Stillwater, Oklahoma in August 1995 and May 1998, respectively. Completed the requirements for Doctor of Philosophy degree in Veterinary Biomedical Science at Oklahoma State University in July 2004.

Experience: Large Animal ICU Veterinarian at Boren Veterinary Medicine Teaching Hospital, Oklahoma State University, Stillwater, Oklahoma, 1998-1999. Veterinary Histology Graduate Teaching Assistant, Oklahoma State University, 1999-2002. Anatomic Pathology Resident, Oklahoma State University, 2003. Lecturer, Anatomic Pathology, Oklahoma State University, 2003-2004.

Professional Organizations: American Veterinary Medical Association, Phi Zeta (Nu Chapter), Licensed by the Oklahoma Board of Veterinary Medical Examiners

Name: Melanie A. Breshears

Date of Degree: July, 2004

Institution: Oklahoma State University

Location: Stillwater, Oklahoma

Title of Study: INVESTIGATION OF THE PATHOGENESIS OF
SAIMIRIINE HERPESVIRUS 1 IN BALB/C MICE

Pages in Study: 141

Candidate for the Degree of Doctor of Philosophy

Major Field: Veterinary Biomedical Science

Scope and Method of Study: The purpose of this study was to investigate the pathogenesis of *Saimiriine herpesvirus 1* (SaHV-1) infection by characterizing the clinical disease and gross and microscopic lesions in experimentally infected mice. To aid in the identification of anatomic sites of viral replication and to trace viral spread in experimentally infected mice, a green fluorescent protein (GFP)-expressing recombinant strain of SaHV-1 was constructed and used in subsequent inoculation studies. Mice were inoculated intramuscularly or epidermally with ten-fold dilutions of virus and sacrificed at 14 or 21 days in endpoint studies or on sequential days in temporal studies. Serum was tested by ELISA and tissues were examined microscopically with routine stains, immunohistochemistry, and confocal microscopy.

Findings and Conclusions: SaHV-1 inoculation of Balb/c mice, either intramuscularly or epidermally, resulted in active infection as indicated by seroconversion, clinical disease, and gross and microscopic lesions. Mice inoculated intramuscularly initially developed skin lesions in the region of inoculation with subsequent development of paresis or paralysis of the inoculated hindlimb in animals receiving higher doses of virus. Lesions in these mice were restricted to the skin and thoracolumbar spinal cord and consisted of necrotizing dermatitis and segmental myelitis with neuronal necrosis. Mice inoculated with SaHV-1 via epidermal scarification developed a more rapidly progressive, severe disease that began in the inoculated epidermis and spread to involve thoracolumbar spinal cord, regional autonomic ganglia, and lower urinary tract. All mice receiving an infective dose of virus by this route developed ultimately fatal disease. GFP expression, indicating viral replication, corresponded with microscopic lesions and was present in keratinocytes of the epidermis, neurons of the dorsal root ganglia, spinal cord, sympathetic ganglia, and colonic myenteric plexus as well as epithelium of the lower urinary tract. SaHV-1 exhibited neurovirulence in Balb/c mice that varied significantly with the route of inoculation.

ADVISOR'S APPROVAL: Jerry W. Ritchey